

2

SANDSTONE-29(EX)
EXTRACTED VERSION

OPERATION SANDSTONE

Scientific Director's Report of Atomic Weapon Tests at Eniwetok, 1948

Annex 8—Gamma-Ray Measurements

Parts I, II, III, IV, and V

AD-A995 396

F. R. Shonka
G. S. Pawlicki
Los Alamos Scientific Laboratory
Los Alamos, NM

DTIC
ELECTE
MAR 20 1986
S D

No Date Available

NOTICE:

This is an extract of SANDSTONE-29, Operation SANDSTONE, Annex 8,
Parts I, II, III, IV, and V.

DTIC FILE COPY

Approved for public release;
distribution is unlimited.

Extracted version prepared for
Director
DEFENSE NUCLEAR AGENCY
Washington, DC 20305-1000

1 September 1985

23 27 026

UNCLASSIFIED

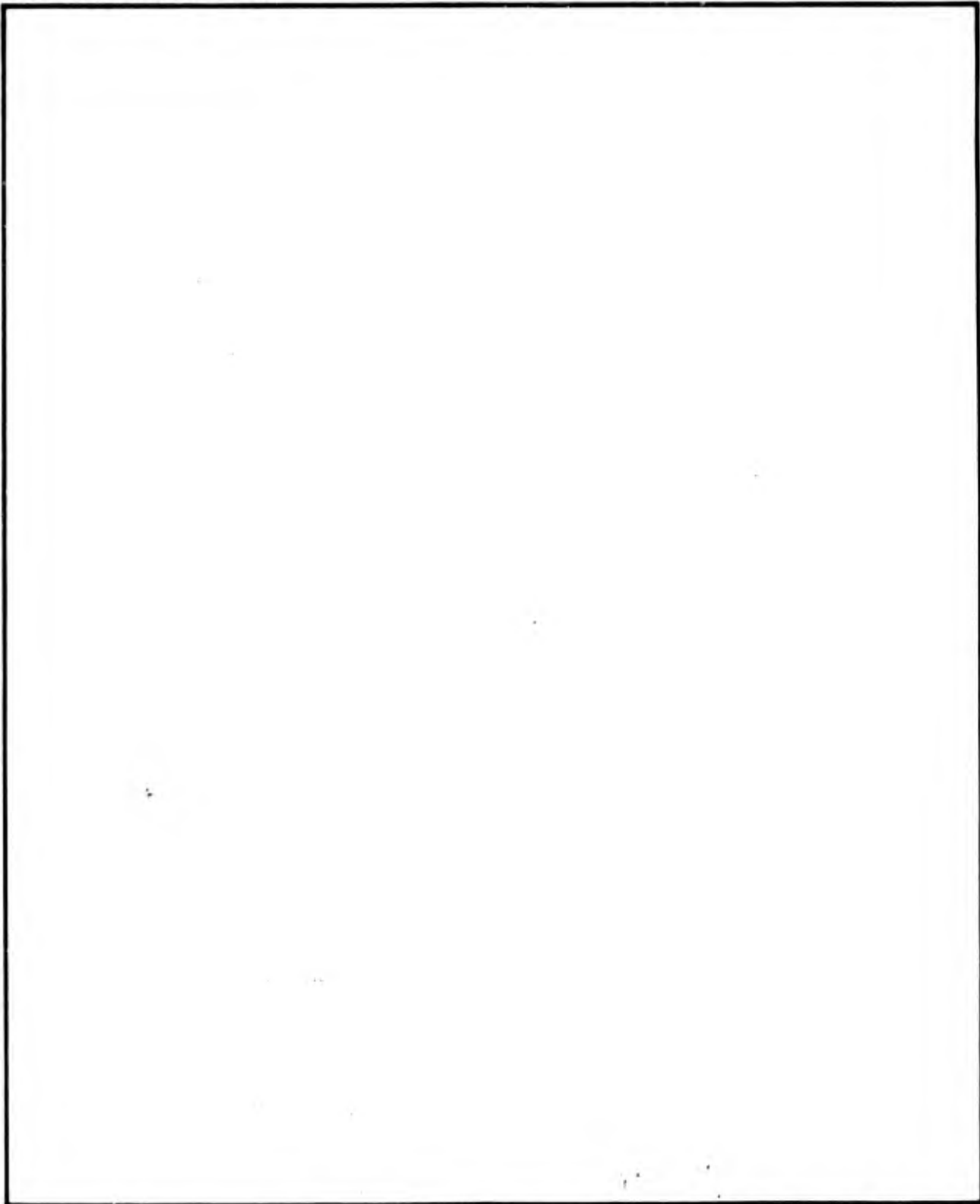
SECURITY CLASSIFICATION OF THIS PAGE

AD-A995396

REPORT DOCUMENTATION PAGE				Form Approved OMB No 0704-0188 Exp. Date Jun 30, 1986		
1a REPORT SECURITY CLASSIFICATION UNCLASSIFIED			1b RESTRICTIVE MARKINGS			
2a SECURITY CLASSIFICATION AUTHORITY N/A since Unclassified			3 DISTRIBUTION / AVAILABILITY OF REPORT Approved for public release; distribution is unlimited.			
2b DECLASSIFICATION / DOWNGRADING SCHEDULE N/A since Unclassified						
4 PERFORMING ORGANIZATION REPORT NUMBER(S)			5 MONITORING ORGANIZATION REPORT NUMBER(S) SANDSTONE-29(EX)			
6a NAME OF PERFORMING ORGANIZATION Los Alamos Scientific Laboratory		6b OFFICE SYMBOL (if applicable)	7a NAME OF MONITORING ORGANIZATION Defense Atomic Support Agency			
6c ADDRESS (City, State, and ZIP Code) Los Alamos, NM			7b ADDRESS (City, State, and ZIP Code) Washington, DC			
8a NAME OF FUNDING / SPONSORING ORGANIZATION		8b OFFICE SYMBOL (if applicable)	9 PROCUREMENT INSTRUMENT IDENTIFICATION NUMBER			
8c ADDRESS (City, State, and ZIP Code)			10 SOURCE OF FUNDING NUMBERS			
			PROGRAM ELEMENT NO	PROJECT NO	TASK NO	WORK UNIT ACCESSION NO
11 TITLE (Include Security Classification) OPERATION SANDSTONE Scientific Director's Report of Atomic Weapon Tests at Eniwetok, 1948 Annex 8—Gamma-Ray Measurements; Parts I, II, III, IV, and V, Extracted Version						
12 PERSONAL AUTHOR(S) Shonka, F.R. and Pawlicki, G.S.						
13a TYPE OF REPORT		13b TIME COVERED FROM _____ TO _____		14 DATE OF REPORT (Year, Month, Day) No Date Available	15 PAGE COUNT 246	
16 SUPPLEMENTARY NOTATION This report has had sensitive military information removed in order to provide an unclassified version for unlimited distribution. The work was performed by the Defense Nuclear Agency in support of the DoD Nuclear Test Personnel Review Program.						
17 COSATI CODES			18 SUBJECT TERMS (Continue on reverse if necessary and identify by block number) SANDSTONE Gamma Radiation Radiation Measurements			
FIELD	GROUP	SUB-GROUP				
18	3					
20	8		19 ABSTRACT (Continue on reverse if necessary and identify by block number) Curves of absorption of gamma rays in boron carbide and a few points on the absorption curve in lead were obtained during the three atomic explosions of Operation Sandstone. Radiation was detected by integrating ionization chambers and by photographic emulsions. A few recording-type ionization chambers were used to give intensities as a function of time. Radiation detectors were located inside of shelters which protected them from blast and shielded them from scattered radiation. Because of geometry, scattered radiation was negligible and the analysis of absorption curves yields the true total absorption coefficient for the radiation.			
20 DISTRIBUTION / AVAILABILITY OF ABSTRACT <input checked="" type="checkbox"/> UNCLASSIFIED/UNLIMITED <input type="checkbox"/> SAME AS RPT <input type="checkbox"/> DTIC USERS			21 ABSTRACT SECURITY CLASSIFICATION UNCLASSIFIED			
22a NAME OF RESPONSIBLE INDIVIDUAL Mark D. Flohr			22b TELEPHONE (Include Area Code) (202) 325-7559		22c OFFICE SYMBOL DNA/ISCM	

DD FORM 1473, 84 MAR

83 APR edition may be used until exhausted
All other editions are obsoleteSECURITY CLASSIFICATION OF THIS PAGE
UNCLASSIFIED



FOREWORD

Classified material has been removed in order to make the information available on an unclassified, open publication basis, to any interested parties. The effort to declassify this report has been accomplished specifically to support the Department of Defense Nuclear Test Personnel Review (NTPR) Program. The objective is to facilitate studies of the low levels of radiation received by some individuals during the atmospheric nuclear test program by making as much information as possible available to all interested parties.

The material which has been deleted is either currently classified as Restricted Data or Formerly Restricted Data under the provisions of the Atomic Energy Act of 1954 (as amended), or is National Security Information, or has been determined to be critical military information which could reveal system or equipment vulnerabilities and is, therefore, not appropriate for open publication.

The Defense Nuclear Agency (DNA) believes that though all classified material has been deleted, the report accurately portrays the contents of the original. DNA also believes that the deleted material is of little or no significance to studies into the amounts, or types, of radiation received by any individuals during the atmospheric nuclear test program.



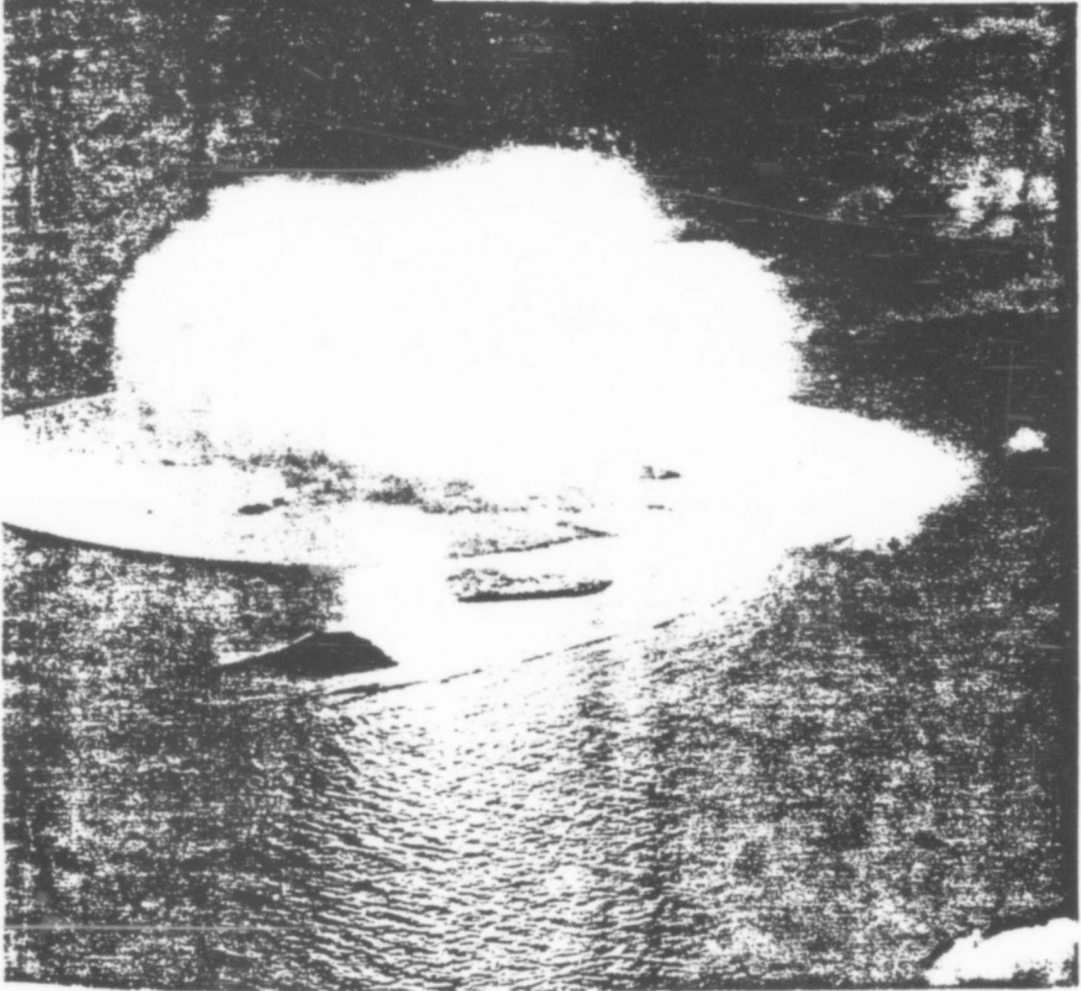
Accession For	
NTIS CRA&I	<input checked="" type="checkbox"/>
DTIC TAB	<input type="checkbox"/>
Unannounced	<input type="checkbox"/>
Justification	
By	
Distribution /	
Availability Codes	
Dist	Avail and/or Special
A-1	

UNANNOUNCED

Sands
RE

29

SCIENTIFIC DIRECTOR'S REPORT OF ATOMIC WEAPON TESTS
ANNEX 8 PARTS I, II, III, IV, AND V
GAMMA-RAY MEASUREMENTS



SCIENTIFIC DIRECTOR'S REPORT
OF ATOMIC WEAPON TESTS
AT ENIWETOK, 1948

Annex 8

GAMMA-RAY MEASUREMENTS

Part I

REPORT OF LAJ-5 ON GAMMA-RAY MEASUREMENT

REPORT OF LAJ-5
ON
GAMMA-RAY MEASUREMENT

Report Written By

F. R. Shonka
G. S. Pawlicki

Group Members

F. R. Shonka
J. E. Rose
G. S. Pawlicki
J. S. Brown
C. Arndt
E. Fudala

Los Alamos Liaison

L. D. P. King

1 September 1948

ACKNOWLEDGMENTS

Mr. J. E. Rose participated in the discussion of these results, although he was unavailable at the writing of this report.

Group LAJ-5 gratefully acknowledges the help and cooperation of D. K. Froman, Scientific Director, and A. C. Graves, Deputy Scientific Director; the valuable consultation with some of the Argonne National Laboratory staff, especially F. C. Hoyt and J. L. Magee; the many valuable discussions with the scientific staff at Sandstone, especially the Los Alamos Theoretical Group; and the assistance of the Property Section and Special Weapons Section in supplying personnel to assist in the experiment.

CONTENTS

ABSTRACT	4
1.1 INTRODUCTION	5
2.1 ABSORBER MATERIAL	6
3.1 SHELTERS	8
4.1 COLLIMATING SYSTEM	10
5.1 IONIZATION CHAMBERS AND THE CHARGE MEASURING SYSTEM	12
6.1 RECORDING ELECTROMETERS	28
7.1 FILM HANDLING AND PROCESSING	30
8.1 OPERATIONAL PROCEDURE	35
9.1 PROCEDURE AROUND ZERO HOUR	38
10.1 CONCLUSIONS FROM TESTS X-RAY, YOKE, AND ZEBRA	39
10.1.1 Conclusions from X-Ray Test	39
10.1.2 Conclusions from Yoke Test	45
10.1.3 Conclusions from Zebra Test	47
11.1 SUGGESTIONS FOR FUTURE EXPERIMENTS	48
APPENDIX A - FILM DATA ON X-RAY, YOKE, AND ZEBRA EXPERIMENTS	51

ABSTRACT

Curves of absorption of gamma rays in boron carbide and a few points on the absorption curve in lead were obtained during the three atomic explosions of Operation Sandstone. Radiation was detected by integrating ionization chambers and by photographic emulsions. A few recording-type ionization chambers were used to give intensities as a function of time.

Radiation detectors were located inside of shelters which protected them from blast and shielded them from scattered radiation. Tubes through the walls of these shelters which faced the zero towers served as collimators. Some of these tubes were aimed at the cabs atop the zero towers and others were directed at several angles of elevation above the cabs.

To get the absorption curve at a given angle of elevation, different thicknesses of absorber were loaded into the collimating tubes at that angle, and the observed intensity of radiation together with the absorber thickness in a given beam defined a point on the absorption curve. Intensity measurements were taken at a position several feet from absorbers in order to minimize the geometry for radiation scattered by the absorber.

Because of geometry, scattered radiation was negligible and the analysis of absorption curves yields the true total absorption coefficient for the radiation.

REPORT OF LAJ-5 ON GAMMA-RAY MEASUREMENT

1.1 INTRODUCTION

Development of new weapons by the Los Alamos Scientific Laboratory had reached a stage early in 1947 where field tests were imperative. Accordingly, a series of three tests was planned for early spring of 1948 and was conducted in April and May of that year under the name Operation Sandstone. The Argonne National Laboratory was requested to assist by supplying personnel to measure gamma-ray absorption curves and gamma-ray intensities as a function of time. These measurements were desired for the following reasons:

1. To determine if there was a high-energy component of gamma radiation;
2. To give a measure of total energy release from the intensity of delayed gamma rays;
3. To measure the air-absorption coefficient for these gamma rays; and
4. To provide data for calculating attenuation by structures and other shields.

In order to avoid a high background of degraded scattered radiation, collimating tubes were installed in shelters built of a special concrete aggregate in which sand and gravel were replaced by iron ore and steel punchings and scrap. Two such shelters were built for the

first test and three for each of the others. Absorption curves were obtained by placing absorbers in the collimator tubes. Thimble ionization chambers and photographic emulsions were used as detectors.

2.1 ABSORBER MATERIAL

Absorbing material, consisting of 83% boron carbide and 17% organic binding material (C_7H_7O) by weight, was molded into 0.750 \pm 0.002-inch-diameter cylinders in lengths of 1.5 inches and 0.75 inch by the Los Alamos Scientific Laboratory. Lead absorbers, used only in the Yoke test, were machined to the same diameter and to specific lengths required. When installed in the collimating tubes, the absorbing cylinders were retained in position by split rings of hard aluminum 0.375 inch long and 0.20 inch wide. These cylinders and rings are shown in Fig. 1.

In the X-ray test, in order to have the same geometry for scattered radiation in all beams, the absorber in each collimator was divided into three parts which were located at the ends and the center of the collimator. In the Yoke and Zebra tests, the collimating tubes with the greatest length of absorber were packed solidly from the incident end, while tubes with lesser absorber lengths had the absorber dispersed in three equal parts throughout the same distance required for the greatest absorber. The precaution of spacing the absorber to maintain the same geometry for the scattered radiation was probably unnecessary since the contribution of scattered radiation was negligible.

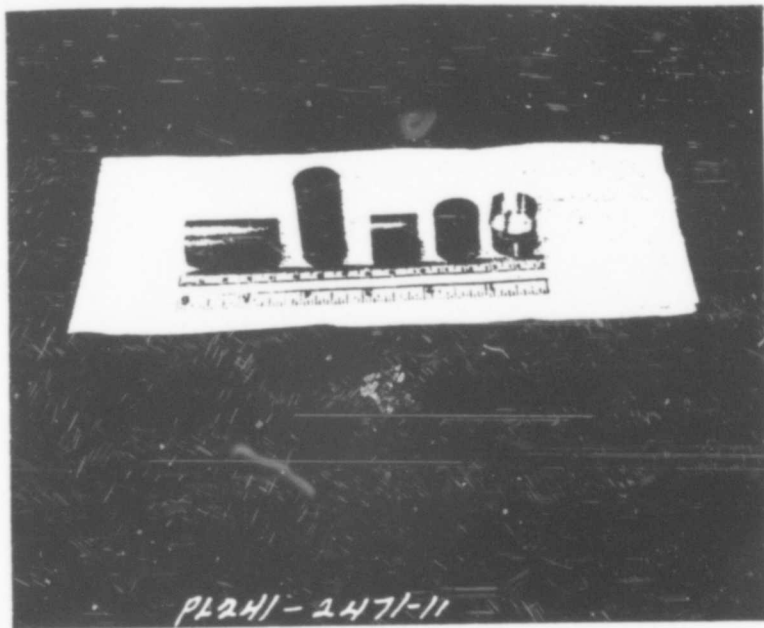


Fig.1 Boron-Carbide Cylinders and Aluminum Retaining Rings
Photographed with a Centimeter Scale

3.1 SHELTERS

The reinforced concrete gamma shelters were of three types and will be referred to as gamma shelters A, B, and C.¹ The walls and ceilings of the shelters consisted of a Portland cement, sand, limonite, iron, and water mixture as used in the Brookhaven shield. The front walls had an opening into which the array of collimating tubes was sealed with the same mix as used for the walls. The shelters were entered through regulation submarine hatches mounted into the rear walls of the A and C shelters and through a double set of standard rectangular hatches in the rear wall of the B shelters. (See Figs. 2 and 3.) The shelter floors were poured of ordinary concrete and were approximately at ground level. Seven holes in the rear walls of the B shelters were provided for lead-in cables from chambers mounted outside of the B shelters.

The inside length of all the shelters, in line of sight with the zero towers, was 7 feet. The other inside dimensions of the A and C shelters were 4 feet each, whereas the B shelters were 7 feet wide and 8 feet high. The thicknesses of the front walls were 4 feet, 3 feet, and 2.5 feet for the A, B, and C shelters, respectively.²

Since the hatches provided insufficient shielding from radiation, additional shielding was added to the back wall. This shielding consisted of 5-gallon-rectangular cans filled with a saturated solution of boric acid in fresh water. These cans were stacked on a roller conveyor

¹"Construction at the Forward Area", R. W. Carlson, J. C. Clark, R. W. Henderson and L. M. Jercinovic, Sandstone No. 39, Parts I and II.

²Ibid.

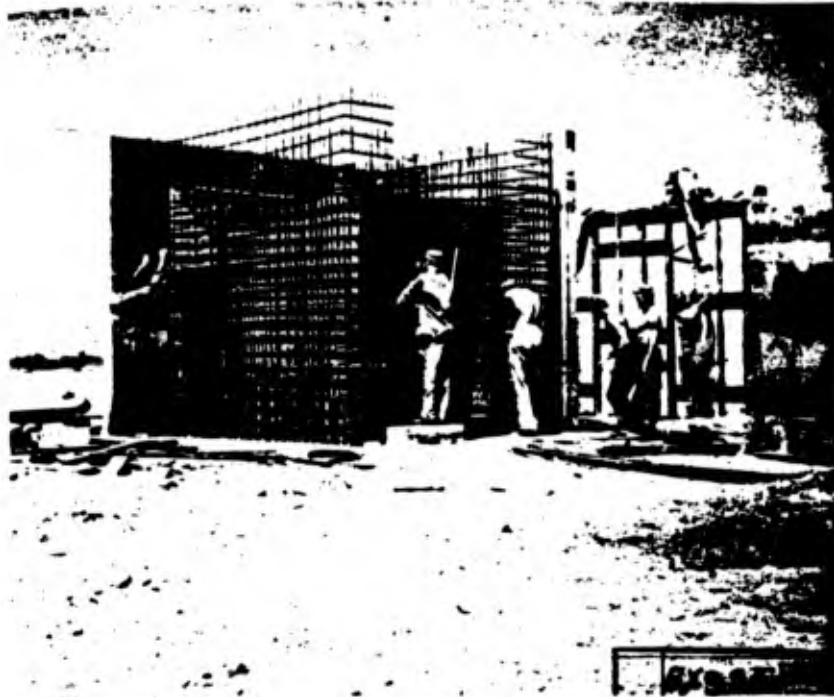


Fig. 2 Construction of Form for Gamma B Shelter, Showing Entrance at Right and Opening for Collimating Tubes at Left

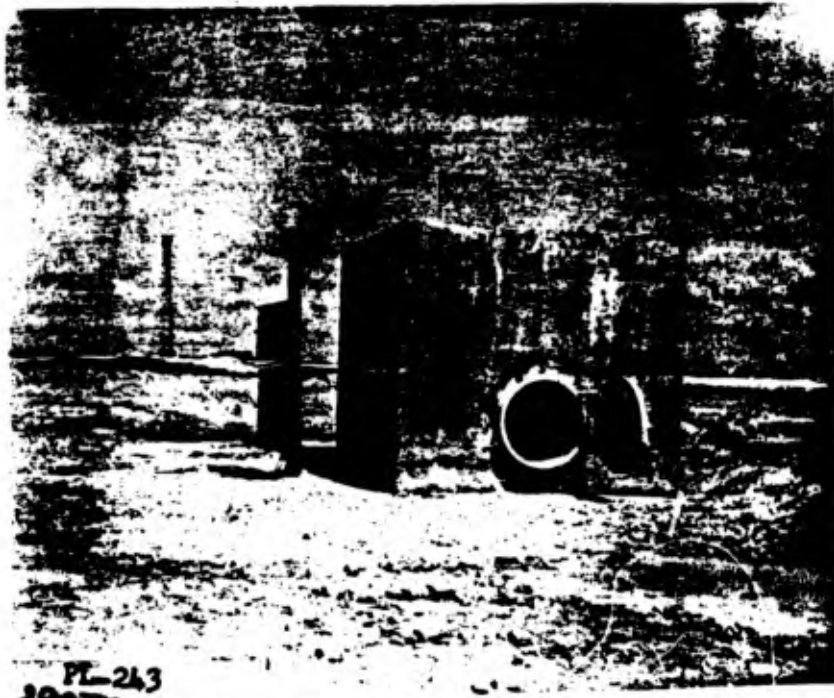


Fig. 3 Completed Gamma A Shelter, Showing Entrance Hatch

platform outside the shelter so that the shields could be moved into position after the hatches were closed. (See Fig. 4.)

The mounting hole for the collimating system and the entrance to a B shelter are shown in Fig. 2. The forward side of a completed B shelter is shown in Fig. 5.

Distances in feet from the zero tower to the various shelters are tabulated below for each experiment.

<u>Shelter</u>	<u>X-Ray</u>	<u>Yoke</u>	<u>Zebra</u>
A	2250	2130	2250
B	3900	3900	3900
C	--	5400	5400

The B shelters were provided with both utility and instrument power, and with timing signals of minus 10 seconds and minus 1 minute.

4.1 COLLIMATING SYSTEM

The collimating system was constructed of precision Shelby steel tubing, 0.754-inch ID, mounted in a welded and annealed angle iron framework with the positioning of the tubes individually adjustable by means of set screws. The collimator tubes were threaded on both ends so that the collars holding aluminum foil dust seals could be attached. The entire array was mounted in the front wall of the shelter and the elevation and azimuth of each collimator were adjusted, after which limonite concrete was packed into the spaces surrounding the exterior of the tubes. Various views of these collimating assemblies are shown in Figs. 5 through

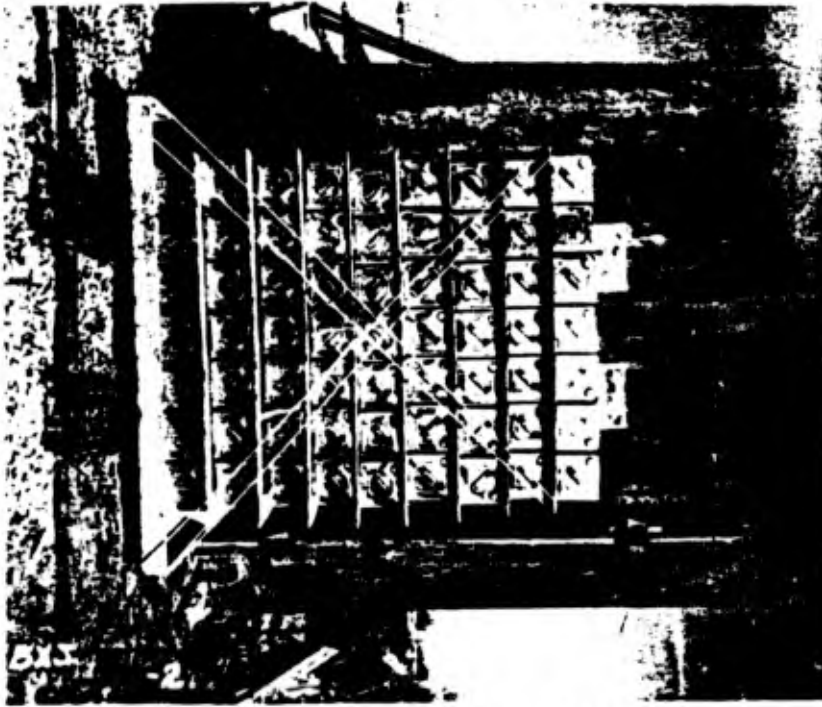


Fig. 4 Back of Gamma B Shelter, Showing Shielding Cans in Position



Fig. 5 Front of Gamma B Shelter, Showing Collimator Tubes

13, inclusive.

Loading of collimator tubes with absorbing material was accomplished by fastening the aluminum dust seal on the inside of the shelter, and pushing absorber slugs in from the outside of the shelter with a rod.

For A shelters the collimating system consisted of seven tubes directed at the zero tower cab and six tubes directed at an angle 10° higher. For the B shelters nine tubes were directed at the zero tower cab, nine tubes each at angles 5° and 15° higher and eight tubes at 30° higher. For the C shelters seven tubes were directed at the zero tower cab and six tubes at an angle 5° higher. The drawings of Figs. 14, 15, and 16 show details of collimator construction for A, B, and C type structures, respectively. The collimators for C-type buildings were the same as for A-type buildings except for the change in angle.

Figures 6, 7, and 8 show front, rear, and side views of the collimator array of an A shelter. Figure 9 shows the array sealed into the A shelter. The front and rear views of the collimator array for a B shelter are shown in Figs. 10 and 11, respectively. Figure 12 shows the collimator array positioned in a B shelter prior to being sealed in with cement. Figure 13 shows the method of loading the absorbing slugs.

5.1 IONIZATION CHAMBERS AND THE CHARGE MEASURING SYSTEM

Integrating ionization chambers were designed to cover the range from 5 to 3000 roentgens. This wide range was obtained by having two sizes of thimble chambers and ten sizes of high insulation condensers varying in value from 100 to 10,000 micro-micro-farads. Thimbles with a

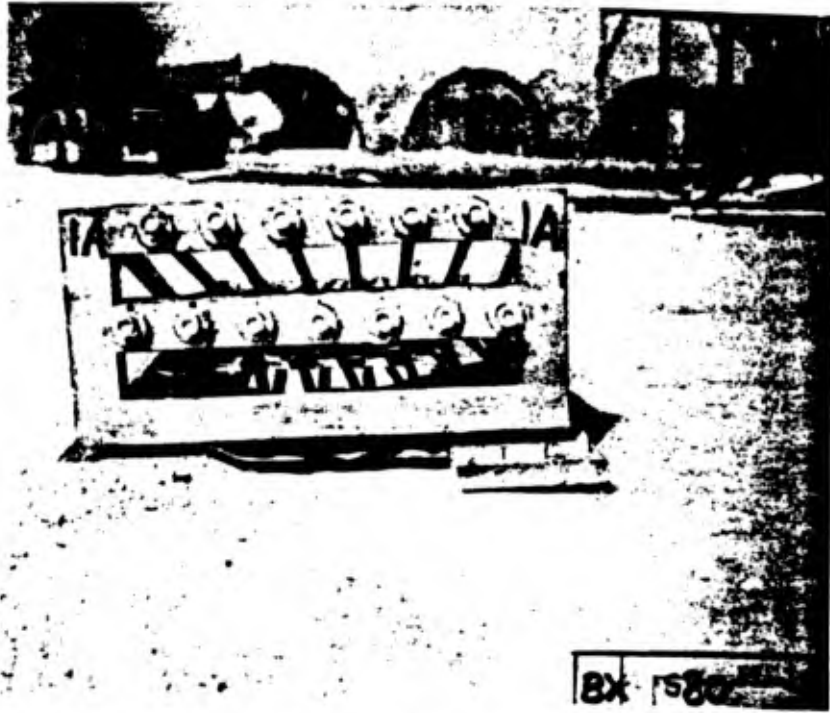


Fig. 6 Front View of Collimator Assembly for Shelter A



Fig. 7 Rear View of Collimator Assembly for Shelter A

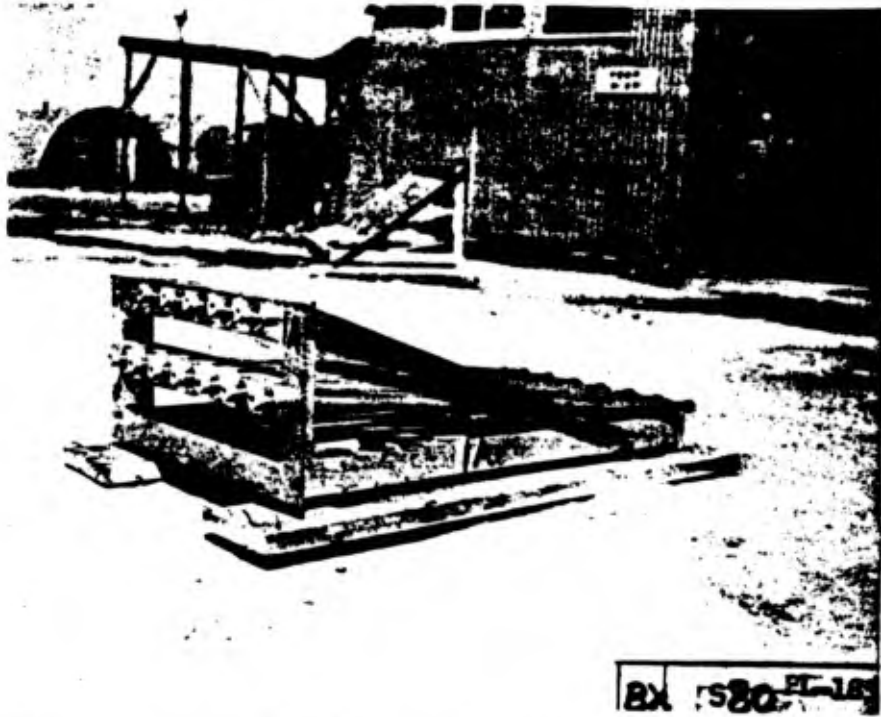


Fig. 8 Side View of Collimator Assembly for Shelter A

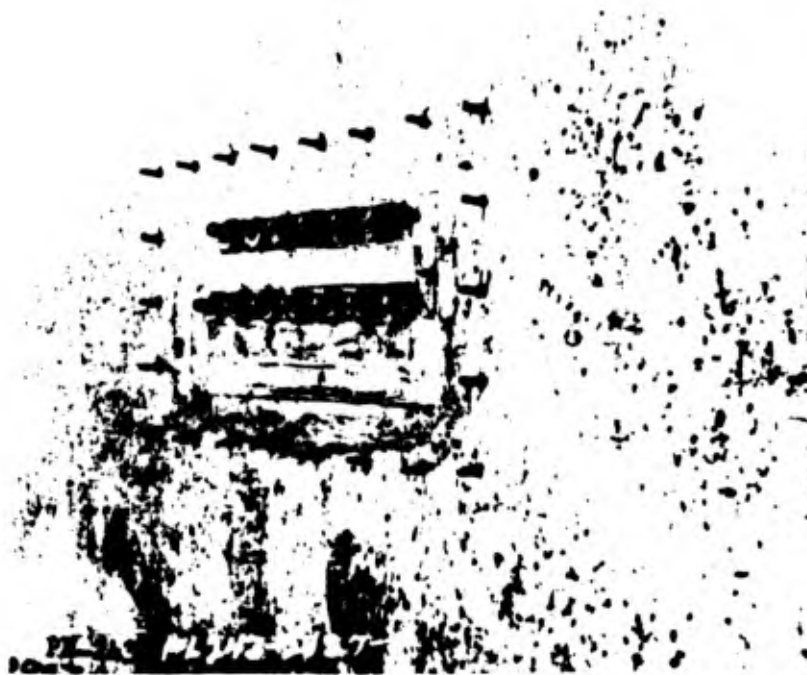


Fig. 9 Collimator for Shelter A Installed

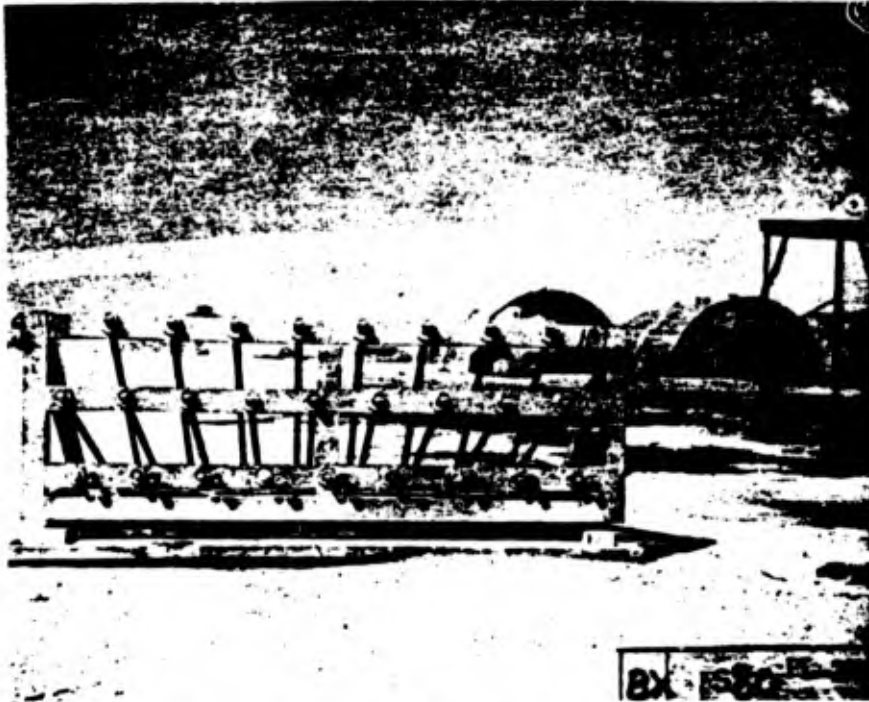


Fig. 10 Front View of Collimator Assembly for B Shelter



Fig. 11 Rear View of Collimator Assembly for B Shelter



Fig. 12 Collimator Assembly in Position in Shelter B

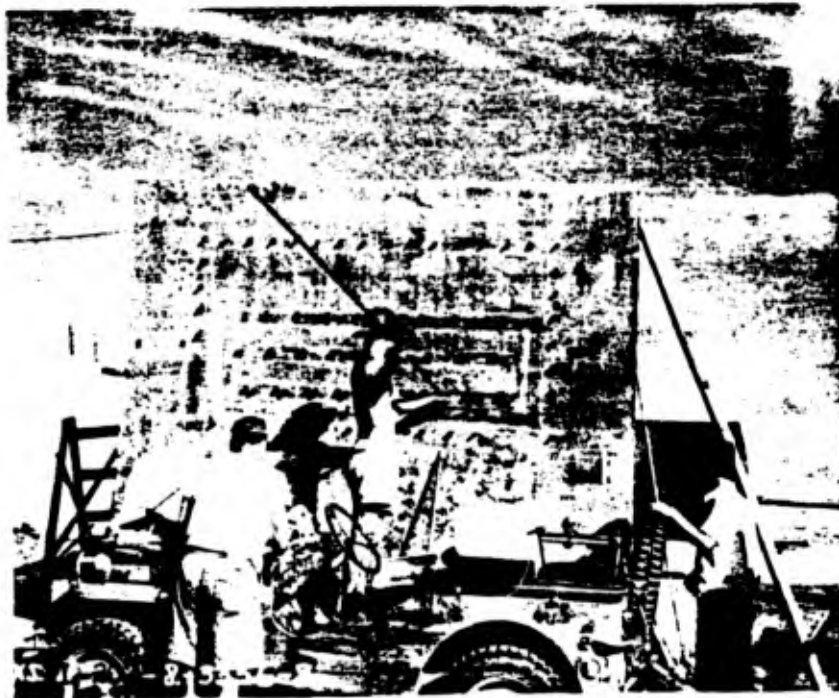


Fig. 13 Loading Absorbers in Collimator of B Shelter

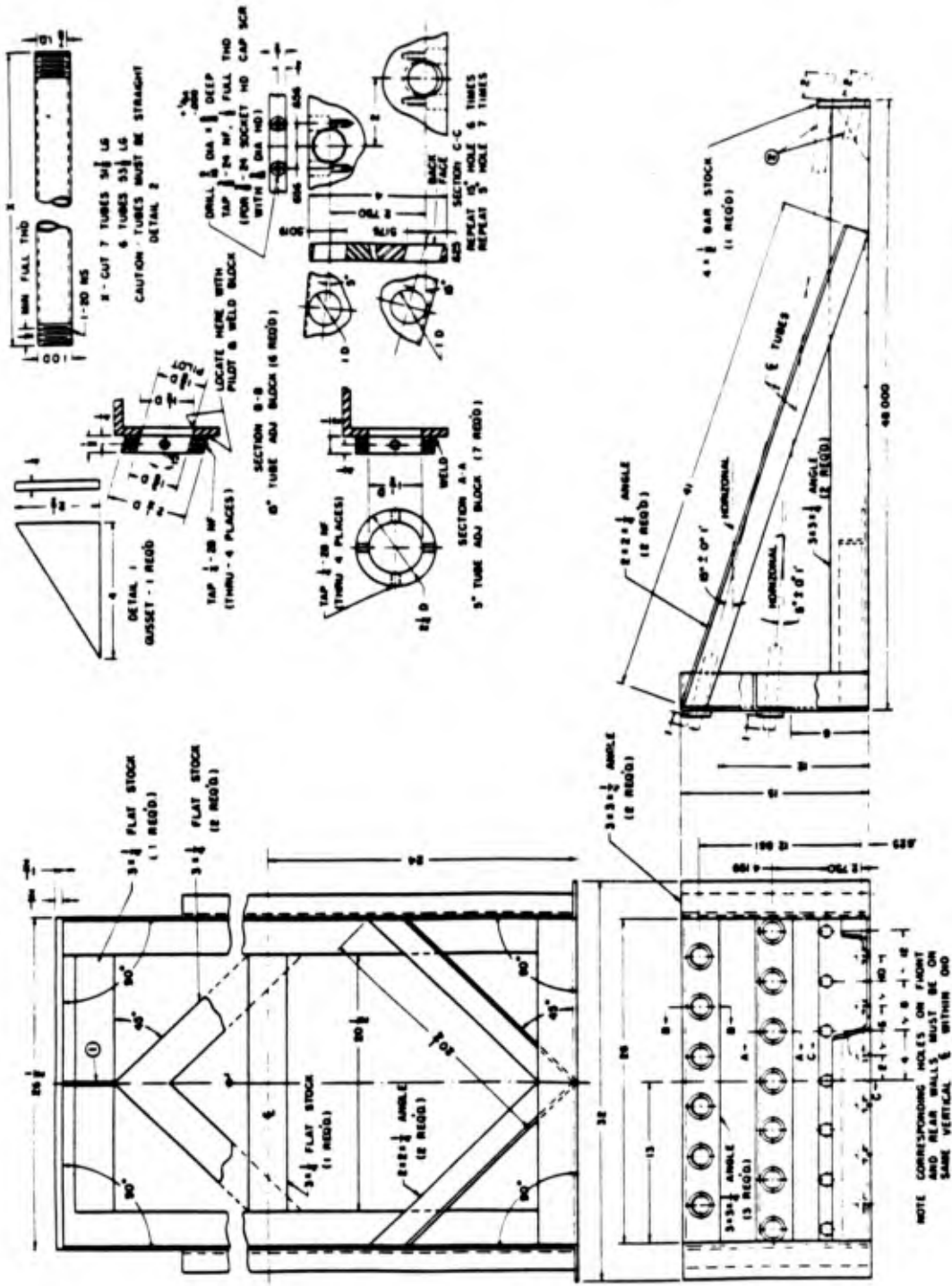


Fig. 14 Design Details for a Collimator for Type A Gamma Buildings

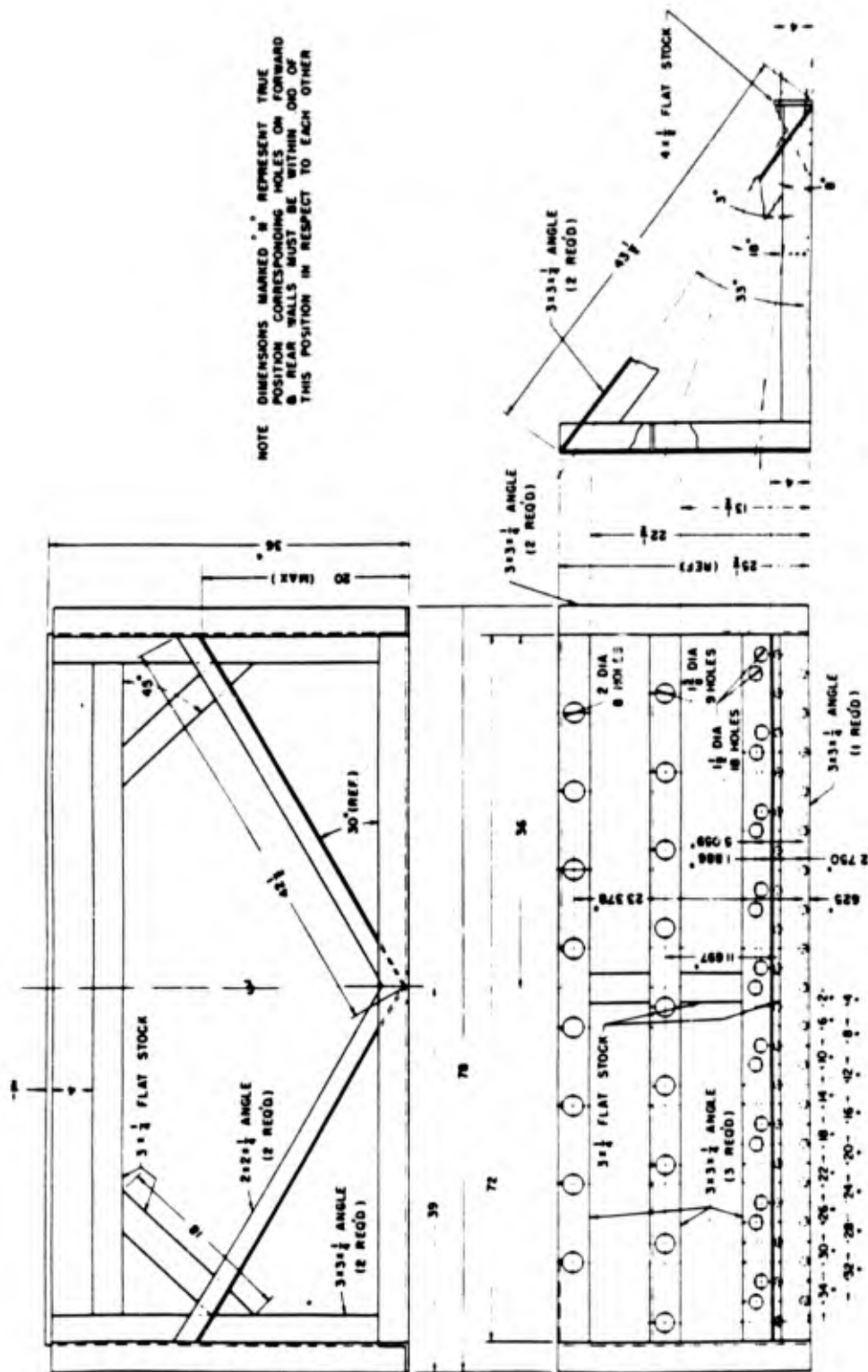


Fig. 15 Design Details for a Collimator for Type B Gamma Buildings

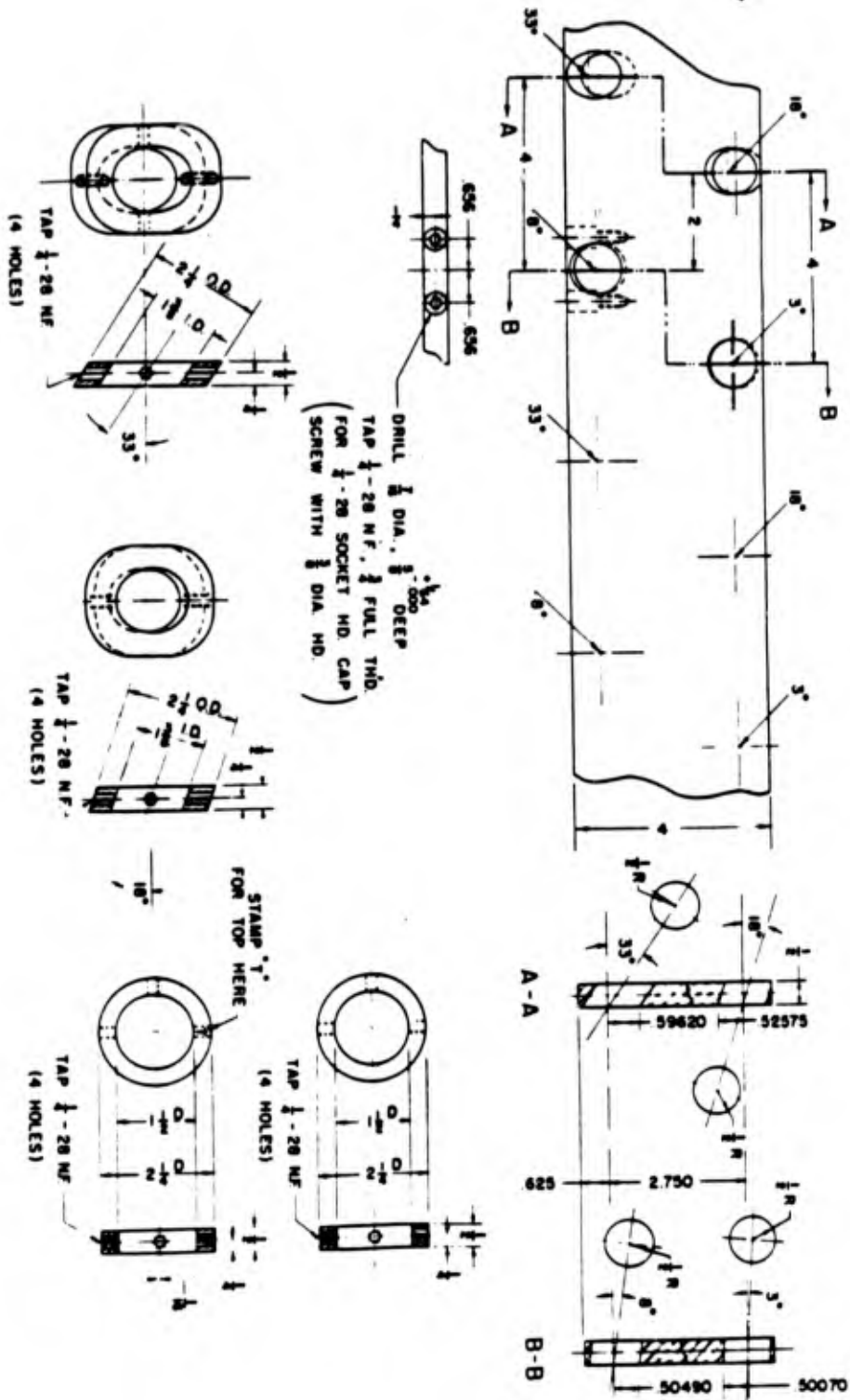


Fig. 16 Design Details for a Collimator for Type C Gamma Buildings

volume of about 1 cubic centimeter were available with either plastic or beryllium walls, while 6-cubic-centimeter chambers were made only of beryllium. The inner surface of the plastic-wall thimbles was grooved with a coarse pitch helical cut filled with conducting paint.

The two sizes of thimbles were threaded into tubular aluminum housings of identical inside dimensions. The condensers were mounted in plastic holders all of which had the same outside dimensions fitting the aluminum housing. Thus, any thimble chamber could readily be assembled with any of the condensers.

The axial lead wire of the polystyrene condenser served as the central electrode of the chamber and was isolated from the entire chamber assembly so that the structure of the condenser determined the leakage of the system. Connection to the center electrode of the ion chamber was accomplished through a radial hole in the side of the aluminum housing and plastic condenser holder. In order to reduce collection of ionization outside of the true chamber volume, the space surrounding the condenser lead wire was made as small as possible. The side hole in the assembly was provided with a plastic plug and a desiccator cap served to exclude moisture and dust from the assembled unit.

Figure 17 shows the parts and method of assembly of the chambers. Figure 18 shows a tray of the integrating chambers with both sizes of thimbles assembled and ready to use.

The equipment for measuring the chamber discharge consisted of a null circuit using a Ryerson-type Lindemann electrometer as the detector.

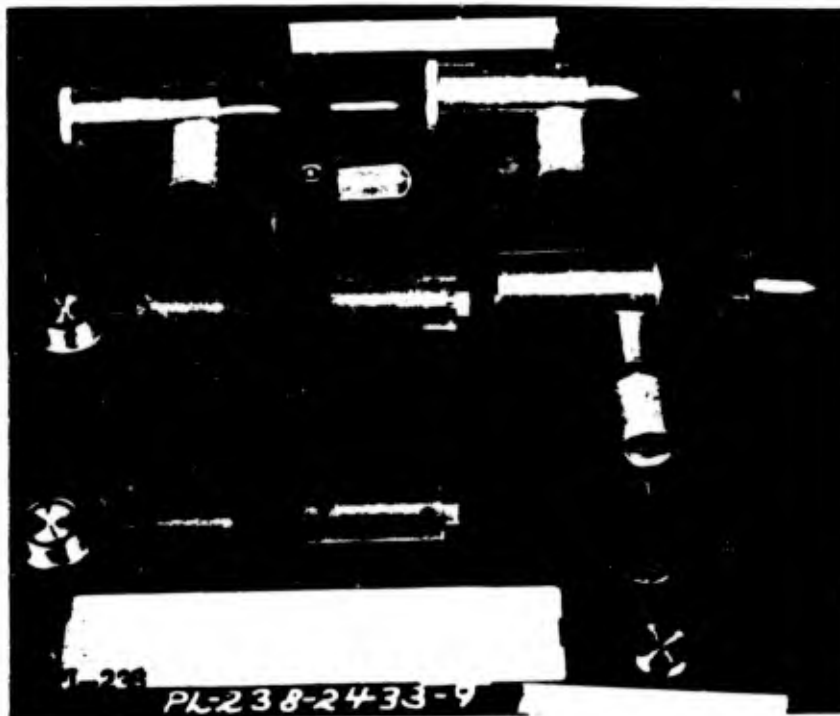


Fig. 17 Thimble Chamber Assembly Shown with Centimeter Scale. Above are Two Sizes of Chamber Assemblies Showing Side Charging Tube with Desiccator Cap in Place. In the Center are Shown the Parts for the Assembly of the Larger Thimble Chamber with Large Condenser. The Parts Below Show How a Smaller Condenser is Fitted into the Same Chamber.

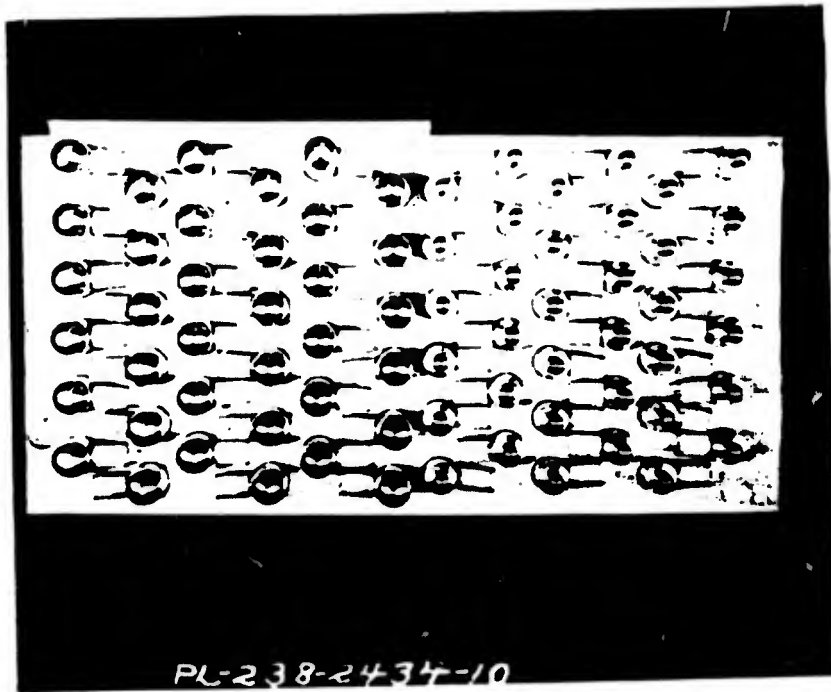


Fig. 18 A Tray Containing Both Sizes of Thimble Chamber Assembled Ready for Use. Scale is Given by Foot Rule Shown Above.

The quadrant circuit for the electrometer was provided with two sensitivities for the sake of convenience in taking readings. The charging voltage for the chambers was adjustable and read with a half-percent voltmeter. Figure 19 shows the complete electrical circuit used and Fig. 20 shows the actual equipment with a 1-cubic-centimeter beryllium chamber attached for measurement.

It should be emphasized that the measuring system which was used measured charge directly and that it was unnecessary to know the electrical capacity of the chamber unit in order to determine charge as is the more usual practice. This is a great advantage when working with a large number of interchangeable condensers, since only their nominal capacity must be known in order to establish in what radiation range a unit should be used.

The chambers were charged to 300 volts and capacities were chosen so that the anticipated dose would reduce the voltage by not more than 100 volts. The condensers were selected from polystyrene condensers manufactured by the Fast Condenser Company so that a leakage of 1 volt or less would be expected over a 24-hour period.

In the X-ray experiment it was found that much smaller radiation was encountered than had been predicted, and it was necessary to provide more ionization chambers for low intensity levels for subsequent experiments. To accomplish this, only the smallest sizes of condensers were used, and a new group of chambers of a radically different design were improvised with available material. These new chambers consisted

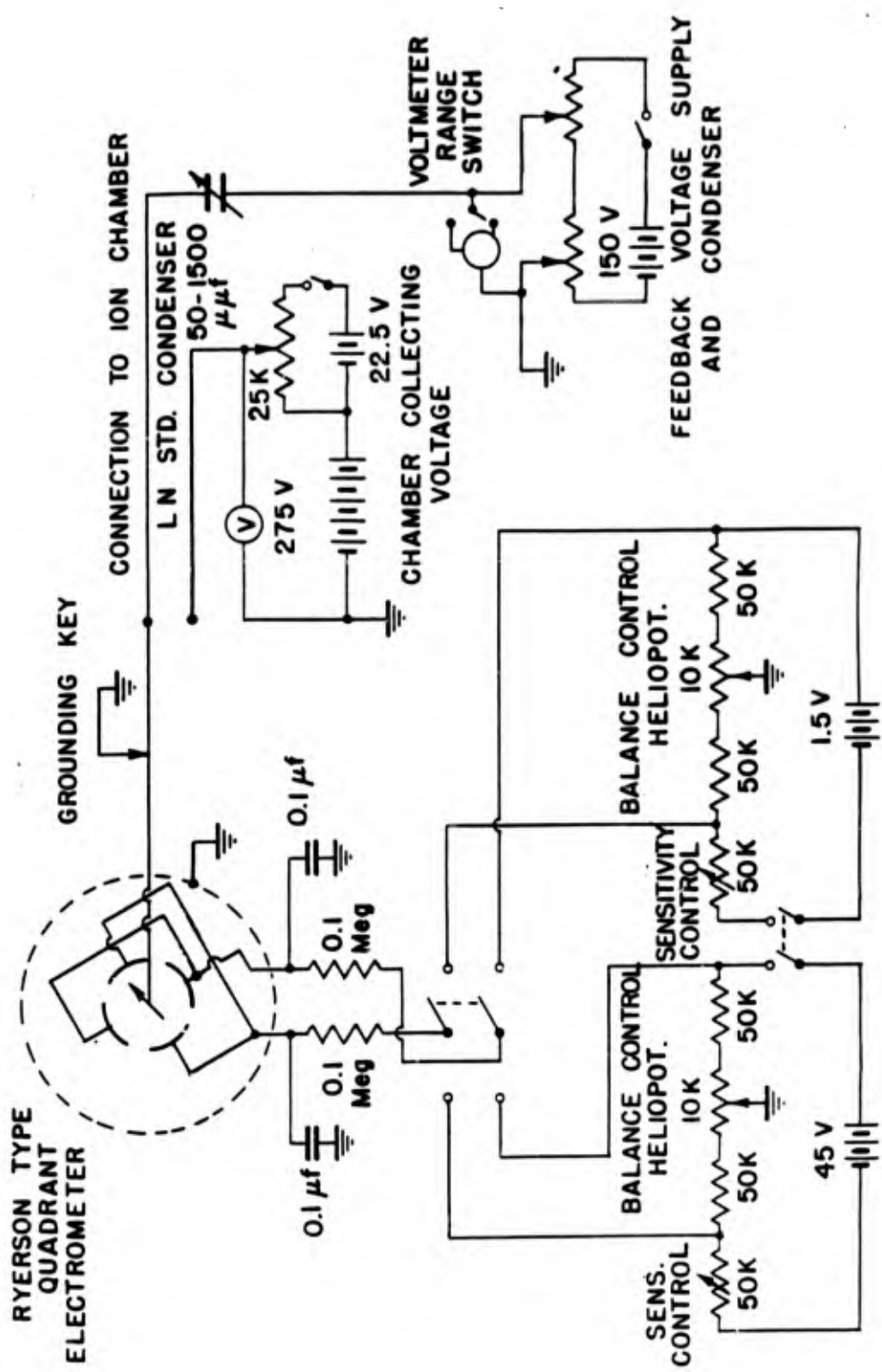


Fig. 19 Circuit for Measuring Chamber Discharge



Fig. 20 Equipment for Charging and Measuring Thimble Chambers

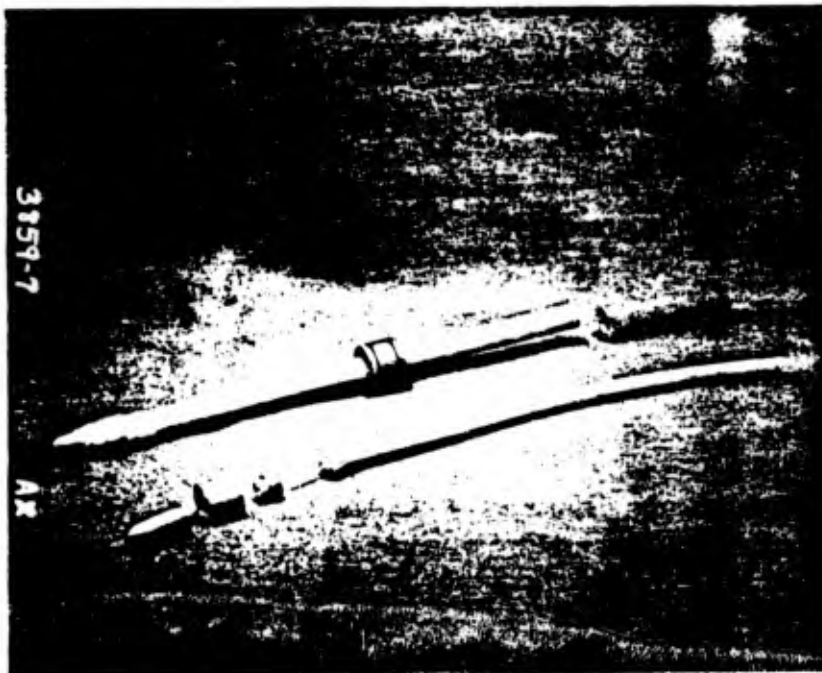


Fig. 21 Exploded View of Polyethylene Dielectric Ion Chamber (AV-5)

of the 1-centimeter beryllium thimbles attached to a 10-inch section of aluminum tubing into which a condenser made of a section of Amphenol RG-9/U cable had been inserted. The center electrode of the chamber was the central strand of the inner conductor of the coaxial cable. Charging and measuring of the condenser were accomplished on the same system used to measure the old design of chamber except for a readily-added adapter so designed that both types of chambers could be measured. The charging and reading of these chambers were done at the end opposite the thimble. This end was then closed with a desiccator cap made of rubber tubing. Due to the difficulty of field construction, it was impossible to minimize the collecting volume at the open end of the tube, but since this end was outside the beam of radiation, the effect was not serious. A photograph of this chamber is shown in Fig. 21.

In the Yoke experiment it was found that the ratio of charge leakage due to insulation and that due to radiation was too unfavorable for reliable results, and it was necessary to construct additional chambers using Amphenol cable. After some experimentation it was decided that the limiting factor on leakage would be the volume resistivity of polyethylene dielectric for lengths of cable greater than about 3 inches. Accordingly, the supply of chambers for the Zebra experiment was made with cable lengths of 3, 6, and 10 inches. Eighty of these chambers were available for the Zebra test.

For the Zebra experiment a half-dozen plastic chambers with heavy walls and thick graphite inner coating were used so that they would be

were nearly in equilibrium with the high-energy radiation indicated by a cursory analysis of the Yoke data. From the Yoke experiment it also became evident that it would be impossible to use the large-size beryllium chambers since they were not completely subtended by the beam. This observation governed the outside dimensions of the newly constructed plastic-walled chambers.

The anomalous shape of the absorption curves obtained in the Yoke experiment was attributed to chamber saturation due to the high momentary intensity of radiation. In an attempt to eliminate this defect the Zebra chambers were provided with center electrodes of 3/16-inch aluminum cylinders which were crimped onto the existing central wire of the chambers.

The chambers were charged in the field some 6 hours before the actual experiment by means of a portable unit consisting of a variable-voltage battery supply which would be read with the same voltmeter used with the measuring device.

All chambers exhibited a slight tendency to improve in their insulation upon being kept fully charged for an extended period of time. Consequently, the chambers were checked for leakage daily and then recharged. This day-by-day record established whether the chambers would be suitable for use in the field. It was noted that this effect of soaking-up charge was more prominent in the polystyrene condensers than in the polyethylene condensers, though the study was not complete.

When bringing the chambers into contact with the measuring system,

a slight motion of the electrometer needle resulted from the changing capacity. In order to correct for this effect the chambers were plugged in an identical manner so that the measurements of leakage also corrected for the change in capacity. The subterfuge of making the effect reproducible was an expediency which should not be resorted to in future work when time permits an improved, low-capacity contacting system from the chamber to the measuring device.

6.1 RECORDING ELECTROMETERS

In order to obtain a time record of some of the chambers, a fast-recording electrometer was developed and three complete units constructed.

The electrometer unit was similar to a Wulff single-fibre electrometer. However, instead of aiming at high sensitivity, which the Wulff electrometer attains due to nearly zero tension in the fibre, the fibre of this electrometer consisted of a 4-centimeter length of a 7-1/2 μ gold-plated tungsten fibre under approximately 500-dynes tension. The tension was adjusted so that the natural frequency of the fibre was of the order of 300 cps. The fibre was suspended through high insulation between two wedge-shaped deflecting plates which were about 3 centimeters in length. With the plates spaced about 3 millimeters apart and with approximate deflecting voltages of plus and minus 180 volts, the full scale sensitivity of the electrometer was of the order of 75 volts and had an inherent capacity of about 2.5 centimeters. Figure 22 shows an assembled electrometer and one with cover plate removed.

This electrometer then replaced the current galvanometer in the

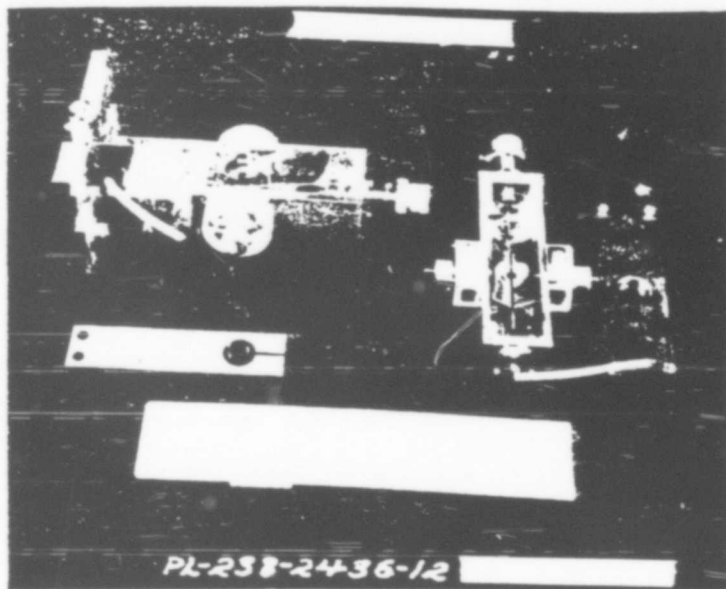


Fig. 22 Assembled Electrometer at Left and Electrometer with Cover Plate Removed at the Right. Dimensions are Indicated by Inch Scale Below.

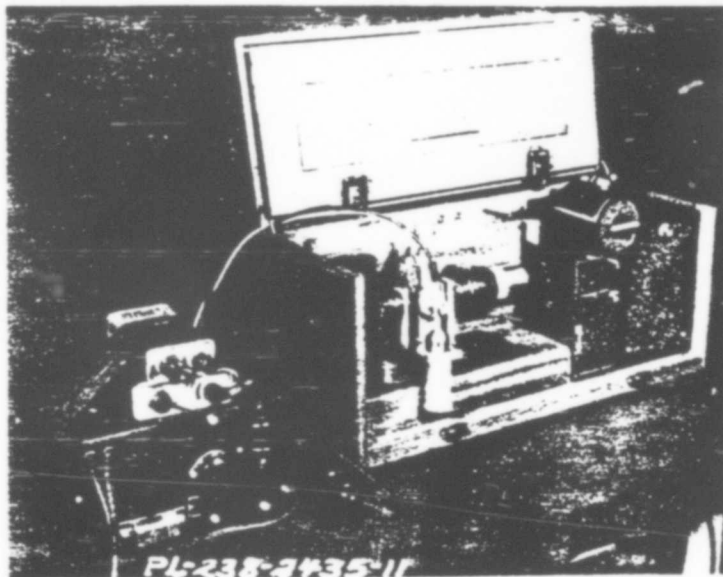


Fig. 23 Recording Electrometer with Portable Power Converter

standard electrocardiograph of the Cambridge Instrument Company. The entire illuminating system, the optical-projecting system, and the moving sensitive-paper system of the electrocardiograph were left unmodified except that the paper speed was nearly doubled on one of the instruments.

Since the time record of the electrocardiograph depends on the speed of a synchronous motor in the instrument, the frequency of the a-c power supply must be known. For this reason a battery-powered vibrator supply was used, the reed of which was resonant at 60 cps. Another reason for the battery supplies was that instrument power at shelter B could not be relied upon after zero time.

A sequence relay initiated by the minus-1-minute timing signal started the recorders at minus 15 seconds. The power supplies were operated for 15 minutes after zero time, after which the sequence relay disconnected the batteries from the converters.

Figure 23 shows the complete recording electrometer with its portable power converter.

7.1 FILM HANDLING AND PROCESSING

Eight photosensitive emulsions were available for use in the experiment. Seven of the emulsions were packaged in standard dental packets as follows: one packet contained DuPont emulsions 552S and 552I which were known as the A and B emulsions; the second packet contained Eastman emulsions 5301, 5302, and translite which were referred to as C, D, and E, respectively; and the third packet contained

Eastman emulsions 548S and 548I which were called emulsions F and G. The emulsions in their alphabetical order represent decreasing sensitivity to gamma radiation with an overlap except for emulsions E and F which do not measure any common range. Except for this lack of overlap which is in the vicinity of 400-800 roentgens, these seven emulsions will cover the range from 0.1 roentgen to 6400 roentgens. The eighth emulsion was Eastman NTB which was available as 34-millimeter roll film. This film was cut and put up in light-tight packets, the same size as dental packets.

The emulsions C, D, and E were calibrated for x-rays and gamma rays to 0.8 Mev with 1-millimeter lead and cadmium filters to determine filters which would minimize the energy dependence of the emulsions. The results are shown in Table 24. From the results of this experiment and previous experience it was decided that 0.046-inch cadmium and 0.081-inch tin filters as well as the emulsion with no filter be used.

The cadmium and tin filters consisted of $\frac{1}{2}$ -inch-wide strips which were folded around the film packet and separated $\frac{1}{2}$ inch from each other. The packet was then placed into a pill box stamped out of 0.022-inch sheet aluminum. Figure 24 shows the film packet with filters and the pill box alongside a scale.

The X-ray experiment showed that the region exposed under the metal filters was smaller than desired because the beam of radiation had a diameter of approximately 0.75 inch. Accordingly, the filters were placed side by side and the ends cut at an angle so that the filters

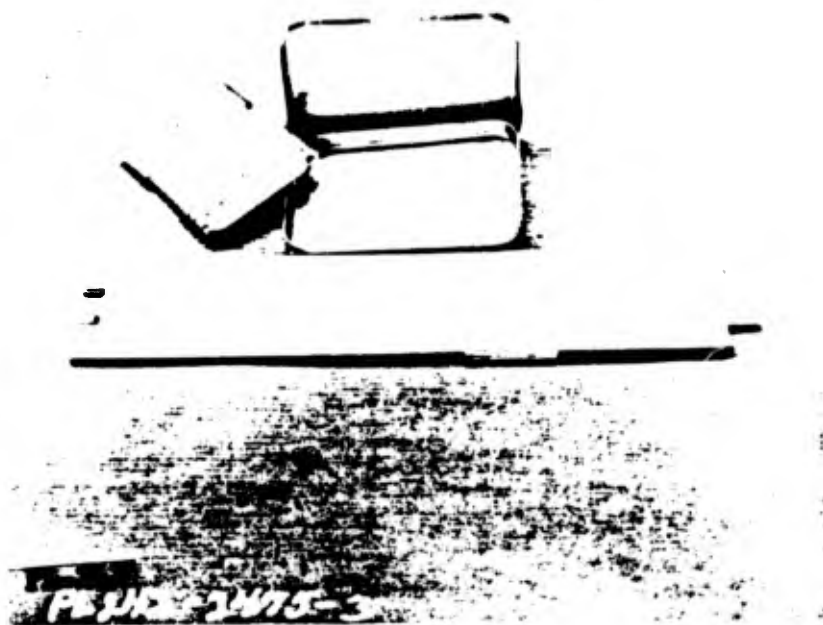


Fig. 24 Film Packet and Pill Box Container. Dimensions are Indicated by Centimeter Scale Below.

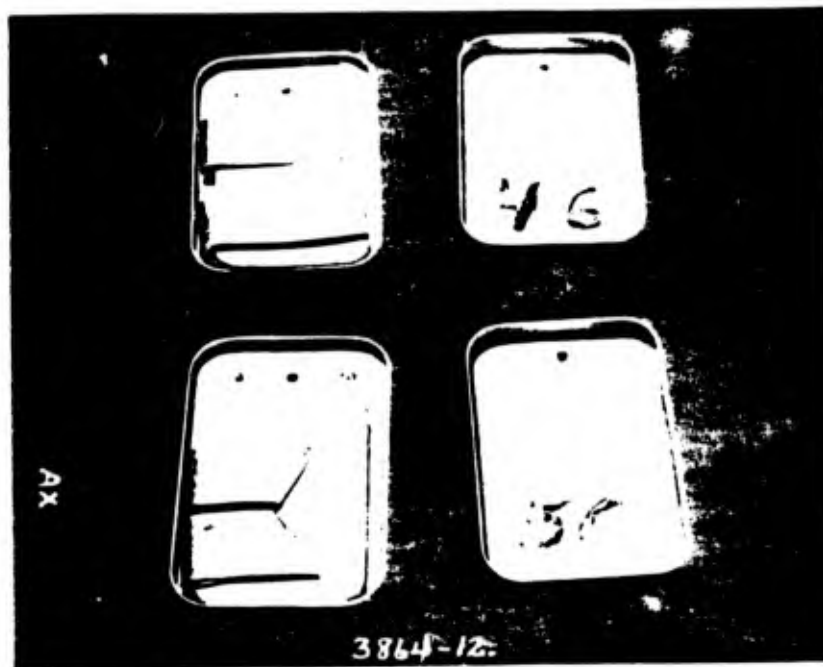


Fig. 25 Lead and Tin Filters Installed on Film Packets. Upper Picture - X-Ray Arrangement; Lower Picture - Later Arrangement.

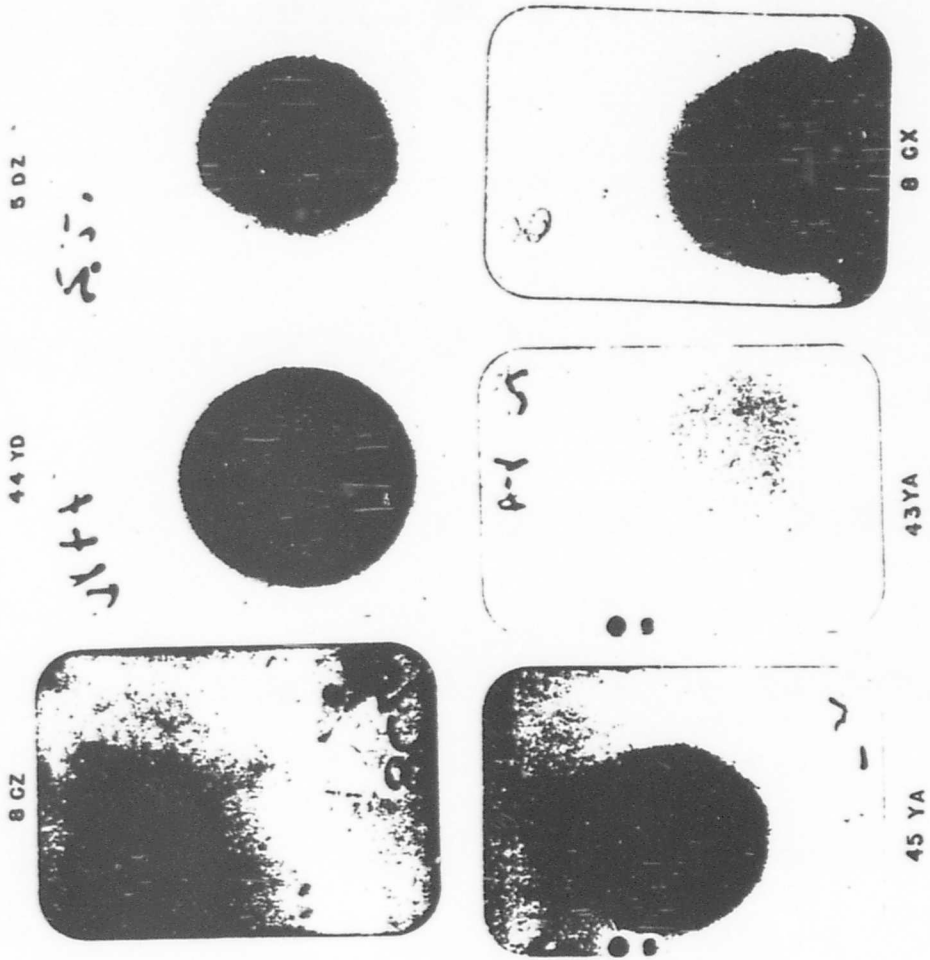


Fig. 26 Films Exposed Under Varying Experimental Conditions

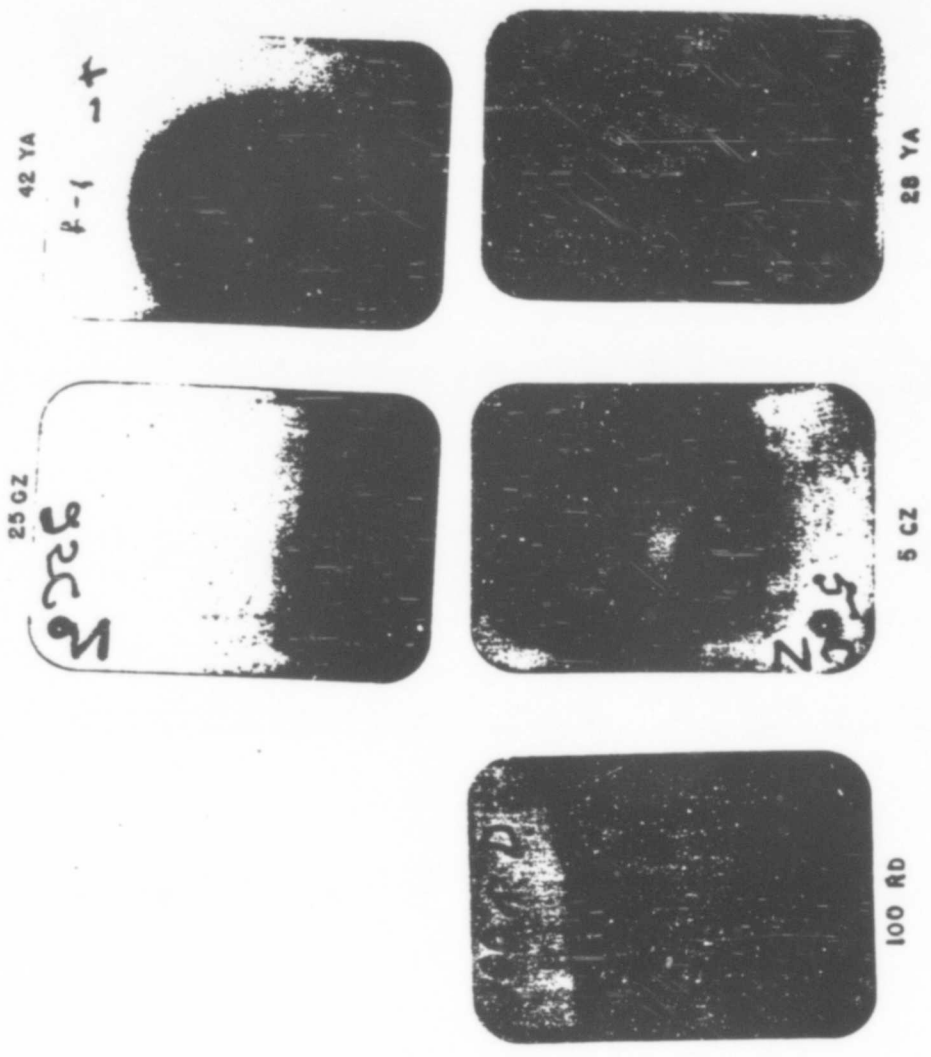


Fig. 27 Films Exposed Under Varying Experimental Conditions

each subtended a 120° sector of the beam. These filters are shown in Fig. 25.

The film was developed with standard DuPont X-ray developer at 65° F for 5 minutes and fixed with DuPont fixing solution for 10 minutes, after which the film was washed for 20 minutes with the final wash in distilled water. The films were then air-dried without wiping. All solutions used were made up with distilled water to eliminate the effects due to a possible variable composition of the ship's water supply.

The films were densitometered in the regions exposed to the direct beam with no filter, with cadmium filter and with tin filter. Similarly, three regions were measured immediately outside the direct beam. To insure stability of the densitometer from line voltage variations, the line voltage was stabilized with a Sorensen regulator.

A complete set of films exposed to a radium standard was included with each batch of film developed so that differences in developing technique would not affect the results. A set of blank emulsions was also mounted in each rack so that if any stray light had caused fogging of the film in the darkroom, it would be known. Typical films are shown in Figs. 26 and 27. Experimental conditions for these films are given in Table 1. (See Appendix A.)

8.1 OPERATIONAL PROCEDURE

Three weeks prior to the arrival of the Task Force at the Atoll, a representative of the Group arrived to assist in the installation,

alignment, and sealing of the collimating system in the shelters.

During the trip to Eniwetok aboard the USS Albemarle, the remainder of the Group set up equipment in the shop and began to take daily readings of chamber leakages.

Upon arrival at the Atoll, installations in the gamma shelters were begun. Wood strips 1 inch by 2 inches for mounting of chambers and films were installed across the inside of the shelters. These strips were just outside the direct beam. Strips for chamber mounting were placed 4 feet from the collimators and film mounting strips were 5- $\frac{1}{2}$ feet behind the collimators. Conduit hangers were used for mounting chambers to the wood strips. This arrangement allowed sufficient adjustment to align the chambers accurately in the beam, which was done by bore-sighting the chamber thimbles through the collimating tubes. By a similar sighting procedure, the position of the film pill boxes was accurately marked on the wood strips.

All shelters were provided with radiation traps shown in Fig. 28 to minimize scattering of the most intense beams from the back wall of the shelter. These traps consisted of a cellular structure of lead bricks.

A timing relay panel and sequence relay were installed in the B shelters. Shield cans filled with boric acid were stacked on platforms supported on roller conveyors at all shelters, as shown in Fig. 4. These preparations were completed several days prior to the experiment.

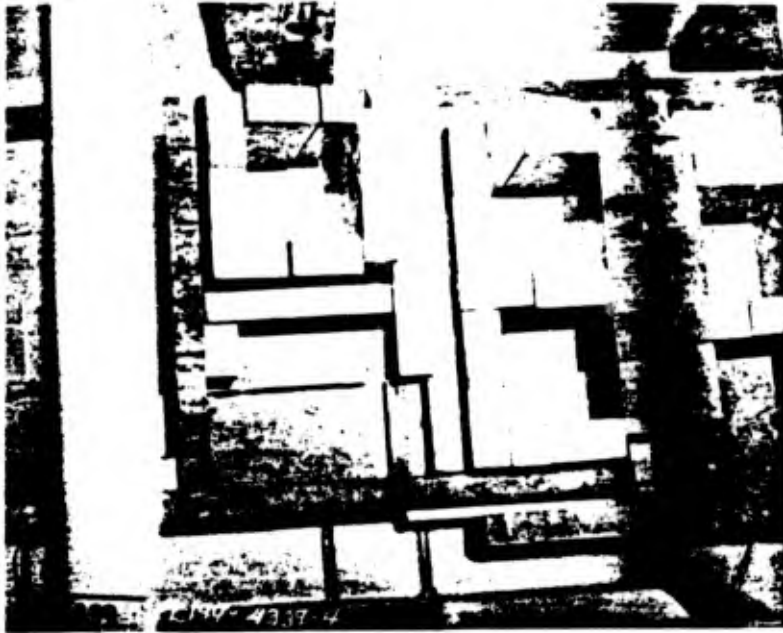


Fig. 28 Radiation Traps Designed to Minimize Scattered Radiation

9.1 PROCEDURE AROUND ZERO HOUR

At minus two days the chambers and recording electrometers were installed. A sealed vinylite tent was built around the assembly. This tent contained 20 pounds of silica gel drier which reduced the relative humidity in the tent from 97% to approximately 30%. After the chambers had been installed, absorber slugs were loaded in the collimating tubes. The chambers were charged at approximately 8-hour intervals and were given their final charge at minus 5 hours. On minus one day, film packets were installed in the positions previously marked. Tools, portable lights, and shielded containers to be used at the time of recovery were left in all shelters. The location of all chambers and films and the amount of absorber in each collimator were recorded in a field data book. After leaving the shelter for the last time, hatches were secured and the shield cans rolled into position against the back walls of the shelters.

Re-entry was made with LCVF boats landing at the end of the island farthest from the zero tower at approximately plus 1- $\frac{1}{2}$ hours. The recovery group for each of the shelters, consisting of a member of the experimental party and a radiological safety monitor, proceeded to the shelters in jeeps which had been left on the island. In addition to regular clothing, assault masks and gloves were worn by all personnel. Upon reaching the shelters, the shield cans were pulled away from the shelter with the jeeps. While gathering the chambers, films, and electrometer chart paper and placing them in carrying cases, gloves

were removed to reduce the possibility of spreading contamination to this equipment. The group reassembled at the LCVP which transferred them to an AVR and returned to the ship.

Upon return to the ship, film was removed from the pill boxes and stored in a refrigerator. At the same time, chambers were read and recharged. Since the elapsed time from charging the chambers until their measurement had been 9 hours, the chambers were read again after a 9-hour period to determine their leakage. The films and electrometer record paper were developed as soon as convenient. After the films had been thoroughly dried, they were densitometered. The procedure followed in all experiments conformed essentially to that outlined above.

10.1 CONCLUSIONS FROM TESTS X-RAY, YOKE, AND ZEBRA

10.1.1 Conclusions from X-Ray Test

As a result of the X-ray experiment, the following results were immediately observable:

1. The intensity was probably one to two orders of magnitude less than had been expected when the chamber design and the amount of absorber had been established prior to the test.
2. From the recording electrometer record, it was seen that the time of exposure was extremely short. In fact, from the amount of overshoot on the record, the recording electrometer could not distinguish between the pulse of radiation it had received and an artificial square voltage pulse applied to it.

3. The size of the beam of radiation from the zero-angle collimators as recorded on the film was only about 0.75 inch in diameter while about a 2.5-inch spot would be expected for an extended source viewed through the zero-angle collimators.

4. For upper-angle collimators there was no blackening on the film detectable above the background darkening caused by scattering from zero-angle beams.

5. The films showed intensification under both cadmium and tin filters, while the standard exposures to x-rays and gamma rays show considerable decrease of blackening under cadmium and tin filters.

Concerning the first observation, the anticipated tonnage for the X-ray experiment was expected to give an intensity from 600 to 1200 roentgens outside of B shelter, on the basis of film measurements made at previous tests. From the scattering coefficients of air the chamber design was established for an anticipated maximum dosage inside the B shelter of about 50 to 300 roentgens, whereas the actual observation in the B shelter was only about 10 roentgens.

No radiation intensity could be noted above the natural leakage of the chambers, though their performance came up to design expectations.

Concerning observations 2 and 3, the small spot on the film showed that the source of radiation was much more nearly a point source than an extended source. This would indicate that a high intensity of radiation is observed in a very short interval of time, whereas it had

been anticipated that very little of the original radiation would penetrate the tamper. The recording electrometer record confirms the fact that a large amount of radiation comes out in a very short interval of time. Due to the relative slowness of the electrometer all that can be said is that the time interval is less than a few milliseconds. This estimate of time is based on a comparison of the experimental chart with that of applied square-wave voltages.

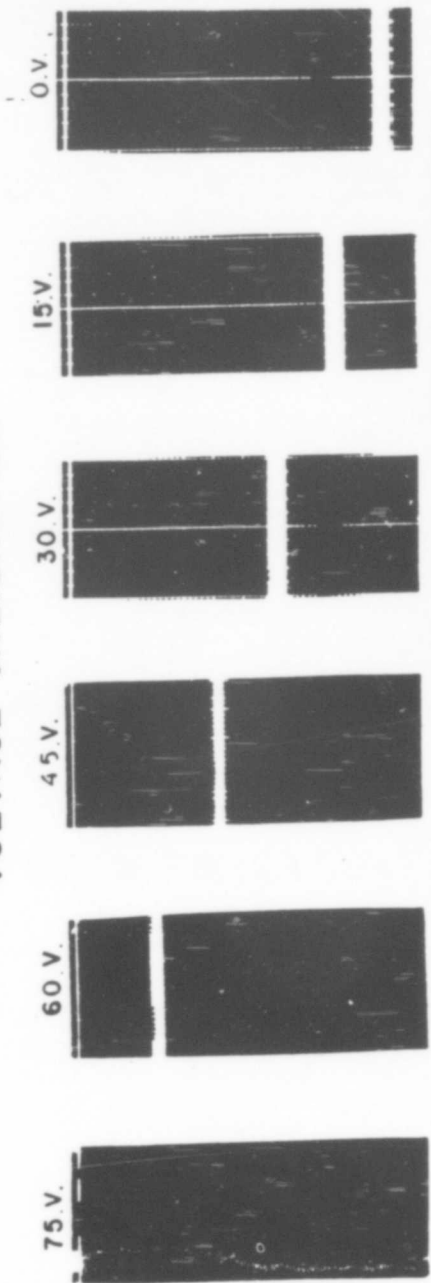
A great deal of interest centered around the size of the spots on the films and the relation of the size of the spot to the size and nature of the source is being investigated by several members of the Los Alamos Theoretical Group. The conclusions from a study of the radial variation of density of the spots on the films will be announced in their report.

Film No. 8CX in Fig. 26 shows the size of the spot in shelter B with 3 inches of boron-carbide absorber. The electrometer records appear identical to those of Figs. 29, 30, and 31.

From the fourth observation it was decided that no accurate absorption curves from the upper angles would be possible. For the Yoke test, films were placed directly over the ends of a few of the upper-angle collimators to determine if there was some radiation coming down these collimators.

Concerning the fifth observation, the cause of the ^{irradiations} identification under the cadmium and tin filters had no unique explanation. Gamma rays with energy greater than 0.8 Mev, fast neutrons, or some

VOLTAGE CALIBRATION



EXPERIMENTAL RECORD SENSITIVITY 0.55 r PER SMALL DIVISION

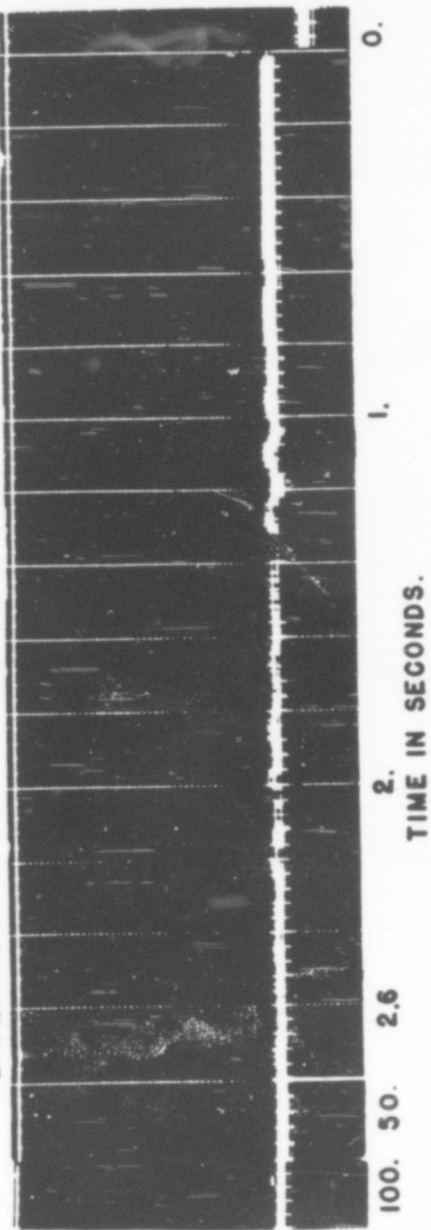
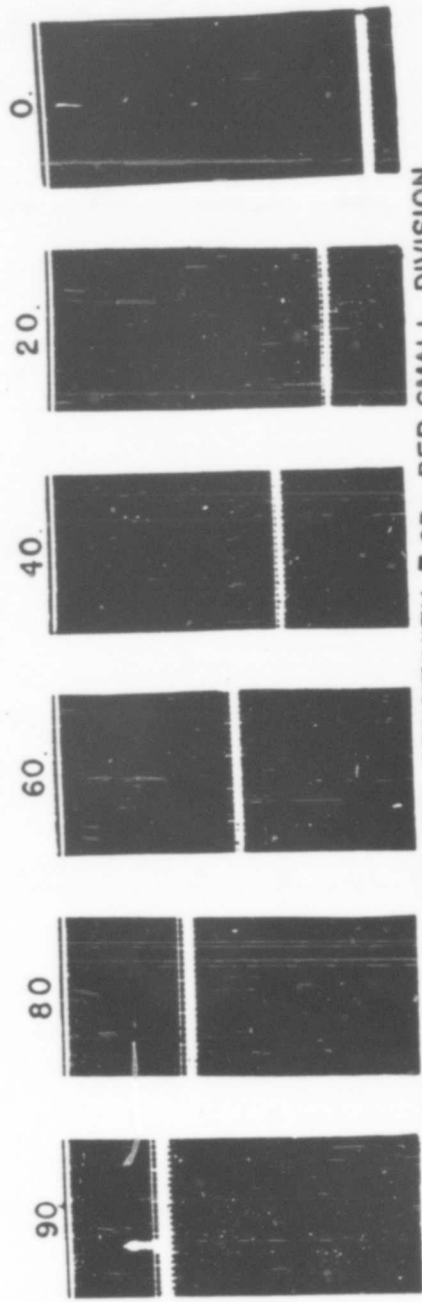


Fig. 29 Zebra Experiment. Beryllium Chamber Located in Beam 5 Inside "B" Shelter. No Absorber.

VOLTAGE CALIBRATION.



EXPERIMENTAL RECORD SENSITIVITY 7.63r PER SMALL DIVISION.

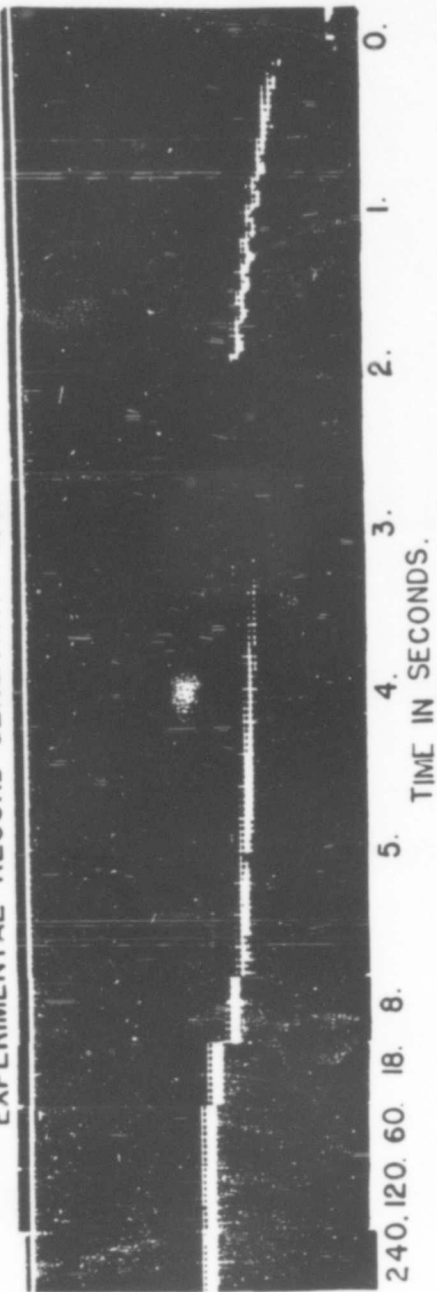


Fig. 30 Zebra Experiment. Beryllium Chamber Outside "B" Shelter.

VOLTAGE CALIBRATION

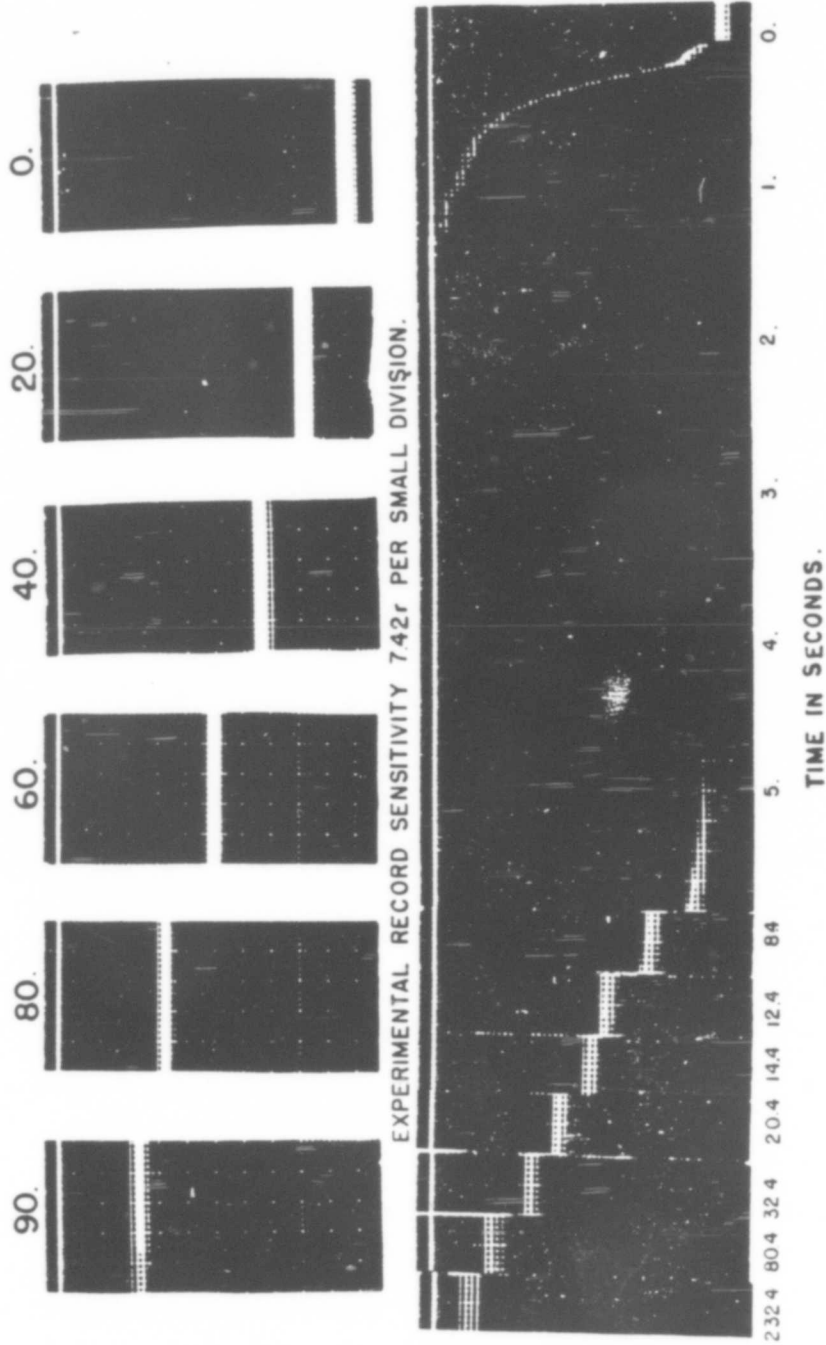


Fig. 31 Zebra Experiment. Plastic Chamber Outside "B" Shelter.

unknown radiation could be considered. As a result of many discussions, three modifications for the Yoke experiment were planned: (1) to settle the problem of slow neutrons or resonant absorption, it was decided to place a 1.5-millimeter cadmium foil at the inner end of the collimating tubes where the geometry for scattering would be less than 1/1000 of what it was with the cadmium in contact with the film; (2) to determine fast-neutron effects, it was decided to take a difference spectrum using two different materials as absorbers, and for this arrangement the Los Alamos Theoretical Group computed corresponding thicknesses of lead and boron-carbide absorbers such that fast neutrons of about 4 Mev would be equally attenuated, while the gamma-ray attenuation would be greatly different; and (3) the Neutron Measurement Group under Linenberger and Ogle was to measure the fast-neutron flux with sulphur samples in the zero-angle collimators without any absorber in shelters A and B.

The tables of film data for standard exposures and experimental exposures are appended to the report. The absorption curves plotted from film without filters are also included.

10.1.2 Conclusions from Yoke Test

Five important observations were made in the Yoke experiment:

1. The intensification under cadmium and tin filters was in evidence just as much as in the X-ray experiment for the zero-angle radiation transmitted through the boron-carbide filled collimators.

2. The amount of radiation transmitted by the collimators loaded with lead absorber at the zero angle was much smaller than the amount transmitted by the collimators loaded with boron carbide.

3. The sulphur sample of Linenberger and Ogle showed a neutron flux at A shelter of neutrons per square centimeter and at B shelter of neutrons per square centimeter.

4. While the use of half the collimators was devoted to lead absorber, a sufficient number of points for the boron-carbide absorber were available to permit drawing absorption curves from ion chamber data. These curves are concave downward indicating inefficient collection of ionization.

5. The films placed in contact with the upper-angle collimators show that some radiation was coming in through these collimators.

The first observation definitely discounts the presence of slow neutrons and almost certainly discounts the presence of any resonance absorption of any other type of radiation.

The second observation from film and chamber data shows that a negligible component producing the readings is due to fast neutrons. This observation is substantiated by the results of the sulphur samples of the neutron group.

As a result of the fourth observation, it was decided to increase the field strength inside the ionization chambers for the Zebra experiment as previously discussed in the apparatus section.

Satisfied with the fifth observation that some radiation

was coming down the upper-angle collimators, it was decided to abandon upper-angle intensity measurements in the Zebra experiment.

Film data were tabulated and plotted for the zero-angle collimators at the three shelters in the Yoke experiment. Reproductions of the emulsions from the upper-angle collimators are also included.

10.1.3 Conclusions from Zebra Test

As a result of the various modifications of the Yoke and X-ray experiments, it was felt sufficient understanding of the problems had been gained to permit accurate absorption curve determinations for the radiation at zero angle in the Zebra experiment.

In addition to the use of chambers and film as detectors behind boron-carbide absorber, three recording electrometers were used. One of these recording electrometers measured the radiation with a beryllium chamber from a collimated beam in the B shelter without any absorber. Another beryllium chamber recorded the radiation outside the B shelter, and the third recorder measured the radiation outside the B shelter with a heavy-wall plastic chamber. Representative data from the three recording electrometers are given in Figs. 29, 30, and 31.

The heavy-wall plastic chambers located in the zero angle at C shelter gave readings roughly three times as high as the beryllium chambers in the same beams. This difference cannot be accounted for by additional wall thickness bringing the chambers more nearly into equilibrium with the radiation, since the optimum thickness of plastic walls for 5-Mev gamma rays would produce only about a 25% increase above

that of the beryllium chambers which were used. The results of ion chamber measurement were recorded and plotted.

Even though the emulsions are known to have considerable energy dependence for gamma radiation, the absorption curves from the film data show reasonable agreement with the ion chamber curves for lower levels of radiation. A summary of the rough analysis of the absorption curves can be found in Table 23.

The air relaxation distances measured from the ratio of intensities at the various shelters are tabulated in Table 22, assuming an inverse square geometry.

Table 20 contains the tonnage ratio determined from readings at A and B shelters.

11.1 SUGGESTIONS FOR FUTURE EXPERIMENTS

With the experience gained during Operation Sandstone, it seems desirable that the work in the future on gamma-ray absorption curves be confined to only one distance from the zero tower. Many more points and a wider range of absorber thickness should be used. The shelter for this absorption measurement should be within 700 yards of the zero tower. Absorption-curve measurements at zero angle and one upper angle would be sufficient. The shelter should be so constructed that high and low intensity beams are completely separated. This would mean one compartment would have the high intensity beams of the zero-angle collimators while the other compartment might contain the complete set of upper-angle beams plus the very weak beams from a few zero-angle collimators. In addition,

each detector should be individually shielded from scattered radiation. More than two compartments would produce a still better setup for reducing background interference.

For air-relaxation-distance measurements, more positions using much simpler types of shield with only one collimator could be designed. These could be constructed with no entrance other than an opening for inserting the detectors. They could be constructed at the laboratory and installed with the aid of light-lift machinery. Since they could be readily moved to new experimental sites, they would not have to be duplicated for each test. The collimators for this shield should view the same field at the zero tower.

The detectors for the measurements should be energy independent because, even if the energy dependence of the detectors were to be known, the analysis of the absorption curves to determine the spectrum of the radiation would be unduly complicated if not impossible. At the present writing, this would indicate that ionization-chamber detectors could be used. They should be designed for the proper radiation levels and so that leakage and efficiency of ion collection would be no problem. The requirement of efficient collection might mean gases at low pressures or even vacuum secondary-emission chambers will be necessary. Balanced chambers, where the background is automatically subtracted from the chamber reading, should be seriously considered.

Although film should not be used as the primary detector for absorption curves, its use is invaluable for showing certain qualitative

aspects of the work such as alignment, collimation, and position of ion chambers. Perhaps the best use of film would be to use a rotating cylinder behind a collimator which gave a flat beam, so as to study time variation of exposure and source size. In practice, a resolution of 0.020 inch per microsecond could be realized by rotating an 8-inch cylinder with film on its periphery.

New types of equipment such as gamma-ray spectrometers using crystal detectors which would give pulses proportional to gamma-ray energy should not be discounted.

From the experience at Operation Sandstone, it is apparent that a liberal supply of spare equipment should be included.

Including two instrument makers in the experimental group during Operation Sandstone proved to be very valuable for making modifications in the experiment. Their services will be found to be indispensable in future experiments.

Experiments are now being planned to study the sensitivity of detectors for neutrons and gamma rays of high energy. This will be useful in clarifying some of the discrepancies in the present data and will be valuable in planning future experiments.

APPENDIX A
FILM DATA
ON
I-RAY, YOKE, AND ZEBRA EXPERIMENTS

Table 1
 DESCRIPTION OF FILM REPRODUCTION

8CX	Original type of cadmium and tin filter; showing intensification under cadmium filter. Spot does not cover tin filter. Located behind 3" of B ₄ C in B shelter. X-ray experiment. Emulsion type C.
42YA	Placed over end of 5° collimator in B shelter with no absorber. Yoke experiment. Emulsion type A.
28YA	Placed over end of 30° collimator in B shelter with no absorber. Yoke experiment. Emulsion type A.
45YA	Placed over end of 15° collimator in B shelter with no absorber. Yoke experiment. Emulsion type A.
44YD	Placed over end of 10° collimator in A shelter. Yoke experiment. Emulsion type D.
100r-D	Standard exposure 100 roentgens showing reduced blackening under both Cd and Sn filters.
5DZ	Film exposed in zero angle collimator in A shelter behind 7½" B ₄ C showing two darkened sectors under Cd and Sn filter. Zebra experiment. Emulsion type D.
5CZ	Same collimator as 5DZ but showing background outside of spot is lighter under Sn filter than for the unfiltered background. Zebra experiment. Emulsion type C.
8CZ	Behind 18" absorber in 10° angle at A shelter, Zebra experiment, showing less blackening under tin filter than for unfiltered radiation. Emulsion type C.
25CZ	Background in A shelter, Zebra experiment, showing less blackening under tin filter than without filter.

Enlargement of emulsions 1: 1.89

Pages 53 through
 89 are deleted

Table 17

ABSORPTION COEFFICIENT IN AIR FOR GAMMA RAYS
(Reciprocal Centimeters) (P215 Heitler)

hv/mc ²	1	2	5	10	20	50	100	1000
abs. coef.	1.11×10^{-4}	$.8 \times 10^{-4}$	$.5 \times 10^{-4}$	$.35 \times 10^{-4}$	$.25 \times 10^{-4}$	$.2 \times 10^{-4}$	$.19 \times 10^{-4}$	$.21 \times 10^{-4}$

HALF THICKNESS FOR GAMMA RAYS

83% B₄C 17% C₇H₇O Density 2 g/cc

pages 91
through 94
are deleted

Table 21
A I R R E L A X A T I O N D I S T A N C E
ZERRA EXPERIMENT
Beryllium Chambers

Inches Boron Carbide	Shelter Ratios Not Corrected for Geometry		
	A Shelter	B Shelter	C Shelter
3	7.04	1	
6	6.76	1	.305
9	7.57	1	.300
12	7.83	1	.283
15	7.59	1	.276
18	7.22	1	.264
21	6.82	1	.250

Half Thickness in Air (Corrected for Inverse Square Geometry)

Average A:B Shelter - 4.13M

Average B:C Shelter - 4.22M

Table 22
 AIR RELAXATION DISTANCE

ZEBRA EXPERIMENT

Inches Boron Carbide	Shelter Ratios Not Corrected for Geometry					
	A Shelter CDE Emulsion	B Shelter CDE Emulsion	AB Shelter AB Emulsion	C Shelter AB Emulsion	C Shelter AB Emulsion	C Shelter AB Emulsion
0	21.1	1	1	1		
3	17.7	1	1	1	.159	
6	14.7	1	1	1	.165	
9	12.3	1	1	1	.162	
12	10.5	1	1	1	.165	
15	8.8	1	1	1	.166	
18	7.42	1	1	1	.168	
21	6.25	1	1	1		

Half Thickness in Air (Corrected for Inverse Square Geometry)

Measured at 0 Absorber A:B - 142 M

Measured at 21 inches Absorber A:B - 480 M

Average of B:C Shelters - 287 M

Table 23
AVERAGE ENERGY FROM BORON CARBIDE ABSORPTION CURVES

Experiment	Shelter	Detector	Half Thickness		Energy Mev.
			Centimeters		
X	A	Film	8.89		2.3
X	B	Film	12.7		4.5
Y	A	Film	8.38		2.0
Y	B	Film	12.5		4.3
Z	A	Film	10.7		3.3
Z	B	Film	15.2		6.2
Z	C	Film	12.5		4.3
Z	A	Chamber	11.4		3.7
Z	B	Chamber	12.2		4.2
Z	C	Chamber	11.4		3.7

Table 24
ENERGY DEPENDANCE OF FILM

Dosage	Filter	41-46 Kev			78 Kev			115 Kev		
		(Energy) (Film Type) C	D	E	C	D	E	C	D	E
25r	Cd (1 mm)	1.15	0.14	0.14	1.80	0.26	0.18	1.80	0.29	0.14
	None		2.66	1.15	2.92	1.62	0.69	2.69	0.57	0.26
	Pb (1 mm)	0.26	0.04	0.09	0.58	0.07	0.04	0.62	0.07	0.04
150 r	Cd		1.15	0.47		1.91	0.88		2.04	0.92
	None			2.42			2.13		2.92	1.40
	Pb	1.69	0.27	0.12	2.55	0.42	0.22	2.59	0.51	0.26
1200r	Cd			2.03			2.55		2.46	
	None			2.92			2.73		2.56	
	Pb	2.09		0.96		2.96	1.39		1.49	
4000r	Cd			2.51			2.68		2.79	
	None			2.81			2.81		2.82	
	Pb			2.61			2.41		2.54	

Table 24 (continued)

Dosage	Filter	330-380 Kev			800 Kev				
		(Energy) (Film Type)	C	D	E	C	D	E	
25r	Cd (1 mm)		1.24	0.17	0.12		1.31	0.18	0.11
	None		1.22	0.17	0.13		1.49	0.20	0.11
	Pb (1 mm)		1.46	0.17	0.14		1.47	0.20	0.13
150r	Cd			1.36	0.76			1.39	0.79
	None			1.46	0.86			1.30	0.84
	Pb			1.46	0.81			1.30	0.92
1200r	Cd				2.33				2.38
	None				2.36				2.41
	Pb				2.38				2.41
4000r	Cd				2.64				2.72
	None				2.64				2.75
	Pb				2.64				2.78

SCIENTIFIC DIRECTOR'S REPORT
OF ATOMIC WEAPON TESTS
AT ENIWETOK, 1948

Annex 8

GAMMA-RAY MEASUREMENTS

Part II

GAMMA-RAY INTENSITIES AT THE SANDSTONE TESTS
IN THE REGION 0 - 1000 MICROSECONDS

GAMMA-RAY INTENSITIES AT THE SANDSTONE TESTS
IN THE REGION 0 - 1000 MICROSECONDS

Work Done By:

F. L. Bentsen
L. D. P. King

Written By:

L. D. P. King

September 1, 1949

TABLE OF CONTENTS

1.1	INTRODUCTION	4
2.1	APPARATUS	8
3.1	EXPERIMENTAL ARRANGEMENT	16
4.1	GENERAL PROCEDURE	26
4.1.1	Procedure for I-Ray Day	27
4.1.2	Procedure for Yoke Day	33
4.1.3	Procedure for Zebra Day	43
5.1	CALIBRATION PROCEDURE	50
6.1	CALCULATIONS AND RESULTS	67
6.1.1	Absolute Gamma Sensitivity of Units	67
6.1.2	Geometry Factors	71
6.1.3	Absolute Gamma Intensities from Bomb	71
6.1.4	Final Results - Gamma Rays and Neutrons	72
7.1	CONCLUSIONS	96
8.1	RECOMMENDATIONS FOR FUTURE TESTS	102
APPENDIX A - NEUTRON SENSITIVITY OF PHOTOMULTIPLIER NAPHTHALENE UNITS		105
APPENDIX B - NEUTRON AND GAMMA-RAY PROPERTIES OF THE BORON-CARBIDE ABSORBER PLUGS		112
APPENDIX C - PROPERTIES OF THE SPECIAL CONCRETE USED IN THE SANDSTONE GAMMA-RAY SHELTERS		115
APPENDIX D - LIST OF PHOTOGRAPHS, FIGURES, AND TABLES		122

ABSTRACT

The intensity of gamma radiation as a function of time was measured at the Sandstone tests using a good geometry. Photomultiplier tubes with naphthalene were used as the detectors of gamma radiation, and oscilloscope records were obtained from 0 - 1000 microsecond. Various thicknesses of boron carbide (lead in one case) placed in collimating tubes give a rough indication of gamma-ray hardness at the 1300-yard station. Peak intensities observed appear to be in good agreement with other independent determinations.

Some of the characteristics of 931 photomultiplier tubes when used at high current densities for short times are described and illustrated.

Measurements on (1) the neutron sensitivity of the photomultiplier naphthalene units and (2) the neutron and gamma-ray properties of the boron-carbide absorber plugs, and the special concrete used in the gamma-ray shelters are described in appendices.

GAMMA-RAY INTENSITIES AT THE SANDSTONE TESTS
IN THE REGION 0 - 1000 MICROSECONDS

1.1 INTRODUCTION

When the Sandstone gamma-ray measurements were planned, essentially only poor geometry, total intensity data were available.

Intensity measurements as a function of time were tried at Trinity⁽¹⁾ over the time interval of a few milliseconds to about twenty seconds. The ionization-chamber recording equipment was saturated, however, during the first ten seconds. Since the experiments were intended to give primarily information on bomb efficiencies from the delayed gamma-ray intensities, the measurements were successful in this respect.

Intensity-versus-time records were obtained at the Bikini Able and Baker tests⁽²⁾ ranging from about one second to twenty minutes. The early portion of the records is in fair agreement with the expected decay of fission-product gamma-rays. The interpretation of the results as a whole is quite difficult, however, due to a lack of knowledge of the exact location of the source, the uncertainty in the

(1) IA-432, Chamberlain, Deutsch, Farwell, Linenberger, Segre, Wiegand.

(2) IAMS-439, J. L. Tuck.

thickness of the shielding produced by various ship components, and the contamination present near the recording equipment.

Initial plans for the Sandstone tests called for measurements of both intensity and energy of the gamma radiation as a function of time. The spectrum was to be measured by using a series of absorbers in good geometry at several well-shielded stations. Short-time measurements were to be made by fast mechanical recorders connected to ionization chambers and by moving film; the longer time records were to be obtained by pointing some of the collimating tubes at a series of vertical angles with respect to the bomb position. Films and chambers placed behind these tubes would give integrated gamma intensities over the several time intervals. Most of these measurements, with the exception of the use of a moving film, were done at least in part by the Chicago group.⁽³⁾

Experiments carried out at several laboratories on the time response and sensitivity of photo-naphthalene detectors indicated that gamma-ray measurements should be possible in the microsecond region without the use of elaborate equipment. It was therefore decided at a rather late date, February 1948, to try to extend the gamma-ray measurements

(3)

Report of LAJ-5 on Gamma Measurement, F. Shonka and G. Pawlicki, Annex 8, Part I (Sandstone No. 29).

originally planned for the Sandstone tests to much shorter times. Such measurements are of considerable importance since the nuclear explosion itself and most of the interesting changes in the bomb configuration take place in the micro-second region.

The shape of the gamma-ray intensity curve after the first few tenths of a microsecond is difficult to predict and interpret. The initial rise, due to prompt gamma rays, is exponential and has been used to measure accurately the multiplication rate of the bomb. Measurements of this type were carried out with great precision in the region 0-0.6 micro-second by the Naval Research Laboratory⁽⁴⁾ for the Sandstone tests. After this initial rise, gamma-ray intensities no longer give a true picture of the nuclear explosion itself, due to many complicating circumstances. A brief description of the possible gamma-ray sources and their time scale may help to indicate what these complications are.

First, one has prompt gamma rays given off from fission practically instantaneously; these are highly attenuated due to the dense, high atomic number, fissile assembly. These are followed by the well-known delay gamma rays which are constant during the first few hundredths of a second and then decay approximately as $t^{-1.2}$.⁽⁵⁾ As the explosion

(4) Operation Sandstone Measurements by NRL, E. H. Krause and staff, Annex 2, Part I (Sandstone No. 11).

(5) The Rate of Decay of Fission Products, K. Way, E. Wigner, Phys. Rev. 73 pp. 1318-1333, 1948.

continues it is obvious that the density of the components decreases. Gamma rays can, therefore, leak out in intensities depending not only on the time rate of change of the source itself, but on the time change of attenuation. Besides these direct gamma rays there is a very important additional source produced by the inelastic scattering and absorption of emitted neutrons. This secondary source will depend also on the time rate of change of the bomb material densities. In addition neutrons can produce an appreciable secondary gamma-ray source by striking the ground in the vicinity of the explosion. The importance of this latter source depends on the proximity and geometry of the detecting equipment with respect to the bomb. Good-geometry experiments considered in this report do not receive many secondary gammas from air scattering or from neutrons striking the ground. Since the bomb expands to approximately air density in about 25 microseconds, it is evident that the varying gamma-ray sources mentioned above present a complicated picture of gamma-ray intensities as a function of time, especially in the early stages.

2.1 APPARATUS

The recording and detecting equipment chosen for this experiment depended on several considerations:

1. The work was undertaken at a late date so that no developmental work was possible and ready-made equipment had to be used.

2. The experiment was considered supplemental to those planned earlier and hence had to be fitted into available space, and the data obtained without seriously interfering with other previously planned setups.

Experiments done at Los Alamos in connection with the time-scale measurements for the bomb tests led to the choice of naphthalene and the 931A or P21 photomultiplier tubes as detectors. A compact, fast, rugged, versatile scope was needed as a recorder. The DuMont Type 256-D (Figure 1) cathode-ray oscilloscope (a revision of the DuMont Type 256B A/R range-scope developed at MIT) seemed to meet these requirements reasonably well. This instrument has over-all dimensions of about 12-inch width 16-inch height and 26-inch depth and comes equipped with the following features:

(1) self-contained power supply, (2) a 5CPA cathode-ray tube with 4,000-volt accelerating potential and focus control giving a clear, fine trace suitable for fast photography; (3) direct vertical deflection ~ 80 volts/in;

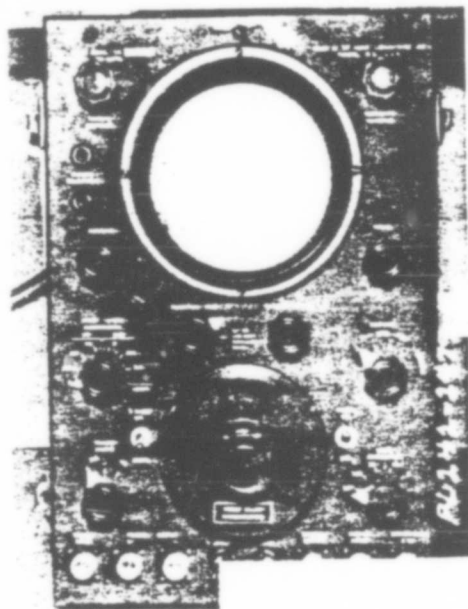
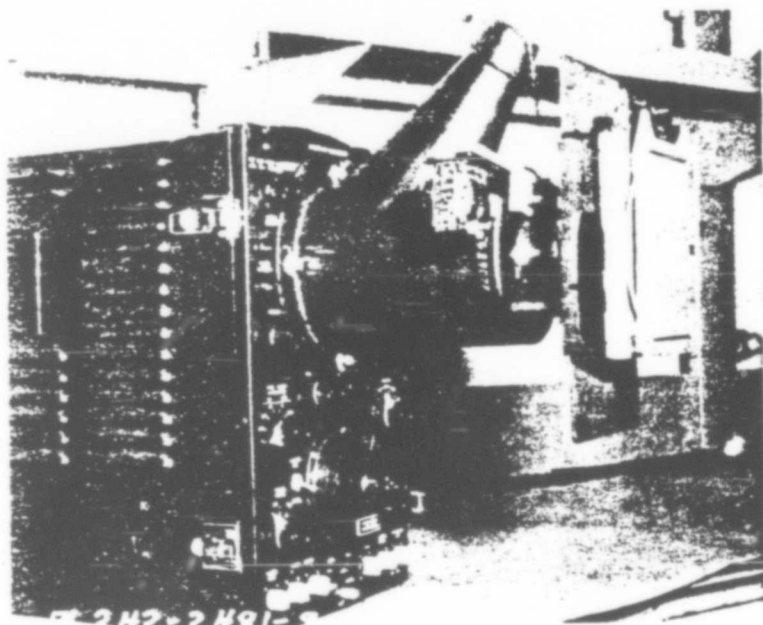


Fig. 1 Dumont Type 256-D Cathode-Ray Oscilloscope and Los Alamos Model Camera.

(4) 4500-, 1000-, 100-, 25-, 10-, 4- microsecond sweeps with speeds of 1100, 300, 30, 6, 2.5 and 1.0 microseconds/inch, respectively; (5) triggering from either an internal variable trigger generator or an external trigger of at least ± 15 volts amplitude is available; (6) outputs of plus or minus polarity at 100-volt amplitudes and 1.0-microsecond width are provided; (7) crystal controlled time markers ($\pm .02\%$) of ± 10 microseconds and ± 50 microseconds as well as a movable marker are provided (markers are available only on internal trigger); and (8) the incoming signal can be viewed directly on the vertical deflection plates or through a video amplifier, 8 megacycles wide, with attenuation ratios of 1:1; 3:1; 10:1; 30:1; and 100:1. These and other features seemed to offer a unit of sufficient versatility and compactness to make it worth while to attempt an experiment without adequate preparation or planning. Through good fortune and the efforts of the purchasing group five such scopes were obtained within about two weeks.

Boron was chosen as the absorber material since it is one of the best materials for discriminating between gamma rays and neutrons over the whole energy spectrum of the incident neutrons. A hydrogenous material would give somewhat higher neutron removal by scattering in the intermediate region, but boron is superior in the low-energy

region. Boron has the additional advantage of giving only 440-kv gamma rays from neutron capture instead of 2-Mev gamma rays as is obtained from hydrogen. A light element is desirable as an absorber, since both the photoelectric effect and pair production contribute a negligible amount to the attenuation of the gamma rays in the region of interest from 1 to 5 Mev. Calculations are considerably simplified if only Compton scattering is present and the Klein-Nishina formula can be directly applied.

The absorber plugs were made of boron carbide with a plastic binder by Group CMR-6 under the direction of J. S. Church. The specifications for the plugs were: diameter $0.750 \pm .005$ inch, length $1.500 \pm .010$ inches; specific gravity $1.96 \pm .02$. These close tolerances assured interchangeability of the plugs and an excellent fit in the Shelby precision tubing used for the collimators. A picture of the plugs and spacers is shown in Figure 2. The latter were used to hold the plugs in any desired position in the tubes. The chemical composition of the plugs was 83% boron carbide + 17% C_7H_7O by weight, the phenol formaldehyde acting as a binder. The boron carbide used was Norbide No. 320. Chemical and spectroscopic analysis of the Norbide showed the following composition: Fe .4%, Si .3%, Al .2%, Ca .01-.1%, Mg .01-.1%, Mn .01-.1%, Na .01-.1%, Mo .001-.01%,

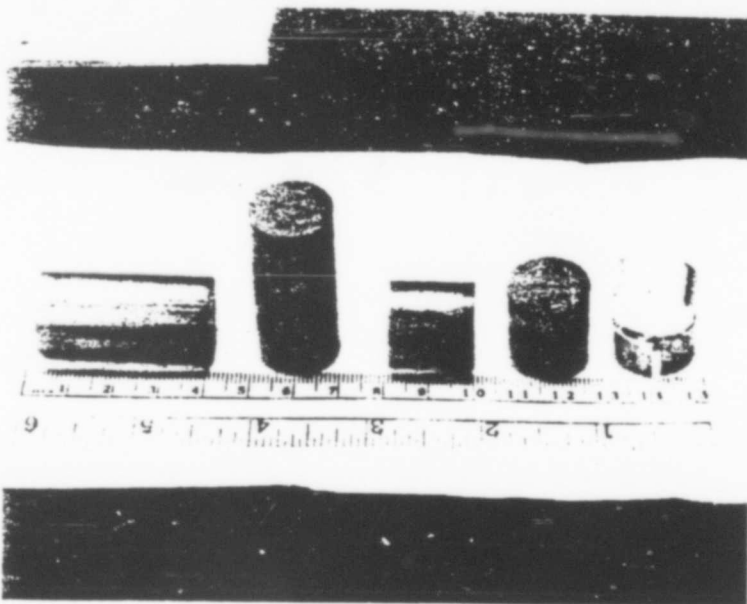


Fig. 2 Boron-Absorber Plugs and Aluminum-Spring Spacers

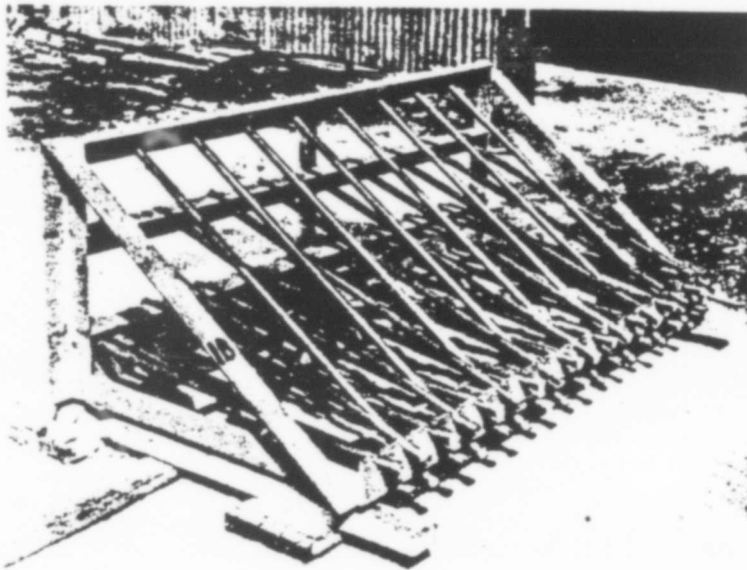


Fig. 3 Collimating Structure Used in the 1300-yard Shelter

Cu .001-.01%, Pb <.001%, Sn <.001%. For additional information on the boron-carbide plugs see Appendix B.

Figures 3 through 7 are photographs showing the collimating structure, the collimator in position, the tubes as seen by the detecting equipment, the general appearance of the 1300-yard shelters, and the borax water-can shield over the door in the rear of the shelter.

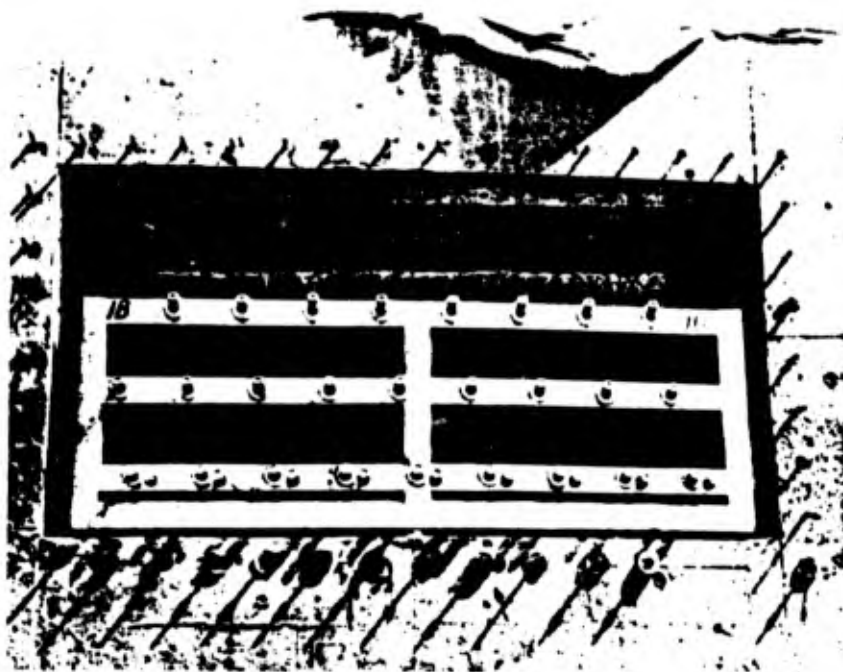


Fig. 4 Outside View of Collimating Structures in Shelter

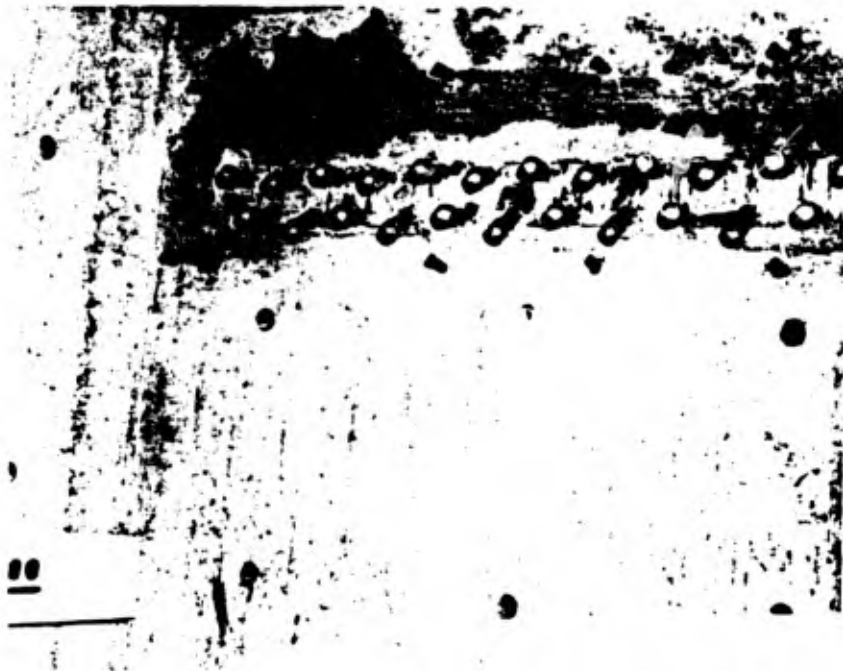


Fig. 5 Collimating Tubes as Seen by Equipment Inside Shelter

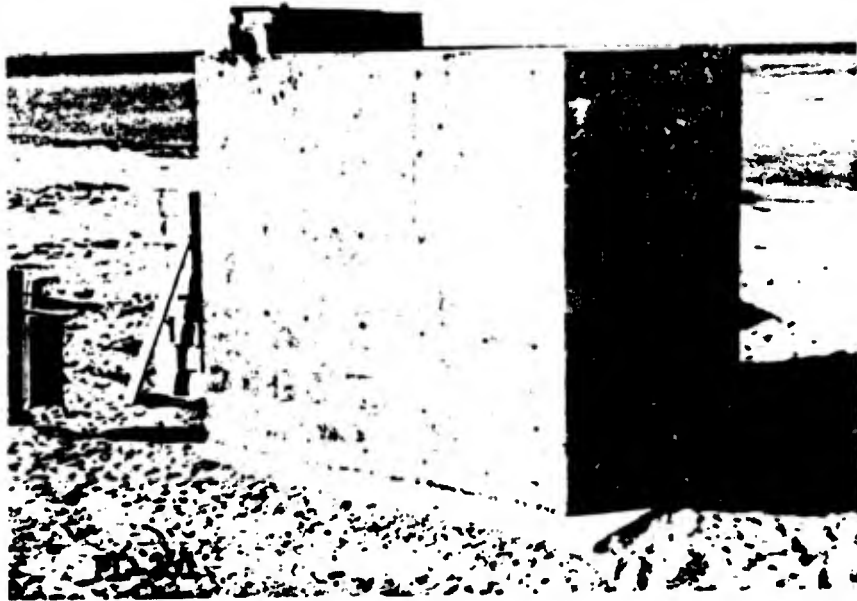


Fig. 6 General Exterior View of 1300-yard Shelter Prior to Shot

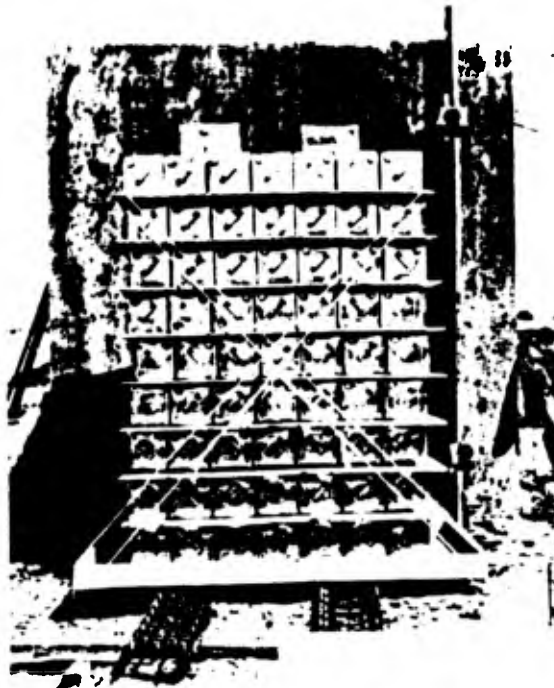


Fig. 7 Rear Borax and Water Shield at 1300-yard Shelter

3.1 EXPERIMENTAL ARRANGEMENT

A schematic layout of the arrangement of the detecting equipment for the zero angle collimating tubes at the 1300-yard gamma B shelter is shown in Figure 8. This Figure does not show the rear door or the three other sets of collimating tubes placed so as to aim at 5° , 15° , and 30° above the bomb position. These additional collimators, along with the thimble chambers and film packs shown, were used by the Chicago group⁽³⁾ and will not be described further here.

The incident gamma rays and neutrons are well collimated by the 3/4-inch I. D. steel tubes placed in the 3-foot special concrete⁽⁶⁾ shield wall. The geometry for all the detectors is good, and as can be seen from the Figure, the collimated beams strike the thimble chambers and film packs before reaching the naphthalene detectors. Any correction due to the absorption by the thin-walled beryllium chambers or film packs has been ignored in this report.

The detecting equipment is shown schematically in Figure 9. The AC power is turned on about one-half hour before zero time to allow the scopes to warm up. At minus one minute a relay closes the battery voltage for the trigger unit and at minus ten seconds power is applied to the

⁽⁶⁾ See Appendix C for properties of special concrete.

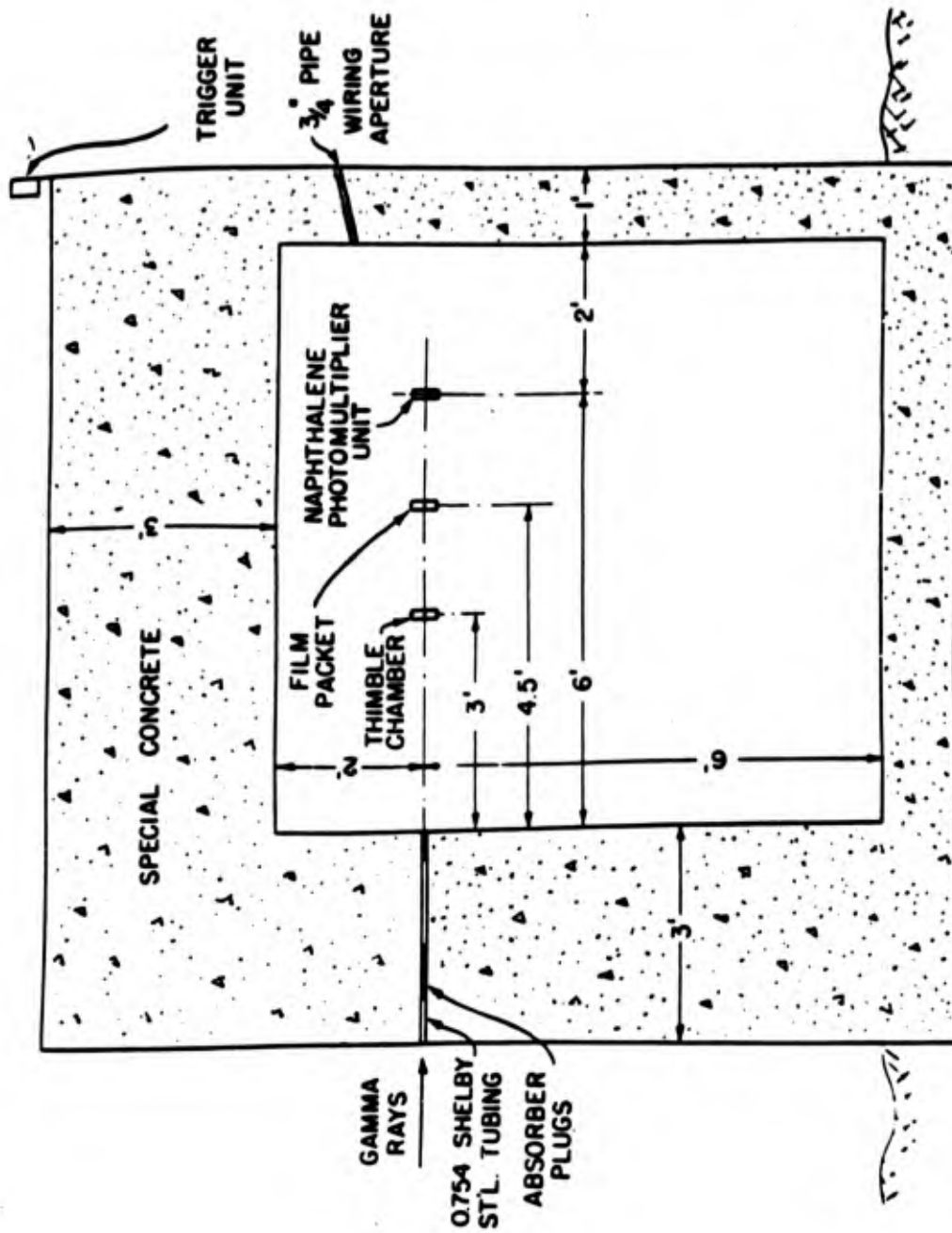
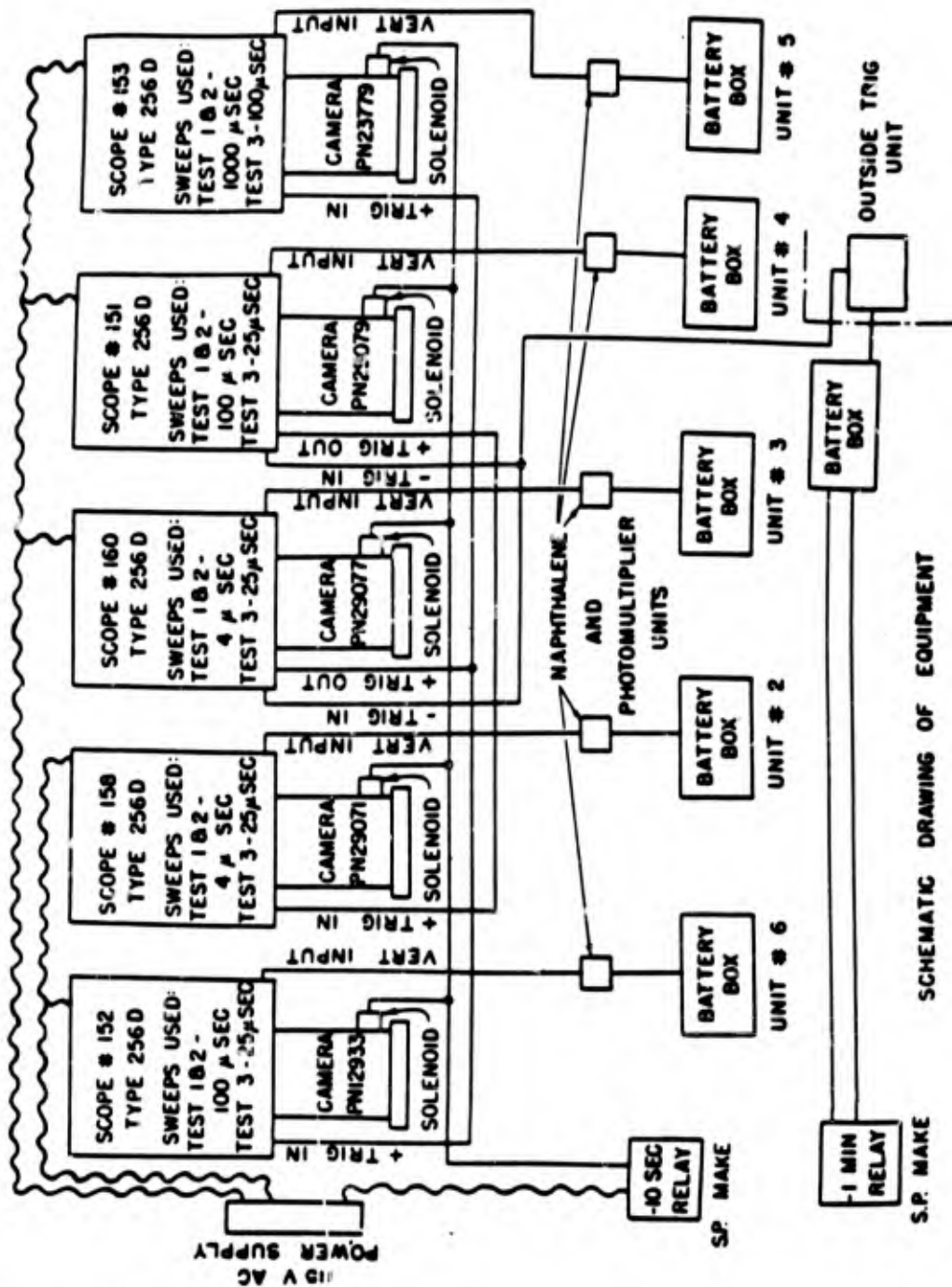


Fig. 8 Schematic View of Equipment and Shelter Used at 1300 Yards



SCHEMATIC DRAWING OF EQUIPMENT

Fig. 9 Schematic View of Detecting Equipment

solenoids which open the camera shutters. A fraction of a microsecond after zero time the gamma intensity from the bomb has built up to sufficient intensity to set off the sensitive outside trigger unit. The negative signal from this unit sets off the internal positive triggers and sweeps of two scopes. The positive triggers from these scopes are used to start the sweeps in the remaining three scopes. This arrangement tended to reduce the attenuation on the incoming trigger pulse and make the probability smaller that none of the units would receive the triggering pulse.

The five oscilloscopes and battery supplies were mounted on a heavy shelf near the rear of the shelter and 18 inches from the ceiling (Figures 10 and 11). The naphthalene units (Figures 12 and 13) were mounted by brackets onto this same shelf. This assured short signal leads. The units were correctly located by tightening the brackets when the pinhole image of the bomb house on the tower was centered on the naphthalene unit. The shelter could be completely darkened by closing the light-tight ship hatch door and capping all but one of the tubes with the available 1/32-inch aluminum discs, before the insertion of the absorber plugs. A small aperture placed on the inside end of the uncapped collimator tube produced a sharp image of the tower surrounded by diffraction rings

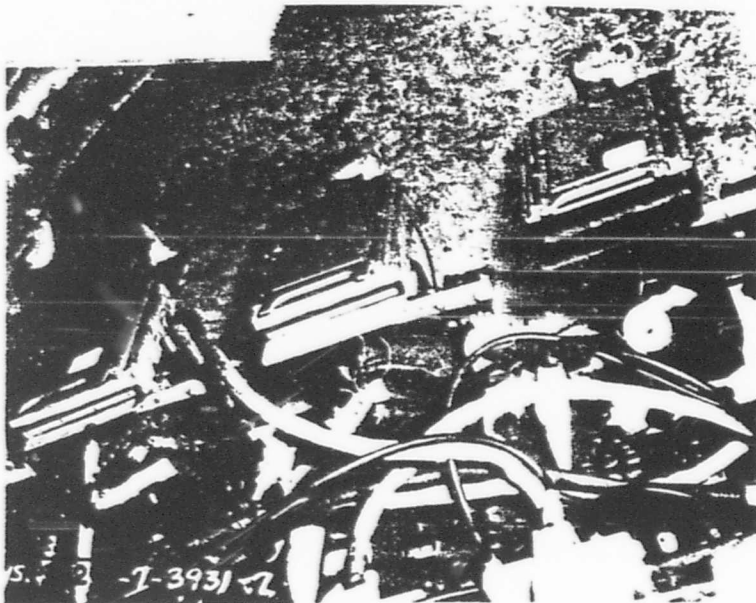


Fig. 10 Recording Equipment Mounted on Shelf Near Ceiling



Fig. 11 Recording Equipment Mounted on Shelf Near Ceiling

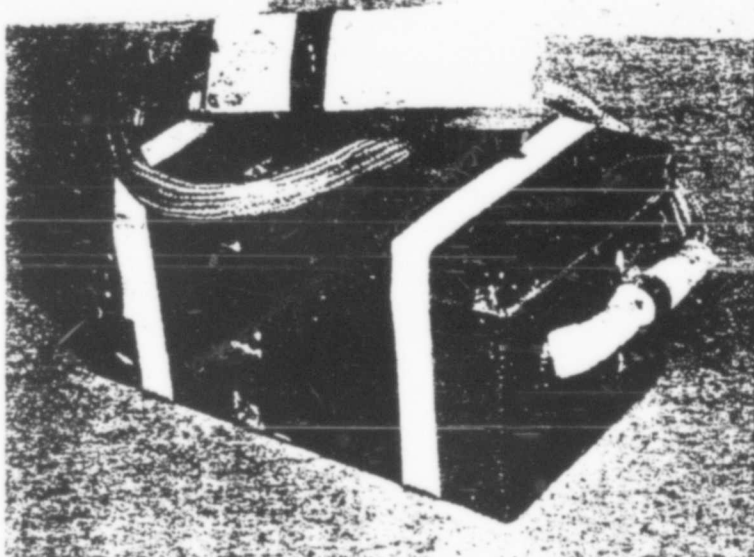


Fig. 12 Naphthalene Detector Unit with Battery Supply Box

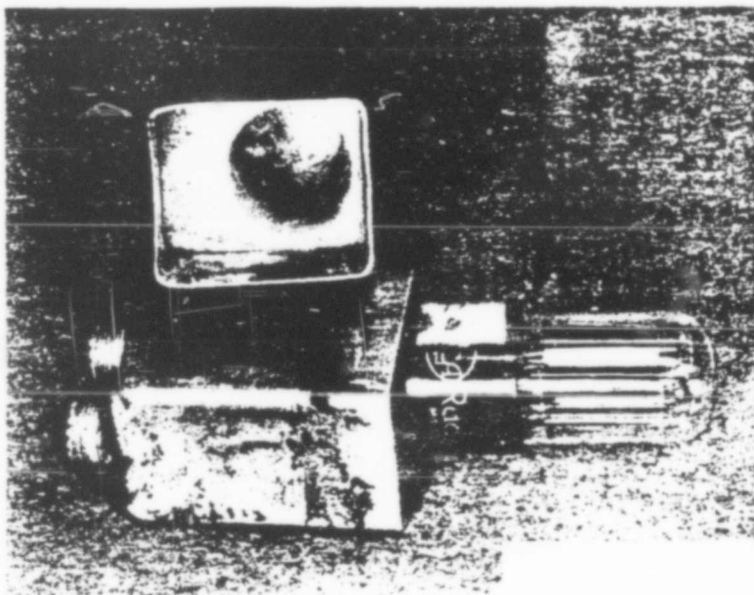


Fig. 13 Detector Unit Showing Naphthalene in Tube Shield Cover

from the shiny tube aperture. This pattern permitted an exact location of the naphthalene units and showed also that the original alignment of the collimating system was good since in most cases the image of the tower house was centered in the diffraction rings.

The trigger unit was mounted on a 2-inch by 10-inch plank placed edgewise against the back of the shelter outside. Signal and battery leads were brought through available pipes in the back of the shelter. Figures 14 and 15 show the trigger unit in place with external leads and sunshade.

Circuit details for the trigger and detecting units are shown in Figures 16 and 17, respectively. The usual bleeder condenser arrangement was satisfactory for the trigger unit only where voltage drops due to large currents were advantageous in preventing damage to the tube. This circuit was convenient also since many fewer leads were required to the batteries mounted inside the shelter. Individual battery connections to each diode were necessary in the detecting tubes, however, otherwise large currents would produce changes in the sensitivity of the units.

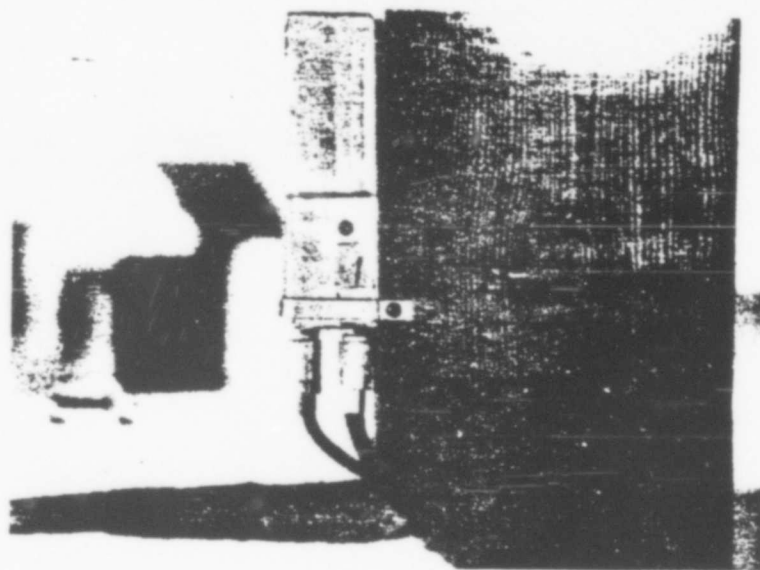


Fig. 14 Close-Up of Trigger Unit Mounting Method

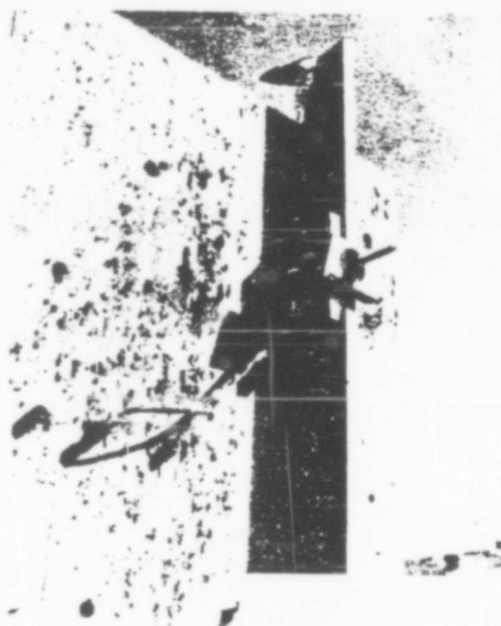


Fig. 15 Trigger Unit Assembly Ready for Test

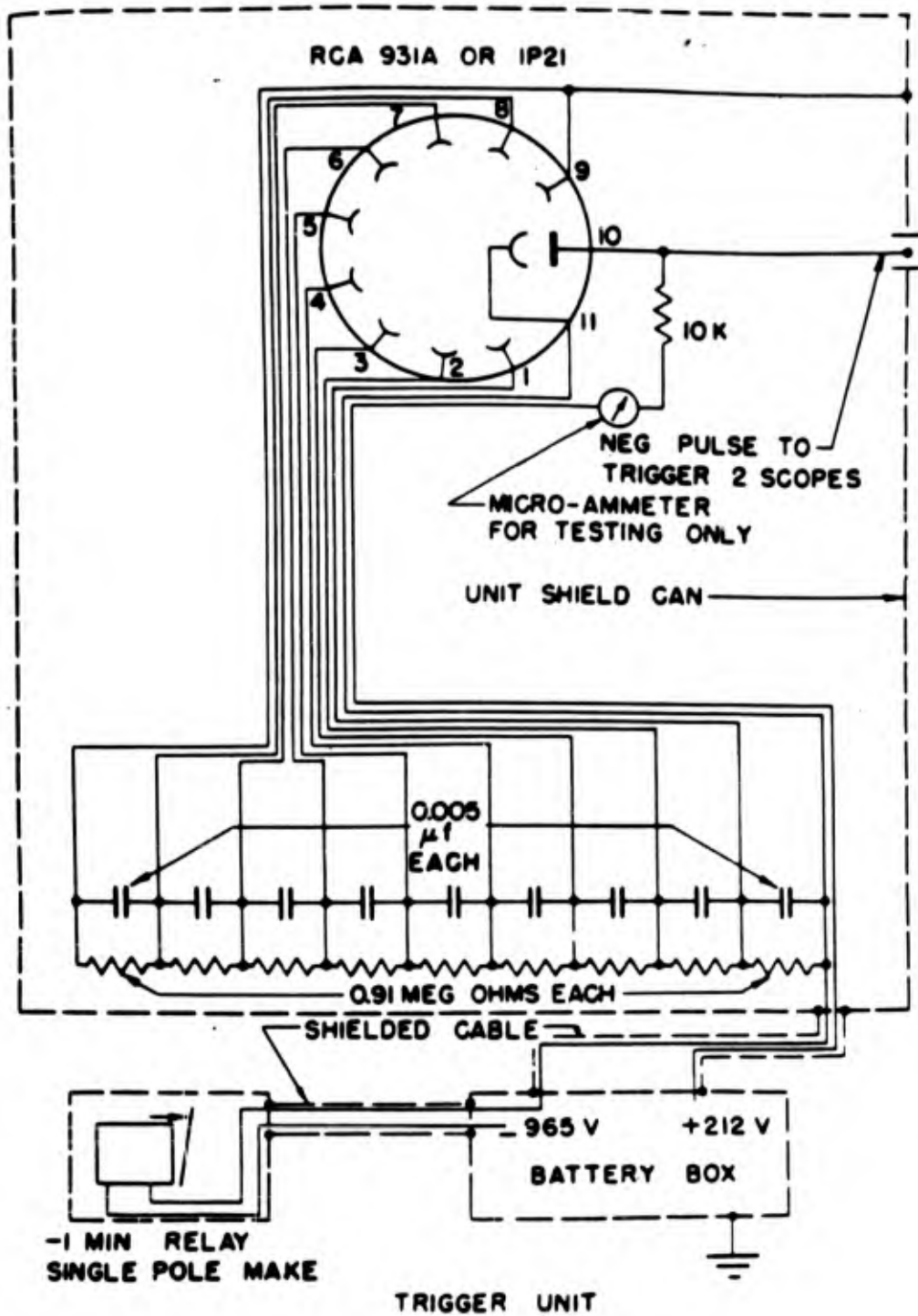


Fig. 16 Schematic Circuit Drawing of Trigger Unit

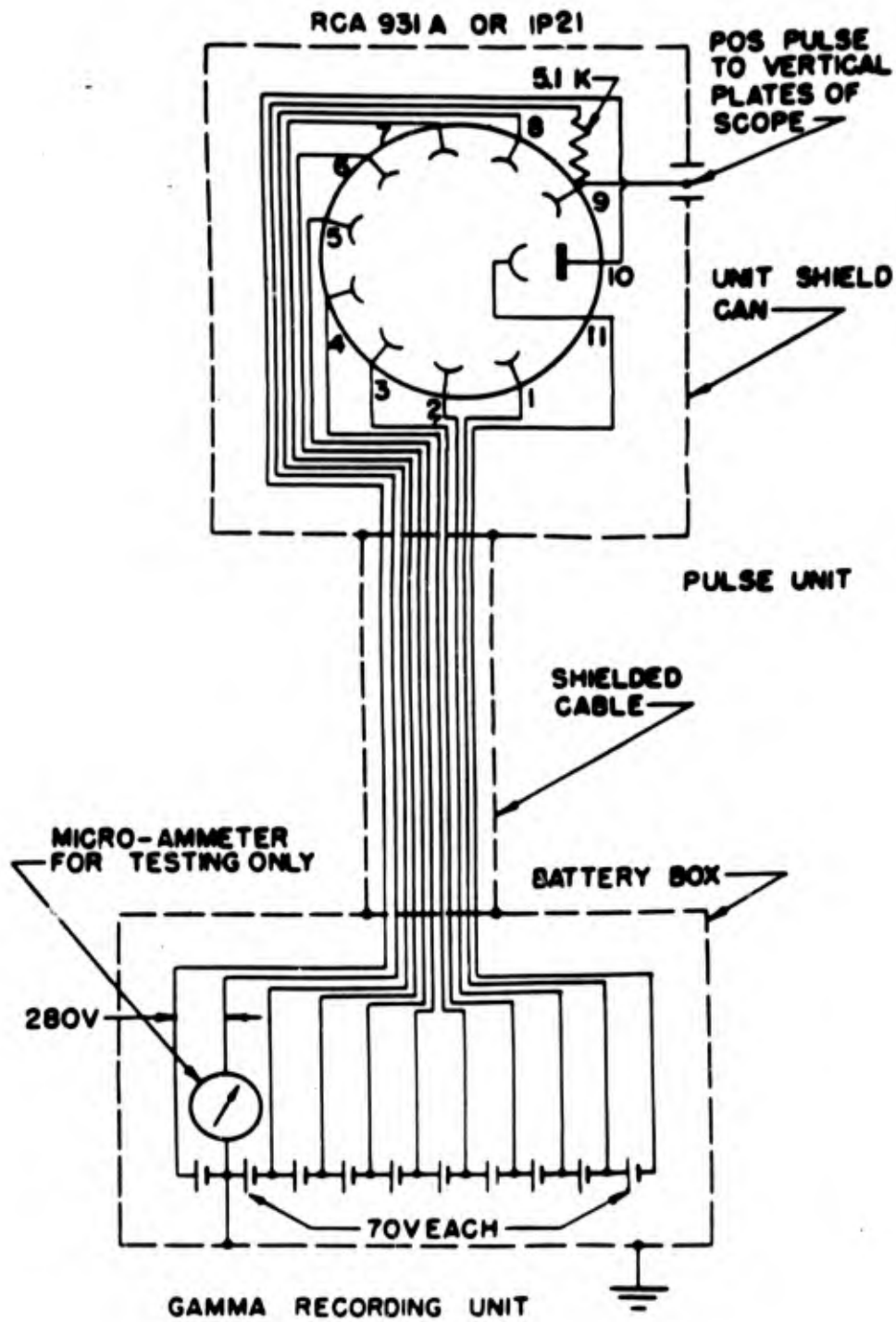


Fig. 17 Schematic Circuit Drawing of Gamma Recording Unit

4.1 PROCEDURE

Calculations and preliminary calibrations with a one-curie RaBe source on shipboard, indicated that the photomultiplier naphthalene unit would be too sensitive for use in the expected geometry inside the 1300-yard gamma shelters. This made it unnecessary to: (1) use high voltages on the dynodes of the multiplier tubes; (2) use the scope amplifiers; or (3) continue work in growing clear naphthalene crystals. In all but the trigger unit where high sensitivity was desirable, low voltages, small load resistors, and less sensitive tubes were used (Figure 16). The most insensitive multiplier tubes were obtained from the large collection on hand of Edgerton, Germeshausen and Grier, Inc.

Since the model 256D scope has approximately a 0.5-microsecond delay between the signal input time and the appearance of a trace on the screen, it was necessary to make some modifications in order to be able to see the initial rise of a fast gamma pulse. Therefore, the input of four of the scopes was fed to a cathode follower and then through fourteen feet of RG65/u delay line before going to the deflecting plates. The positive output signal from the detecting units (Figure 17) made it possible to drive a delay line directly with a cathode follower. RG65/u cable

has a delay of 0.042 microsecond per foot at 5 megacycles, a capacity of 42 micromicrofarads per foot and a resistance of 7 ohms per foot. Signals were impressed directly on the plates of the fifth scope so that this unit was not used for the fastest sweep speeds.

Previous experimental data and the modifications in bomb design used in the Sandstone tests made calculations of the expected gamma intensities as a function of time rather uncertain. It seemed advisable, therefore, to cover as wide an intensity and time range as possible with the five scopes for the first test.

4.1.1 Procedure for X-Ray Day (Test No. 1 on Engald)

1. The trigger or unit No. 1 was made very sensitive in order to start the scope sweeps as early as possible. The best available tube was picked (a 931 A); a large load resistor and high diode voltages were used (Figure 16). This unit had a plate current of 50 microamperes when a one-curie RaBe source was placed 20 centimeters from the tube cover. The unit was mounted outside the shelter (Figures 14 and 15) and, although in full view of the blast, it survived all three test shots with no appreciable change in sensitivity. The unit was wrapped with waterproof tape at all points and an aluminum sunshade placed overhead to

reduce any high temperature from the rays of the sun.

2. Unit No. 2 was the least sensitive unit, the output diode current being only 3 microamperes when the cesuric RaBe source was placed in contact with the tube cover box. This unit was used with a 4-microsecond sweep and 6-inch boron-carbide absorber.

3. Unit No. 3 was quite sensitive giving 52 microamperes with the source in contact. This unit was used with a 4-microsecond sweep and $1\frac{1}{2}$ inches of boron carbide.

4. Unit No. 4 had a sensitivity of 4 microamperes with source in contact and was used with a 100-microsecond sweep and 6 inches of boron carbide.

5. Unit No. 5 had a sensitivity of 57 microamperes with the source in contact and was used with a 1000-microsecond sweep and $1\frac{1}{2}$ inches of boron carbide. This unit had no delay line and the signal went directly to the plates of the scope.

6. Unit No. 6 had a sensitivity of 50 microamperes with the source in contact and was used with a 100-microsecond sweep and 3 inches of boron carbide.

By using an insensitive unit with a thick absorber and sensitive tube with a thin absorber, a considerable range in sensitivity was obtained. Pairs of units with similar over-all sensitivity were then used with two sweeps

4- and 100-microseconds respectively. One unit was used on the longest sweep (1000 microseconds) which would more than cover the total time during which the complete source of gamma rays would remain in the field of view of the collimators.

Only three out of five records were obtained on X-ray. For some unknown reason the main supply voltage dropped to about 90 volts just prior to the shot, so that two of the solenoids did not open the camera shutters and the four-microsecond sweep records were lost. Two 100-microsecond and one 1000-microsecond record were obtained from units four, six, and five (Figures 18, 19, and 20, respectively). These records indicated that the trigger and detecting units were working satisfactorily and the sensitivities used were only slightly high.

Due to a change in the sensitivity of units three and five after the test, a lack of adequate intercalibration between units, and the voltage drop in the main power which changed the scope sensitivity and shifted the beam zero (sweep axis), these records have not been used other than to give rough intensity values. The traces of Figures 18, 19, and 20 have superimposed axes. These axes were obtained after the shot and the true position may be different due to the above-mentioned voltage drop.

pages 30 through
32 are deleted

Table I summarizes the static calibrations of all the units throughout the test period. Table II shows the unit arrangement for each of the tests and Table III indicates the absorbers available for each shot. These absorber arrangements were chosen to meet the requirements of the experiments being carried out by the Chicago group.⁽³⁾

4.1.2 Procedure for Yoke Day

To prevent the possible recurrence of a shutter not opening due to low voltage, all of these were adjusted so that the solenoids would operate on 90 volts or more.

From Table I it is evident that there was some change in sensitivity in the units after X-ray. The large change which occurred in unit No.3 is known to have occurred by accidental over-exposure to light during some calibration experiments. It is not definitely known if this was also true for unit No.5. It can be seen from the table that unit No.3 partially recovered in a short time, and that all the units maintained their sensitivity in a very satisfactory manner for Yoke and Zebra days as well as for all the final calibration work described below.

The traces from X-ray day, Figures 18, 19, and 20, indicate that the signal intensity was high as expected. It was therefore advisable to try to reduce the signal

TABLE III

Collimating apertures in the 1300-yd shelter aiming at tower		Absorbers in Collimators		
Numbers are from left to right when facing tubes inside shelter	I-ray	Yoke		Zebra
		Cd in all holes 15" from inner end		
1	1.5" B ₄ C*	12"	B ₄ C*	18" B ₄ C
2	3 " B ₄ C*	9.75"	B ₄ C*	12" B ₄ C*
3	6" B ₄ C*	6"	B ₄ C*	6" B ₄ C
4	15" B ₄ C	3"	B ₄ C*	3" B ₄ C
5	36" B ₄ C	0	Open hole	0 Open hole
6	24" B ₄ C	3.75"	Pb	3" B ₄ C*
7	9" B ₄ C	7.5"	Pb*	9" B ₄ C*
8	6" B ₄ C*	12.25"	Pb	15" B ₄ C*
9	1.5" B ₄ C*	15.05	Pb	21" B ₄ C*

* Collimators chosen from those available to use for experiment in this report. The absorbers in the collimators were chosen for experiment of Chicago group. (3)

response on the scope further, especially since the Yoke test was expected to be larger by a factor of 1.3. This was accomplished in part by the change in sensitivity of the units mentioned above and in part by increasing the thickness of the boron-carbide absorber on some of the units. Since part of the collimators were to be filled with lead absorbers by the Chicago group for Yoke day, it was thought worth while to use one unit with a thick lead absorber (7.5 inches) to measure the background readings in the shelter.

From Table II and Table IX one can determine that for 2-Mev gamma rays the total decrease in sensitivity of the units for Yoke as compared with X-ray (due to change in unit and absorber) was, for unit No.2, $1.5 \times 3.6 = 5.4$; for unit No.3, $3.3 \times 1.5 = 5.6$; for unit No.4, $1.14 \times 1 = 1.14$; for unit No.5, $1.78 \times 1.38 = 2.5$; and for unit No.6, $1.55 \times 10,300 = 16,000$.

Since no 4-microsecond traces were obtained on X-ray, it was decided to use the same sweeps for Yoke.

Records were obtained for units 2, 3, 4, 5, and 6 from the second test (Figures 21, 22, 23, 24, and 25, respectively). These traces appeared rather good but still with too high sensitivity, so that a portion of each was near saturation. The most surprising result was the high

intensity of unit No.6 (Figure 25) which was expected to give no signal.

4.1.3 Procedure for Zebra Day

Due to lack of time between tests and the apparent stability which the units had attained, it was not thought advisable to attempt any change in the units to further reduce their sensitivity. Fortunately, it was expected that the intensity of the Zebra test would be lower than that for Yoke by a factor of three. It was hoped also that a further reduction could be achieved through the use of thicker absorbers. Requirements of the Chicago group, however, although in the right direction, as seen in Table III, did not permit the use of much thicker absorbers so as to appreciably decrease intensities.

The records of X-ray and Yoke indicated that the shape of the curve for times shorter than 50 microseconds was probably the most interesting and it would be worth while to make an effort to measure the hardness of the gammas in this region. To do this the units and absorbers were matched to give roughly equal sensitivities when using the maximum absorber thickness available. The relative sensitivities (see Table II and Table X) were about 1.5, 0.99, 2.4, 1.2 and 0.81 for units 2, 3, 4, 5, and 6 respectively.

Four of the units were set with 25-microsecond sweeps for good intercomparison in the interesting time region. Unit No. 5 was run with a 100-microsecond sweep for comparison with the previous tests.

It can be seen from the five traces (Figures 26 through 30) obtained from Zebra that the intensity was too great and most of the units are near saturation. (The hoped-for reduction in incident intensity from the changed bomb construction and available absorbers was insufficient to give good records.)

5.1 CALIBRATION PROCEDURE

A detailed and careful intercalibration of the units was begun before Zebra and finished during the following week. No complete calibration was possible prior to the tests due to lack of time and only a few measurements were available for Yoke. Since, however, the units maintained the same sensitivity throughout Yoke, Zebra, and all the calibration period, it is felt that the behavior of the units was well known during these two tests.

The calibration consisted of three main steps:

1. The static gamma-ray sensitivity determinations of the photomultiplier naphthalene unit by itself. A 1-curie RaBe source was used in a definite geometry and the dinode or plate current measured with a sensitive microammeter.
2. The time response of the complete photomultiplier and oscilloscope combination (less naphthalene) was determined by using light pulses. A fast pulse (0.3 microsecond to peak) was obtained from an argon spark and a somewhat slower pulse (1 microsecond to first peak) from an argon discharge tube.
3. The absolute sensitivity of the oscilloscopes was obtained in inches/volt by applying known voltages directly to the oscilloscope deflection plates. The relative sensitivity of the scopes plus cathode followers was determined

by comparing their signal outputs for the same signal input (i.e., same light pulse and photomultiplier unit connected to all scopes), see Figure 31. Throughout the calibrations the unmodified oscilloscope (no delay line or cathode follower, scope No. 153) together with its naphthalene photomultiplier unit (No. 5) was used as the standard and all other detecting units and scopes compared with it.

The geometry used for the static gamma-ray calibrations is shown in Figure 32 and Table I indicates all the relative sensitivity measurements made. Los Alamos source No. 43⁽⁷⁾ was used in contact with the naphthalene cover box. From this geometry one can obtain the absolute sensitivity of each unit in terms of microamperes per gamma ray per unit solid angle. The largest error occurs in estimating the effective solid angle subtended at the unit by the source as compared with that seen for the tests. Calculations of these quantities are given in the section on calculations and results.

The light sources used for the dynamic tests were kindly furnished by Dr. H. E. Edgerton. The argon spark source was a burned-out automobile headlamp which was arced by connecting a small capacity, charged to 2000 volts, across the terminals. This unit gave a smooth pulse rising

(7) One-curie gamma source.

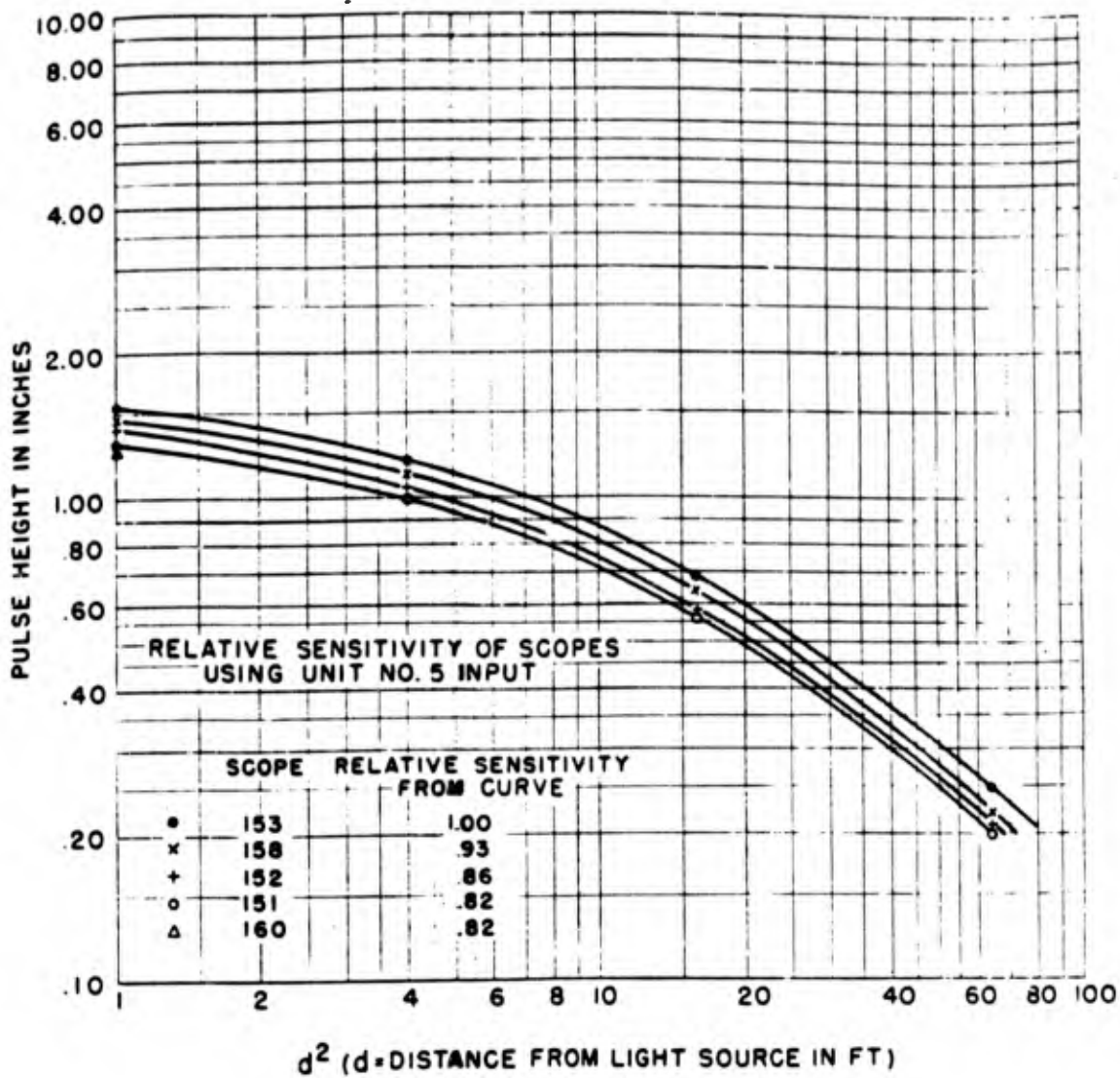
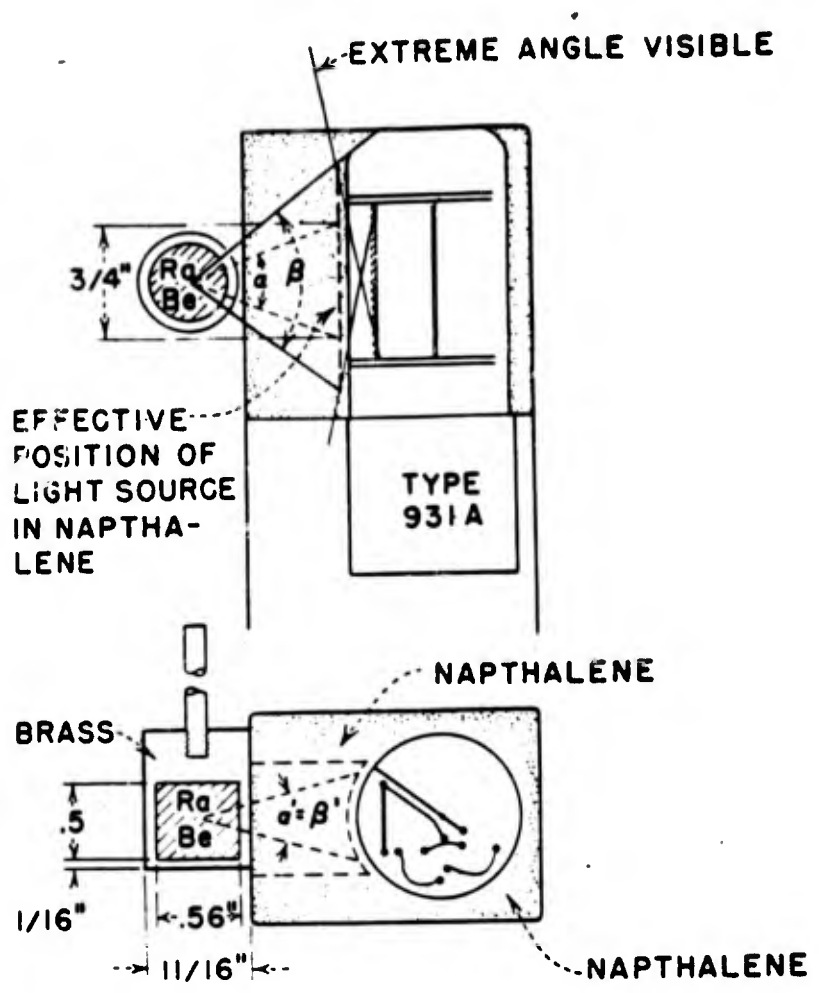


Fig. 31 Relative Sensitivity of Scope Assemblies



CALIBRATING GEOMETRY
FOR UNITS USING 1 CURIE SOURCE
 FULL SIZE

α & α' = Effective angle subtended for 3/4" collimation
 β & β' = " " " " no collimation

$$\frac{\text{Area subtended by } \beta \text{ \& } \beta'}{\text{Area " " " } \alpha \text{ \& } \alpha'} \sim 2$$

Measured Ratio = 2.2

Fig. 32 Geometry Used for Gamma Calibration

to a maximum intensity in 0.3 microsecond decreasing to 1 per cent in about 2 microseconds. This source was used to test the rise-time response of the complete units. Figure 33 is a photograph of what is believed to be the true shape of this light source. This was obtained after return to Los Alamos, by means of a very fast scope and photocell connected directly to the deflecting plates. The sweep speed used in the Figure was 0.8 microsecond/inch and the several curves were obtained by placing the light source at different distances. The rise-time of this fast scope and photocell combination was such that a vertical trace was obtained from a square pulser when a sweep speed of 0.15 microsecond/inch was used.

The argon discharge source is a commercially available unit known as a Strobotak. This source gives a very irregularly shaped pulse with many peaks. The first maximum occurs at 1 microsecond, and the intensity drops to 1 per cent in about 50 microseconds. The similarity in rise-time and drop off of this light pulse to that found in the bomb tests make it an excellent calibration source. Figures 36a, 36b, and 36c illustrate the shape of the Strobotak pulse for several light intensities and sweep speeds of 25, 100, and 1000 microseconds, respectively. The multiple peaks seem to be accurately reproducible, and their position was used to

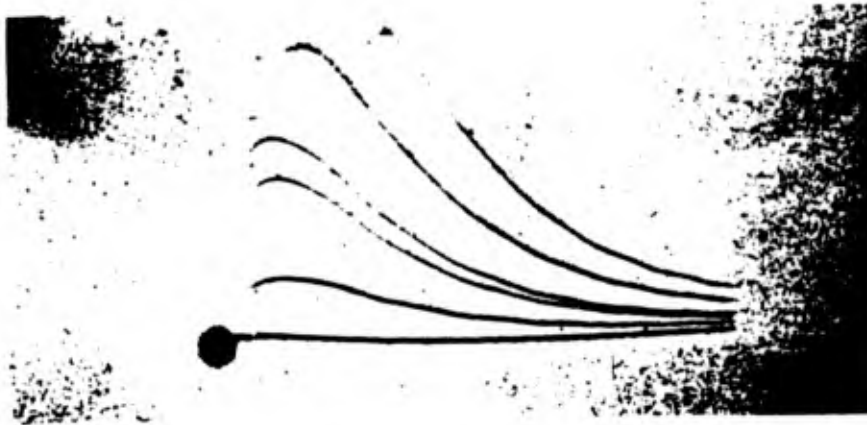


Fig. 33 Response of a Photocell to Argon Spark Light Pulses of Different Amplitudes. Sweep Speed 0.8 Microsecond per Inch.

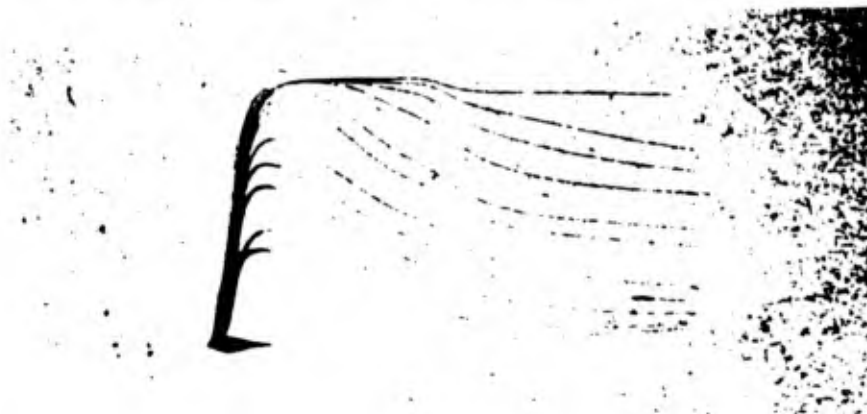


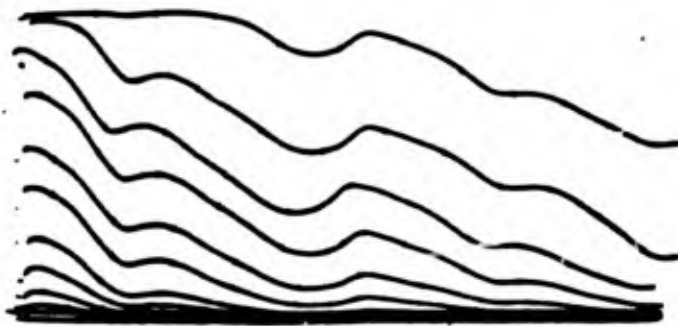
Fig. 34 Effect of Small Delay Line Reflection as Pulse Amplitude is Increased. Unit No.3 with Argon Spark Light Sources. Sweep Speed 0.88 Microsecond per Inch.



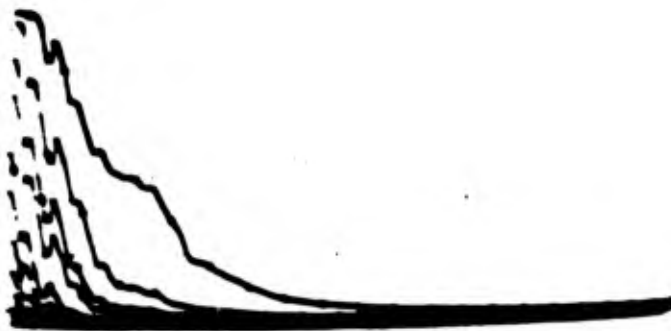
Fig. 35 Effect of Light Pulse Amplitude on Peak Position for Insensitive Unit No.2. Sweep Speed 0.94 Microsecond per Inch. Note Contrast to Figures 33 and 34.



(a)



(b)



(c)

Fig. 36 Strobotak Light Source Pulse Shape
(a) four-microsecond sweep
(b) one-hundred microsecond sweep
(c) one-thousand microsecond sweep

advantage in comparing zero times for the different sweep speeds.

The general dynamic calibration procedure, carried out on shipboard, was to take many photographs of the oscilloscope traces obtained from the light pulses of the argon spark and Strobotak. The same sweep speeds used on the tests were used for each unit and the light intensity from the sources changed in a known manner by making use of the inverse square law. Source-to-detector distances were varied from six inches to twenty feet.

The pulse amplitudes at various sweep times were measured for such a family of curves. A log-log plot of the pulse height versus the square of the distance was then made for each time interval. A linear response to intensity would give a straight line at 45° for each of the times plotted. Only the response of the photocell (Figure 33) gives such a straight line over the entire range. A measure of non-linearity was obtained for every unit by subtracting the actual points from the straight line for linear response.

The response of each unit, modified for non-linearity by a correction curve, was then compared to the true pulse shape. Small changes in some of these calibrations were then made so that each unit when corrected by its own curve gave the same final shape for various signal amplitudes.

Such a complete correction to linearity from a single calibration curve was not possible for fast-rising pulses and the fastest sweep speeds when close to saturation (>1 microsecond to maximum). Pulses near saturation, especially for some units, were difficult to correct also, due to a slight reflection from the delay line between one and two microseconds (Figures 37 and 38). These figures indicate the argon spark record for several intensities, with a 4-microsecond sweep on units No. 2 and No. 3, respectively. The reflected wave is negative and is not affected by saturation effects so that, while the main signal remains essentially constant, the reflected wave can contribute more and more with increased signal amplitude. This effect is seen also in Figure 34. The difficulty of correcting for fast-rising pulses of different amplitudes is illustrated in Figure 35 (very insensitive 931A tube, unit No. 2) by a series of argon spark signals. It is evident on this photograph that the position of the maximum of the pulse appears to be moving towards longer and longer times. Figure 34 illustrates the much better behavior in this respect of a more normal 931 tube (unit No. 3). Figure 33 illustrates the absence of such a distortion when an ordinary photocell connected directly to a fast scope is used. Here the amplitudes are so great that two of the traces

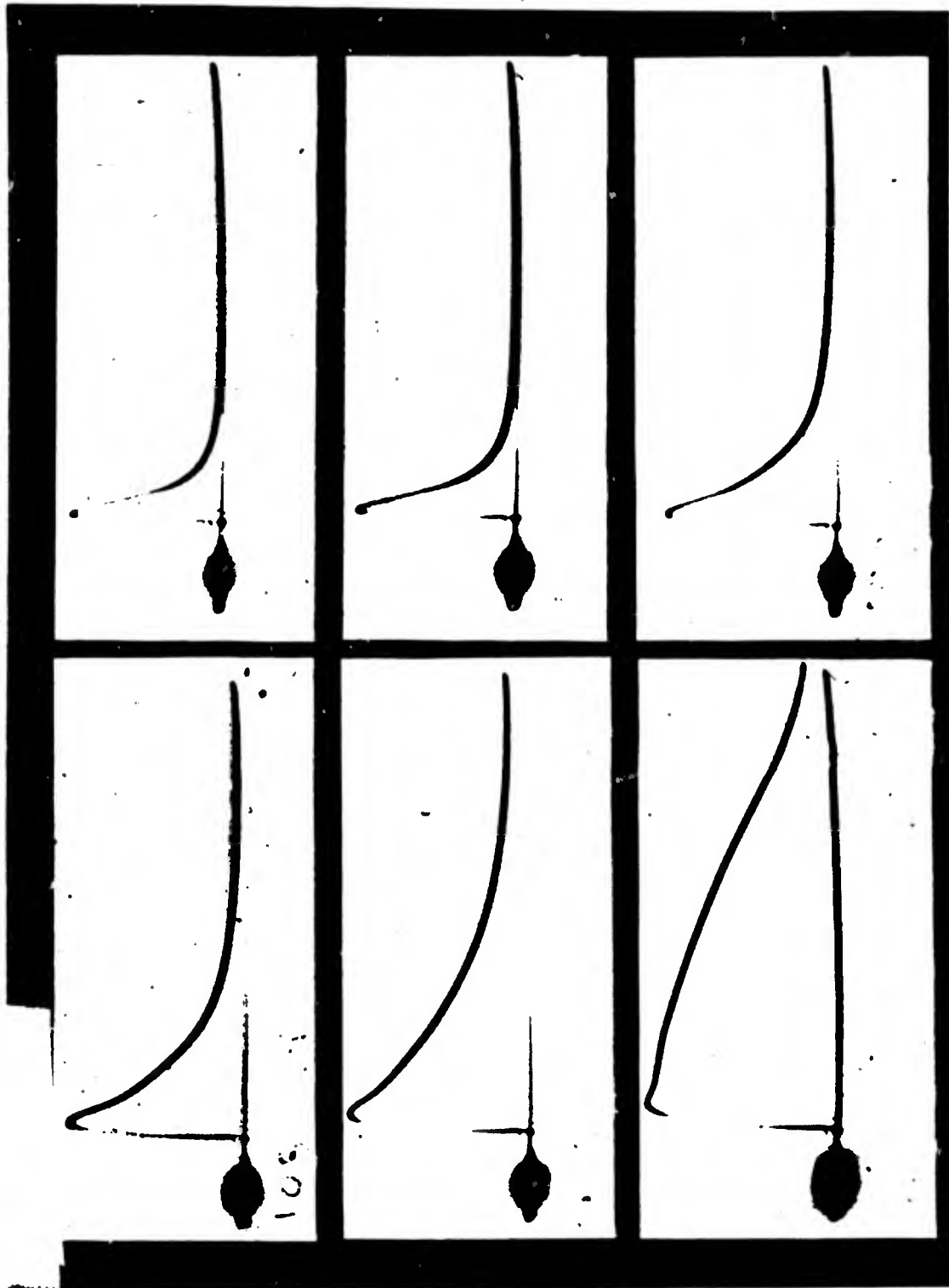


Fig. 37 Effect of Light Pulse Amplitude on Record of Unit No. 2 in Presence of Slight Delay Line Reflection. Argon Spark Source; Three Microseconds Full Sweep Axis.

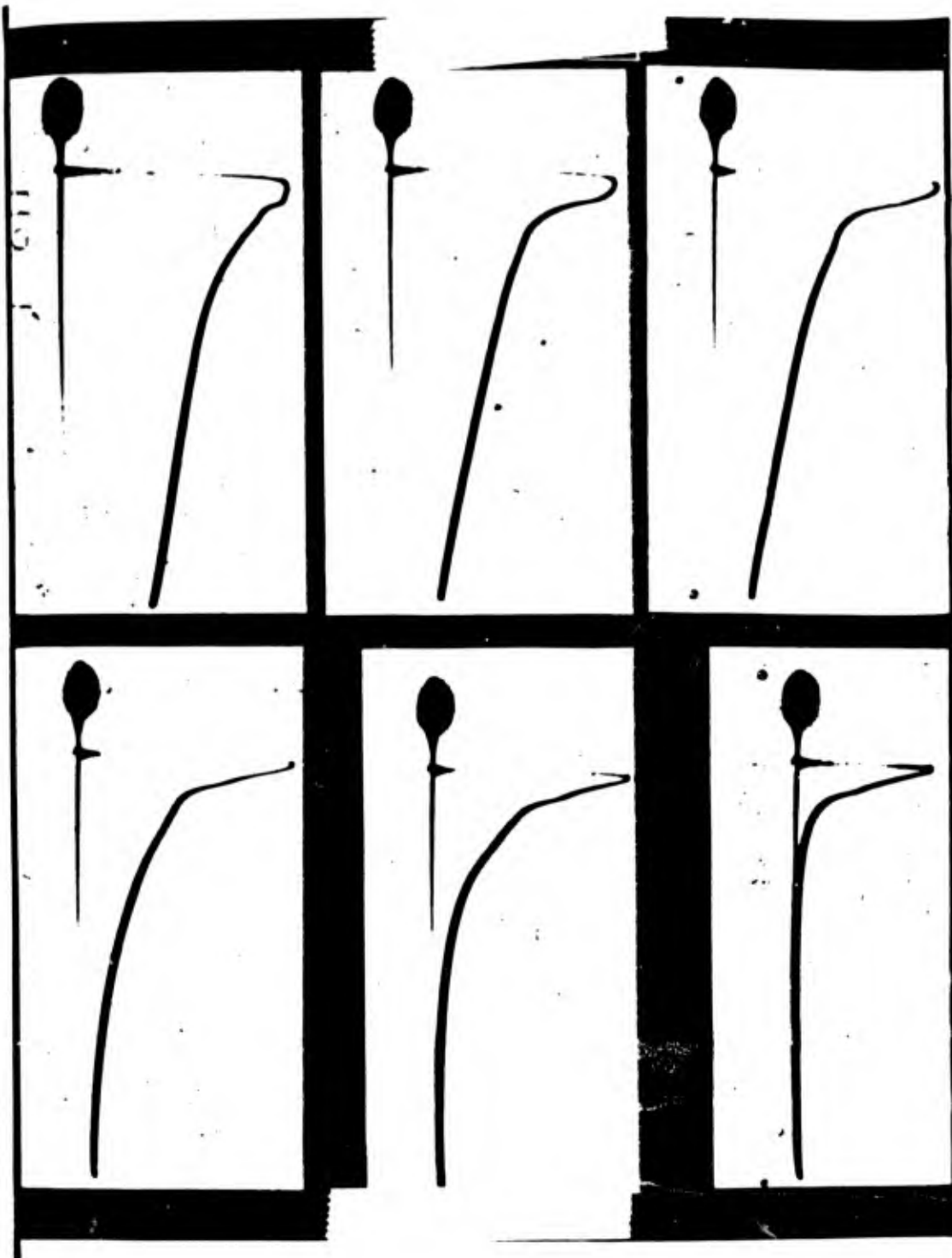


Fig. 38 Effect of Light Pulse Amplitude on Record of Unit No. 3 in Presence of Slight Delay Line Reflection. Argon Spark Source; Three and One Half Microseconds for Full Sweep Axis.

are distorted and cut off by the edge of the scope before a maximum is reached. In order to be able to choose the proper correction curve for such a peak-shift distortion some prior knowledge of the pulse size and rate of rise is required. An attempt was made to choose a suitable correction for the first microsecond on the two 4-microsecond traces obtained for Yoke. To do this a family of correction curves at 0.1-microsecond time intervals was plotted from the spark traces. Then by estimating the incident intensity of the signal the order of magnitude of the signal at each sweep time could be obtained.

Figures 39, 40, 41, 42, and 43 are the calibration curves used for obtaining the final curves. It is seen that all of these curves have a portion which appears to be almost exponential. The curve for unit No. 5 which used no delay line or cathode follower seems to give the truest exponential over a long region and then saturates quite rapidly. Units No. 2 and No. 4 have the shortest exponential section and also showed the worst behavior for different pulse amplitudes (Figure 35). These two units had the extremely low sensitivity photomultiplier tubes.

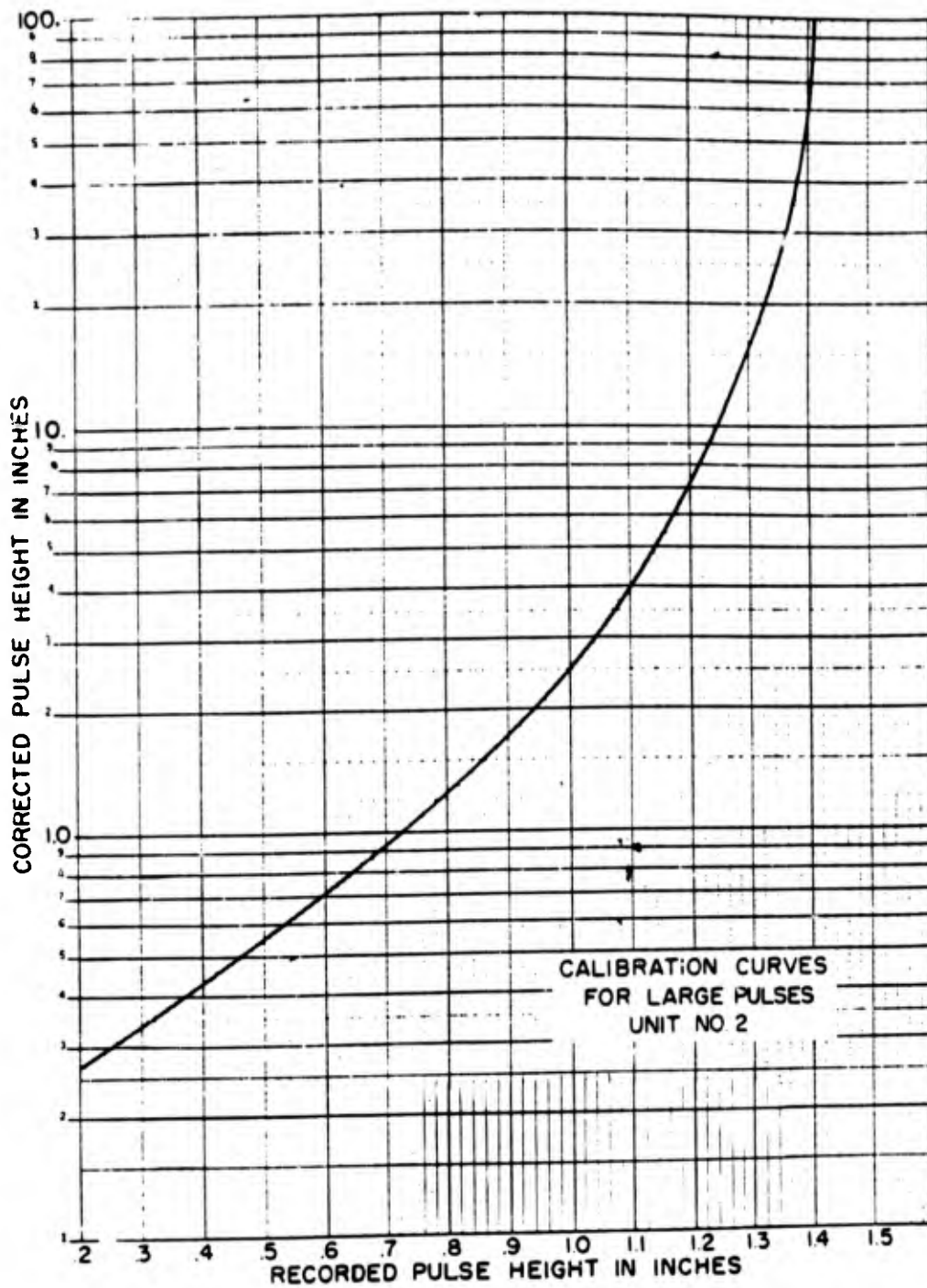


Fig. 39 Calibration Curves for Non-Linearity

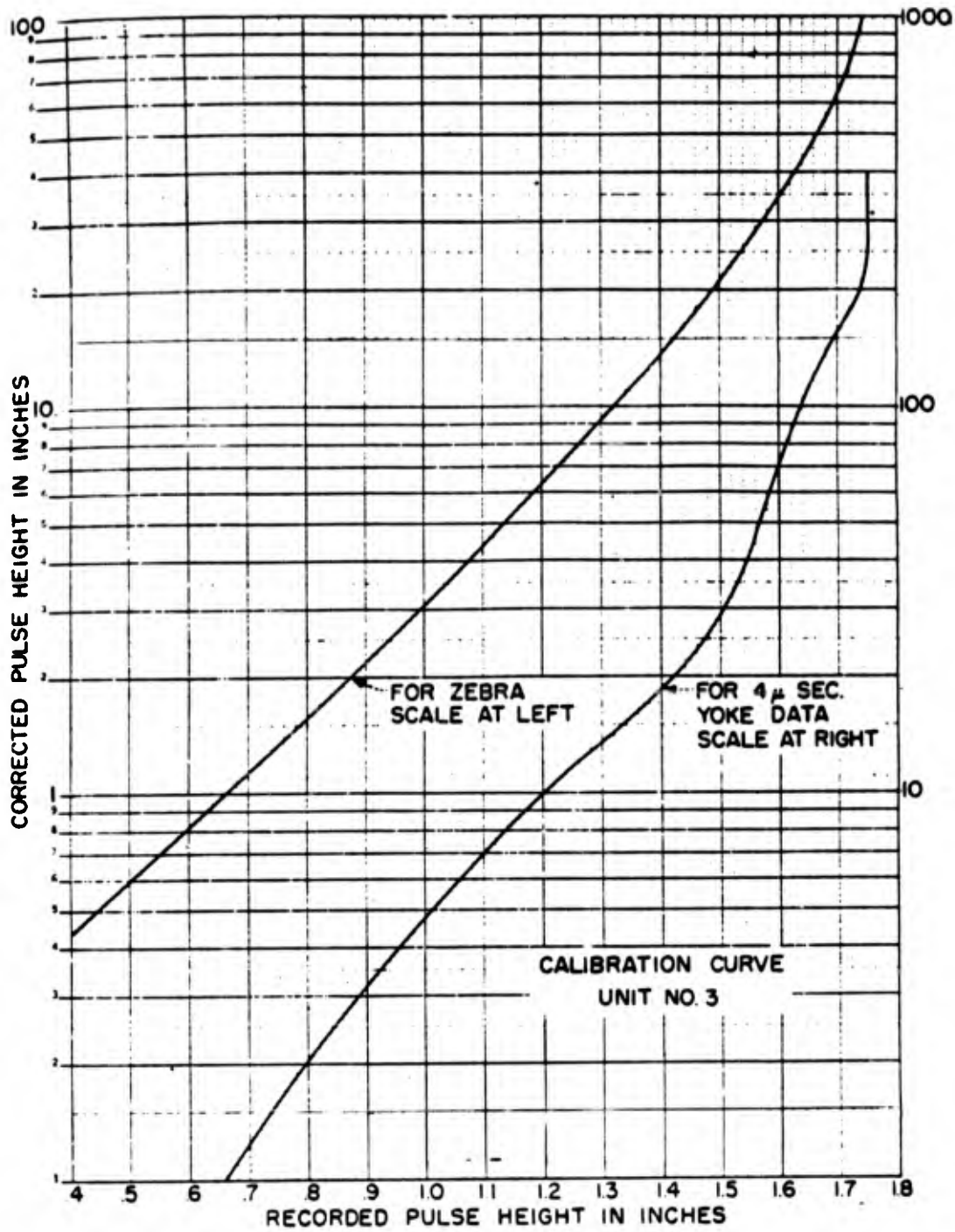


Fig. 40 Calibration Curves for Non-Linearity

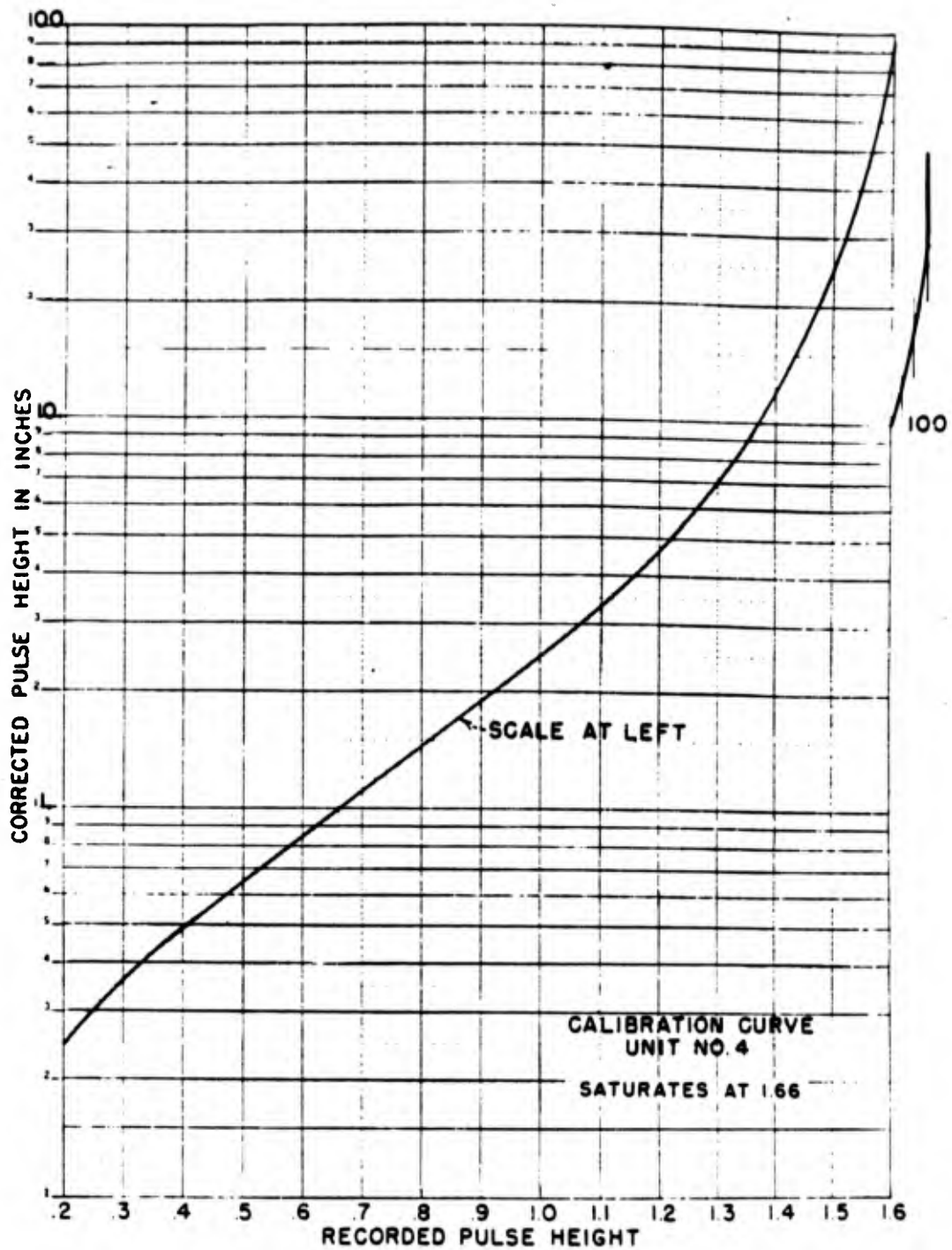


Fig. 41 Calibration Curves for Non-Linearity

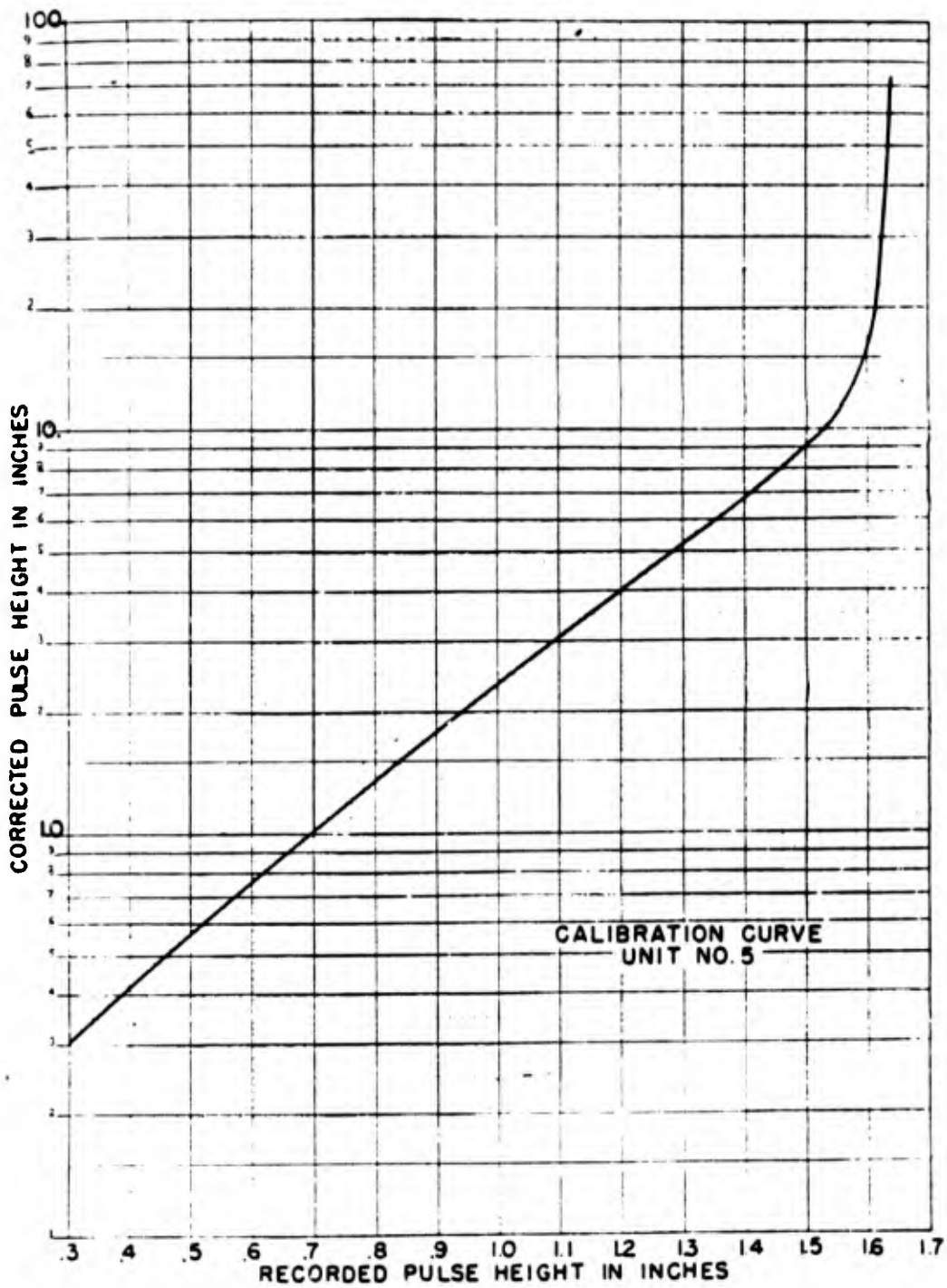


Fig. 42 Calibration Curves for Non-Linearity

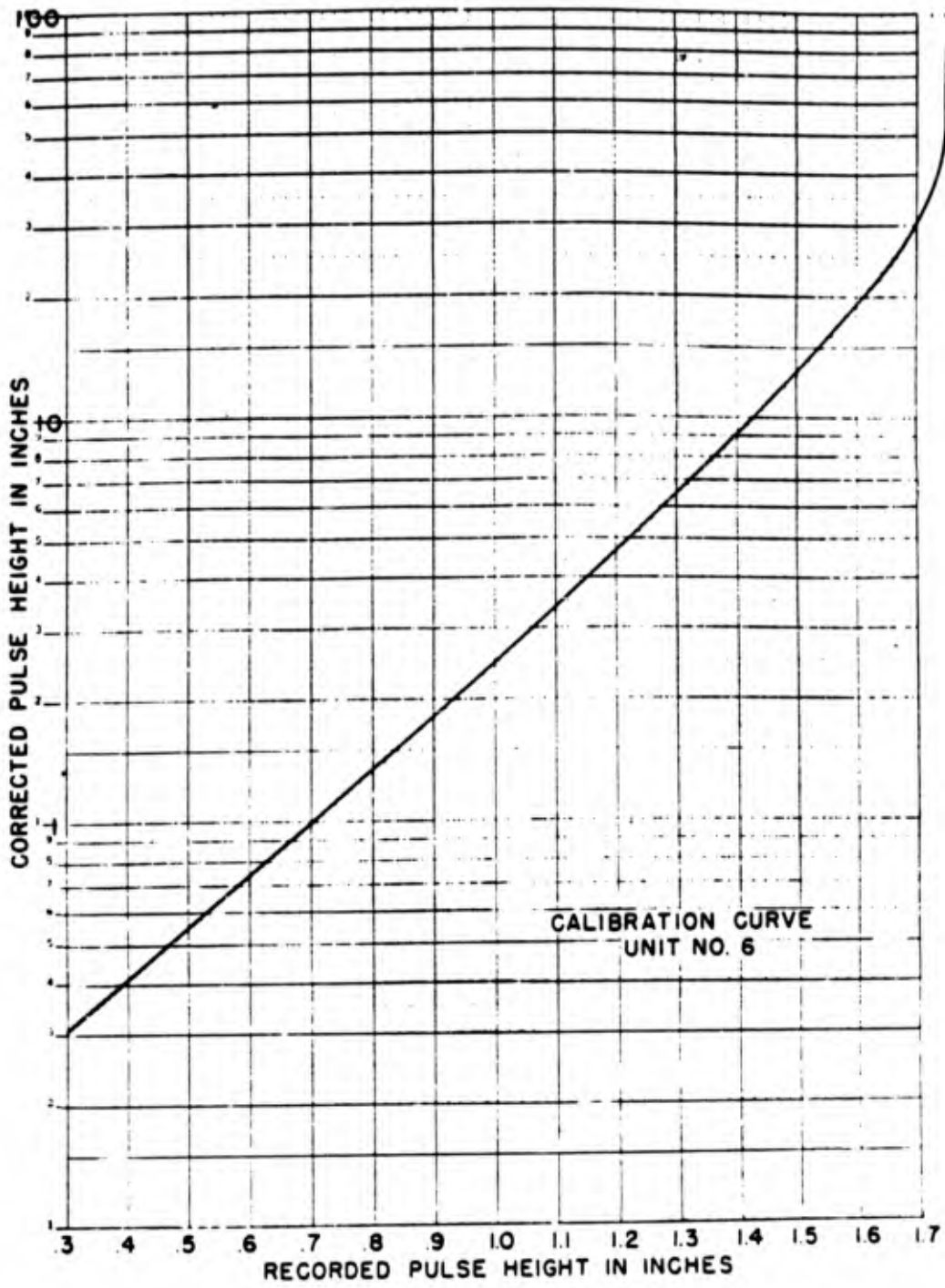


Fig. 43 Calibration Curves for Non-Linearity

6.1 CALCULATIONS AND RESULTS

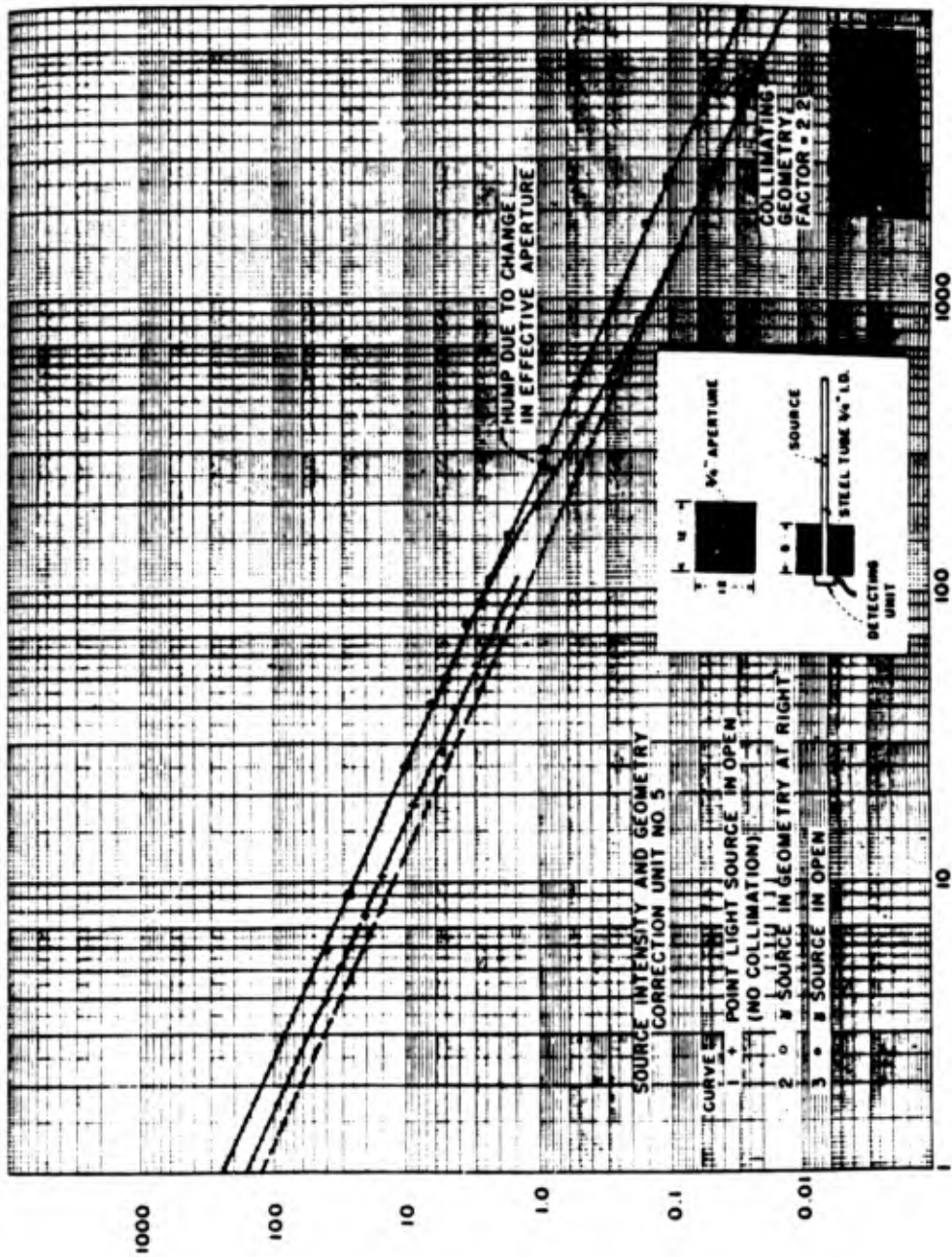
In order to convert the corrected pulse amplitudes to absolute gamma intensity values of the bomb, several factors have to be considered.

6.1.1 Absolute Gamma Sensitivity of Units

Gamma-ray responses were originally obtained by using a one-curie source in the standard geometry shown in Figure 32. The calibration values are listed in Table I. These values give relative sensitivities. Absolute response requires a knowledge of the linearity of the units for the currents obtained in the calibrating geometry; a value of the effective solid angle subtended by the source on the naphthalene photomultiplier unit; and the ratio of the effectiveness of the standard geometry to the collimated geometry used in the bomb tests.

Curve 1 of Figure 44 indicates the response of a typical unit for a constant light source whose intensity has been adjusted so as to give the same plate currents as are obtained in the standard geometry with the gamma source. It is seen that the points lie on a straight line, which for the plot used, is an indication of true linearity.

Curves 2 and 3 of the same figure are the corresponding results when the gamma-ray source is used in the standard geometry and a 3/4-inch collimated geometry (to simulate



D² (D-EFFECTIVE DISTANCE BETWEEN SOURCE & UNIT)

Fig. 44 Source Calibration Curves

bomb test geometry). In taking the data for curve 2 there is an uncertainty as to the exact distance between the source and the detector, especially for the short distance used in the standard geometry. This uncertainty arises from the unknown effective depth of the naphthalene as a radiation source. If one uses an effective depth of 1 millimeter (2.35 centimeters from source centers in standard geometry),⁽⁸⁾ the data lie on the straight line indicated by curve 2. Such a small effective depth appears quite reasonable since, as mentioned earlier, the naphthalene used was made in a polycrystalline form (mothball appearance) to reduce the unit sensitivities.⁽⁹⁾

The effect of the collimating geometry is obtained from the difference in intensities indicated by curves 2 and 3 at large distances. The departure of curve 3 from a straight line is due to the change in collimating aperture

(8)

The effective depth was checked in another manner when the gamma source was accidentally placed on the wrong side of a unit during calibration. The ratio of currents obtained should be inversely proportional to the effective distance from the source. Intensities observed were 56.5 microamperes and 17.5 microamperes or a ratio of 3.2. Using 1-millimeter effective thickness gives $\frac{(4.1)^2}{(2.35)^2} = 3.0$.

(9)

Independent measurements made on carefully cooled translucent naphthalene indicated that thicknesses in excess of one centimeter were still effective.

as the source is moved close to the detector. The geometry ratio obtained from the curves is 2.2. A rough geometric estimate indicated in Figure 32 gives a value of 2. A similar geometric estimate for the effective solid angle subtended by the source in the standard geometry gives $3.7 \times 1.5 = 5.55$ square centimeters at 2.4 centimeters from the source center.

The total number of gamma rays⁽¹⁰⁾ from the one-curie source detected in the standard geometry is

$$\frac{3.7 \times 10^{10} \alpha/\text{sec} \times 2.3 \gamma/\alpha}{4 \pi R^2} = 1.22 \times 10^9 \gamma/\text{cm}^2/\text{sec}$$

where $R = 2.35$ cm.

Unit No. 5 gives 35-microamperes plate current in the standard geometry

$$\frac{1.22 \times 10^9 \gamma/\text{cm}^2/\text{sec}}{35 \mu\text{a}} = 3.48 \times 10^7 \gamma/\text{cm}^2/\text{sec}/\mu\text{a}$$

Scope 153 used with unit No. 5 has a voltage sensitivity of 87 volts/inch deflection. A 5,100-ohm load resistor was used in all the detecting units.

$$\therefore \frac{87}{5.1 \times 10^3 \text{ ohm}} = 17.1 \times 10^3 \mu\text{a}/\text{inch pulse height}$$

Absolute sensitivity of unit No. 5
in standard geometry =

(10)

On the average, each atom decaying through all stages of radium in equilibrium with its decay products emits 2.3 quanta of gamma radiation of average energy of about 0.8 Mev.

$$\frac{3.48 \times 10^7 \text{ } \gamma}{\text{cm}^2 \times \mu\text{a} \times \text{sec}} \times 17.1 \times 10^3 \frac{\mu\text{a}}{\text{inch}}$$

$$= 5.95 \times 10^{11} \text{ } \gamma / \text{cm}^2 / \text{sec} / \text{inch pulse height}$$

Absolute sensitivity in 3/4 inch collimated geometry =

$$5.95 \times 10^{11} \times 2.2 = 1.31 \times 10^{12} \text{ } \gamma / \text{sec} / \text{inch pulse height.}$$

6.1.2 Geometry Factors.

Total reduction of the gamma rays at the 1300-yard (1189 meters) station due to attenuation and geometry are assuming 340 meters (4.6 Mev) for the mean free path of the gamma rays at this distance.

$$A_t = \frac{e^{-R/340}}{4 \pi R^2} = \frac{e^{-1189/340}}{4 \pi (118,900)^2}$$

$$= .0302 \times 5.63 \times 10^{-12} = 1.7 \times 10^{-13}$$

$$1/A_t = 5.88 \times 10^{12}$$

6.1.3 Absolute Bomb Gamma Intensity.

It was for this reason that efforts were made to make the units insensitive by using low voltage, polycrystalline naphthalene, insensitive multiplier tubes and large absorber thicknesses when possible. A unit giving a 35-microampere current with the standard source and with a scope sensitivity of 17×10^3 microampere per inch deflection was expected to give a deflection with no absorber of about 20-200 inches on a linear scale. The use of absorbers and the non-linearity of the unit were expected to make the records satisfactory. The results indicate that these estimates were approximately correct and that if somewhat thicker absorbers could have been used no part of the records would have reached complete saturation.

Tables IV, V, VI, VII, and VIII summarize the data obtained for each unit. Figure 45 is a plot of the corrected intensities as observed at 1300 yards for all usable

TABLE IV UNIT #2

- * A Time in microseconds from sweep.
- B Corrected sweep time from calibrations.
- C Amplitude of trace on 7.5 enlargement print from enlarged negative.
- D Actual trace height $\frac{\text{Reduction of camera enlargement of print}}{7.5} = 4/7.5 = .53$; correction due to paper stretch 1.023 for Y & Z.
- E Corrected to saturation value obtained from calibrations.
- F Height of record from nonlinearity correction curve.
- G Scope face distortion correction.
- H Normalization to unit #5; factor 19.6 for Yoke; 20 for Zebra.

Note: Unit #2 saturates with light pulses at 1.41; axis for Zebra adjusted slightly.
The correction curve used for Yoke is based on large amplitude spark data with 4 μ sec sweep. For Zebra correction curve is based on large amplitude spark data using 4 and 25 μ sec sweeps.

TABLE V UNIT #3

- * A Time in microseconds from sweep.
- B Corrected sweep time from calibrations.
- C Amplitude of trace on 7.5 enlargement print from enlarged negative.
- D Actual trace height reduction of camera = $4/7.5 = .53$.
Any correction due to paper stretch included in this column; 1.024 for Yoke; 1.02 for Zebra.
- E Corrected to saturation values observed from calibrations after Zebra.
- F Height of record from non-linearity correction curve.
- G Scope face distortion correction.
- H Normalization to unit #5; factor 2.7 for Yoke and 2.38 for Zebra.

Note: Unit #3 saturates at 1.74 (column D) during calibration tests. The correction curve used for Yoke is uncertain due to dependence of calibration on incident pulse intensity; the curve used is based on large amplitude spark data with 4 microsecond sweep. The Zebra calibration is based on large amplitude spark data with 25 μ sec sweep. The ripples appearing at 10 μ sec are known to be due to delay line reflection.

TABLE VI UNIT #4

- * A Time in microseconds from sweep.
- B Corrected time due to starting time loss.
- C Amplitude of trace measured on 7.5 enlargement print from enlarged negative.
- D Actual trace height $\frac{\text{reduction of camera}}{\text{enlargement of print}} = 4/7.5 = .53$, any stretch in paper included in this column;
- E 1.017 for Yoke and Zebra prints.
- F Corrected to saturation value as observed in calibrations.
- G Height of record from non-linearity correction curve.
- H Scope face distortion correction.
- I Normalization to unit #5; factor of 12 for Yoke and 12.5 for Zebra.

Note: Unit #4 saturates at 1.66 with calibrating light pulses after Zebra. This factor was used to make corrections in axis position for Yoke. The calibration curve used for the largest amplitudes was based on spark data for both the 100 μ sec and 25 μ sec data since the Strobotak intensity was insufficient for values greater than 1.4 inches.

• 7 •

page 80 is
deleted

TABLE VII UNIT #5

- * A Time in microseconds from sweep.
- B Corrected sweep time due to starting time loss.
- C Amplitude of trace measurement on 7.5 enlargement print from enlarged negative.
- D Actual trace height $\frac{\text{reduction of camera}}{\text{enlargement of print}} = \frac{2}{7.5} = .53$ correction due to paper stretch included in this column; none for Yoke; 1.023 for Zebra print.
- E Corrected to saturation value observed in calibrations after Zebra.
- F Height of record from non-linearity correction curve.
- G Scope face distortion correction.
- H Normalization to Unit #5; factor 1.09 for Yoke; 1 for Zebra.

Note: Unit #5 saturates at 1.62 with calibrating light pulses after Zebra. Correction curve based entirely on Strobotak data since sweep times are large.

Page 82
deleted

TABLE VIII UNIT #6

- * A Time in microseconds from sweep.
- B Corrected time due to starting time loss.
- C Amplitude of trace measured on 7.5 enlargement print from enlarged negative.
- D Actual trace height $\frac{\text{reduction of camera}}{\text{enlargement of print}} = 4/7.5 = 53$ (paper stretch of print used included, $Y = 0; Z = 1.019$).
- E Corrected to saturation value observed in calibrations.
- F Height of record from non-linearity correction curve.
- G Scope face distortion correction
- H Normalization to Unit #5; factor .85 for Yoke day, .89 for Zebra day.

Note: Unit #6 saturates at 1.74 μ s with calibrating light pulses from the Strobotak after Zebra. This value has been used to make slight corrections in location of axis for Yoke test. The dip occurring in the Zebra record at 1.5 microseconds is known to be due to a delay line reflection and has no significance on the record.

records. In this Figure the attenuation by the absorbers has not been taken into account so that one would expect only a similarity in shape between curves.

Table IX lists the attenuation factors for the absorbers used assuming various incident gamma-ray energies. The data plotted in Figure 45 should give a single curve for each bomb test if the correct gamma-ray energy is used, since then, the attenuation factors should be such so as to give equal incident intensities. The only curves showing any disagreement are the two 4-microsecond traces for Yoke Day where the signal appeared slightly higher for a 2-inch boron-carbide absorber than for a 9.75-inch absorber. However, as pointed out above, the correction for the peak intensity for these particular records is extremely uncertain.

the portion of the curve marked "neutron corrected" is

TABLE IX

Transmission Through B₄C and Pb Absorbers

Thickness B ₄ C	<u>Energy in Mev.</u>						
	1	2	2.5	3	3.5	4	4.5
1.5"	.63	.73	.75	.77	.787	.80	.811
3"	.394	.527	.566	.594	.619	.639	.657
6"	.157	.278	.317	.357	.383	.411	.432
9"	.062	.151	.179	.212	.237	.262	.284
9.75"	.049	.124	.156	.186	.210	.235	.254
12"	.024	.076	.101	.127	.147	.167	.186
15"	.010	.040	.057	.076	.091	.106	.122
21"	.0015	.011	.018	.027	.035	.044	.059
γ_{cm}^{-1}	.309	.210	.191	.172	.160	.149	.140
<u>For Lead Absorbers</u>							
7.5"(19.05cm)			.000105	.00014			.00013
3.75"(9.53cm)	.0004	.00737	.0103	.0116			.0113

page 87 and 88
are deleted

obtained in the following manner:

The Yoke data shown in Table VIII corrected for attenuation in the lead absorber give good agreement with the resultant curve of Figures 46 and 47 when an absorber thickness of 3.75 inches of lead is assumed. (It was pointed out above that the records of the Chicago group indicate 7.5-inch lead absorber in this collimator and 3.75-inch lead in the adjacent collimator.) The agreement for the lead absorber is good up to 25 microseconds, thereafter the intensity values are many times too great. If one assumes that this portion of the curve is primarily due to neutrons, a different and smaller attenuation factor is necessary.⁽¹²⁾ The difference between the resultant lead curve and the resultant gamma curve of Figure 46 with the use of attenuation factors for gammas and neutrons should be a measure of the relative incident neutron intensity. Figure 48 is such a plot for neutrons, the ordinates being the same as for Figure 46. The rise of this curve should represent the relative number of neutrons of different energies from the bomb since it corresponds to a time-of-flight measurement. The upper scale indicates neutron energies determined from the known distance (1189 meters) and times of arrival. The resolution of the curve is uncertain since the neutron pulse length from the

⁽¹²⁾ Neutron cross sections measured for the boron-carbide plugs used are given in Appendix B.

*page 90 is
deleted*

bomb is unknown. The absolute-intensity scale is obtained from measurements described in Appendix A.

-
- (13) LA-252.
(14) LA-253 LA-253A

*Page 92 is
deleted*

(15) LAMS-255 and LAMS-256 (under Group F-2 progress report).

- 93 -

*pages 94 + 95
are deleted*

7.1 CONCLUSIONS

An examination of the separate curves of Figure 45 and the resultant curves of Figures 46 and 47 leads to several conclusions.

(16)

Operation Sandstone Report by Groups LAJ- 4B, LAJ- 12A, N.E. Grier and E.H. Edgerton of Edgerton, Germeshausen and Grier, Inc., Annex 3, Parts I, II, and III (Sandstone Nos. 15, 16, and 17).

(17)

Gamma-Ray Intensity as a Function of Time for the Third
Sandstone Test, N. Nereson, Annex 8, Part III
(Sandstone No. 29).

*page 98 is
deleted*

(18)

Investigation of Fission Gamma Rays by Deutsch and
Rotblat. LA-170.

(19)

Gamma Rays Produced by Fission of U^{235} by Kinsey, Hanna
and Van Patter. BM-1369.

(20)

Threshold Detector Measurement of High Energy Neutrons,
G. A. Linenberger and W. Ogle.

- 100 -

*page 101 v.
deleted*

8.1 RECOMMENDATIONS FOR FUTURE TESTS

The results of the experiments reported here indicate that with more preparation and improved equipment accurate results for the gamma intensities and spectrum as a function of time may be possible.

Equipment giving a continuous recording over the desired time range can give much more information than integrated results obtained by film packs or non-recording chambers.

An experiment using a moving film behind a suitable collimator, as originally planned for Sandstone, might give information on the gamma-source size as a function of time. No information of this type is at present available.

B. Suydam has calculated, on purely geometrical grounds, that the film spot size obtained by the Chicago group for X-ray indicates a source size of about six yards. This radius is reached by the ball of fire in about 13 microseconds.

The data obtained using a lead absorber indicate that, with a somewhat better neutron detector, records of the total neutron intensity as a function of time, as well as the neutron spectrum, might be obtained with a similar geometry

to that described in this report. The intensity values would be obtained at small distances and the spectrum measurements at large distances in order to make use of the time-of-flight technique.

The main difficulties encountered in the described experiments were the following: (1) accurate calibration of units; (2) inability to locate the zeros of the scope axis precisely during each test; (3) delay in starting time of scopes; (4) too great a sensitivity of detector units; and (5) attempting to do the experiments of several groups simultaneously with the same collimators and shelters.

The calibration of the units is difficult since they are neither linear nor logarithmic and the units are each different. The use of a linear detector, although offering some advantages, might be difficult due to the large range, ~ 1000 , necessary. A careful pre-selection of tubes or the use of photocells with logarithmic amplifiers might simplify the calibration problem.

For accurate results it is absolutely necessary to know precisely how the complete equipment is behaving just prior to the test. A sweep trace and test pulse a few seconds prior to the shot should eliminate worries about effects from possible power voltage fluctuations or changes in the overall response of the equipment.

The use of faster scopes should make it possible to obtain much better records in the 0-1 microsecond time region than were obtained here.

The fact that the 931-A multiplier tubes were too sensitive in the geometry used could be overcome in several ways; (1) a greater signal attenuation by using more absorbers, going to greater distances, or decreasing the size of the collimators; (2) developing photomultipliers with a lower over-all gain and larger current capacity; and (3) the use of photocells with logarithmic amplifiers.

In conclusion it seems that good geometry experiments, i.e., using collimators, in conjunction with several different absorbers and continuous recording equipment, may offer the simplest method for obtaining intensity and energy measurements as a function of time for both neutrons and gamma rays. A similar geometry with a thin aluminum window and moving film might give estimates on the rate of growth of the gamma-ray source.

APPENDIX A

NEUTRON SENSITIVITY OF THE PHOTOMULTIPLIER NAPHTHALENE UNITS

Figure 50 is a schematic arrangement used to determine the neutron sensitivity of the units. The source was a special arrangement of the Los Alamos homogenous reactor to give a fission spectrum of neutrons and gamma rays.

Beam transmission measurements were made using bismuth, lead, iron, and boron-carbide absorbers. A photo-naphthalene unit (Unit No. 6 used at Sandstone), a U^{235} fission chamber with and without cadmium, and a U^{238} fission chamber were used as detectors. The bismuth absorbers were distributed inside the 3/4-inch collimating aperture, as well as immediately at the beam exit, to test scattering effects of the collimating geometry; the same results were obtained for both absorber positions.

Figure 51 summarizes the results obtained. It is seen that the naphthalene unit gives a much steeper initial drop off than either the U^{235} or U^{238} fission chambers which measure essentially slow- (thermal) and high-energy neutrons (> 1.2 Mev) respectively. The final slope of the curve from the naphthalene unit becomes the same as that for the neutron-detector curves.

The close resemblance and near linearity of the fast and slow-neutron curves is to be expected when bismuth is used

GEOMETRY USED FOR MEASUREMENTS
DESCRIBED IN APPENDIX A, B AND C

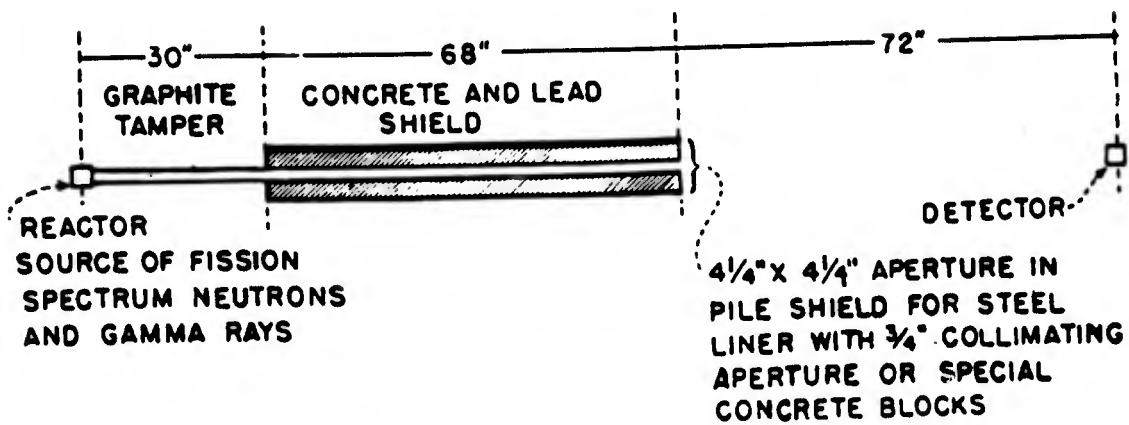


Fig. 50 Geometry Used in Experiments Described in Appendices A, B, and C

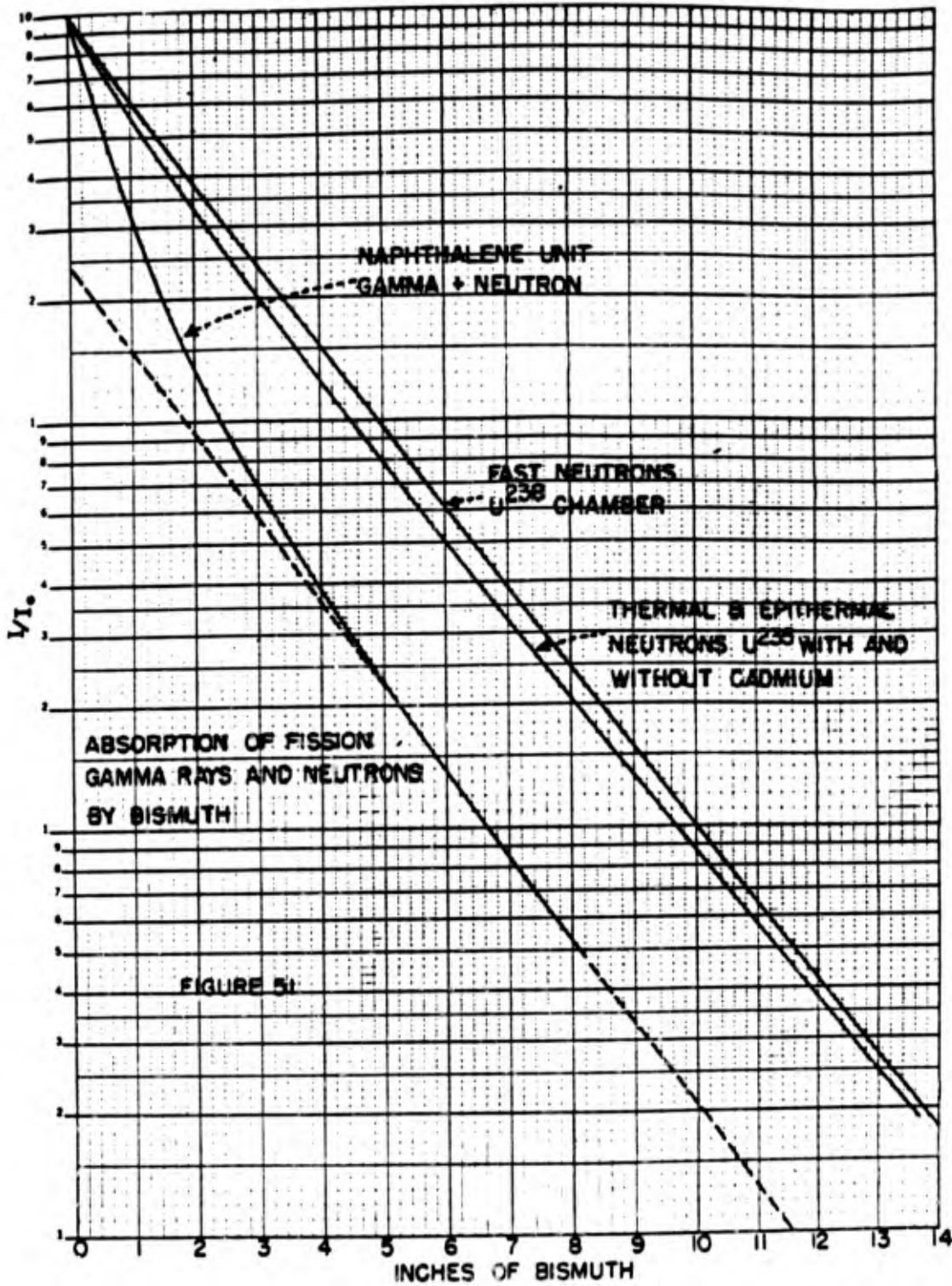


Fig. 51 Relative Neutron Sensitivity of Naphthalene Units

for the absorbing material since its total cross section is essentially constant over a wide range in neutron energy.

The shape of the naphthalene photomultiplier curve can be interpreted as being due to both gamma rays and neutrons. The final slope, which has an impossible gamma-ray absorption coefficient, corresponds closely to that of the neutron detectors. A subtraction of the slope of this part of the curve from the initial portion leaves the gamma-ray component. Such a "peeling off" gives relative sensitivities of about 76 per cent and 24 per cent for the gamma rays and neutrons from the reactor hole, respectively. A knowledge of the ratio of neutrons to gamma rays emerging from the reactor would permit an absolute neutron calibration of the naphthalene unit.

Unit No. 6 gave a total current of 2.2 microamperes from the 1-inch reactor beam shown in Figure 50. With the above relative sensitivities this represents 1.65 microamperes due to gamma rays and 0.55 microamperes for neutrons. Using the calibration value for Unit No. 6 (in the standard geometry with the 1-curie source) this current represents a gamma intensity of

$$3.48 \times 10^7 \text{ } \alpha / \text{cm}^2 / \text{sec} / \mu\text{a} \times \frac{35 \mu\text{a}}{50 \mu\text{a}} \times \frac{1.65 \mu\text{a}}{5 \text{ sq. cm.}} = 8 \times 10^6 \text{ } \gamma / \text{cm}^2 / \text{sec}$$

if the gamma-rays had the same energy as the RaBe calibrating source. For 2-Mev gamma rays the intensity would be $8 \times 10^6 \times 1.3 = 1.4 \times 10^7$ $\gamma/\text{cm}^2/\text{sec}$. This value is in fair agreement with estimates of the gamma intensity from the reactor based on geometry and power which gives about 1.1×10^7 2-Mev γ/cm^2 under similar running conditions. A direct estimate of the neutron intensity from the reactor is 9.8×10^6 neutrons/ cm^2/sec . Using this value one obtains the absolute neutron sensitivity of the naphthalene unit for fission neutrons to be

$$\frac{9.8 \times 10^6 \text{ neutrons}}{.55 \mu\text{a}} \times 5 \text{ sq. cm.} = 8.9 \times 10^7 \text{ neutrons}/\text{cm}^2/\text{sec}/\mu\text{a}$$

The approximate agreement gives one somewhat more confidence in the neutron measurements of this experiment which required several doubtful assumptions.

Similar experiments using lead, iron, and boron-carbide absorbers established that the final slope of the photo-multiplier naphthalene unit corresponds to that obtained by the fast-neutron detector (U^{238} chamber) rather than to the slow-neutron curves (U^{235} detector with and without cadmium). This result indicates that the naphthalene unit is more sensitive to fast neutrons. This is to be expected since a greater ionization is produced by a fast recoil proton than for a slow one.

The slow and fast-neutron curves obtained for these absorbers are, of course, in contrast to those from bismuth, far from linear and are also quite different from each other, due to the change of cross section with neutron energy.

The geometry used in these experiments appears to be satisfactory for the determination of total cross sections since the values obtained for the slow-, epithermal-, and fast-neutron detectors agree well, for all the detectors used, with known values.

The gamma-ray energy determined by the naphthalene detector was consistent for all the absorbers used. The average value obtained is about 1.9 Mev. This energy presumably represents the energy of the prompt and delay gamma rays in an equilibrium mixture obtained from several hours of continuous reactor operation. This value is in rough agreement with the gamma-energy measurements mentioned above, references 6 and 18, where an approximate value of 2.5 Mev was obtained for both prompt and delay gamma rays.

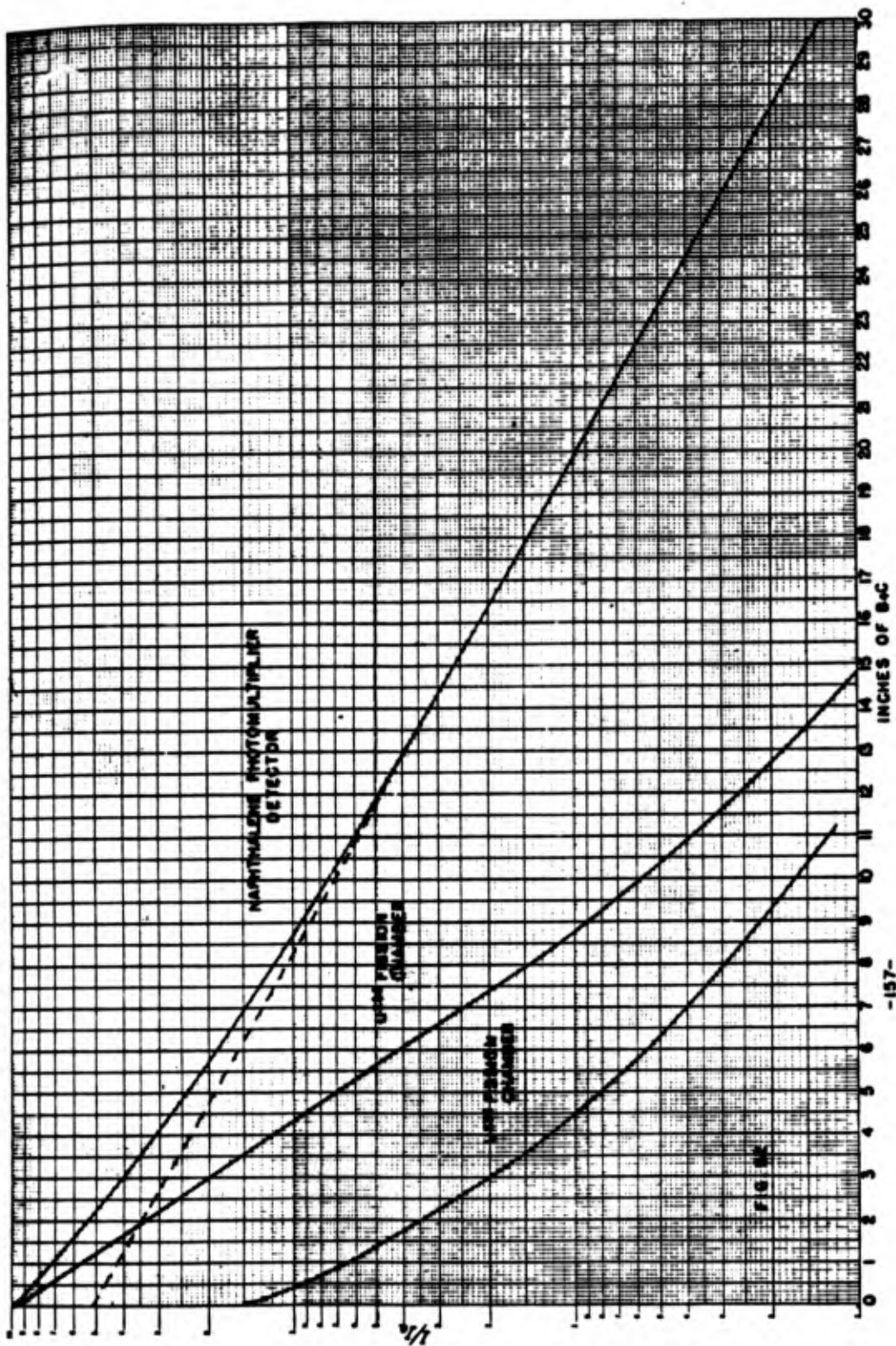
APPENDIX B

NEUTRON AND GAMMA-RAY PROPERTIES OF THE BORON-CARBIDE ABSORBER PLUGS USED AT SANDSTONE

The total cross section for fission gamma rays and neutrons was determined for the boron-carbide plugs in the geometry shown in Appendix A, Figure 50. The absorbers were placed in a 3/4-inch hole of the steel liner in the concrete shield of the pile. The geometry of absorber and detector is very similar to that used in the gamma B shelters at Sandstone.

To test the effect of absorber position a 1-1/2-inch plug was moved from the outer end of the steel tube to 50 inches inside the steel tube; a negligible effect was observed by the detectors placed 6 feet from the end of the collimator. The absorption data reported here were taken with the plugs centered about a point 1/4 inches inside the collimator with absorbers ranging from zero to 24 inches in thickness. The detectors used were: (1) one of the naphthalene photomultiplier units used at Sandstone; (2) a U^{235} fission chamber; and (3) a U^{238} fission chamber.

The results are shown in Figure 52. It is seen that the boron-carbide plugs are an efficient absorber for both the slow and fast neutrons. The curve with the slow-neutron detector shows an extremely rapid drop in neutron intensity (~ 370 barns) in the first 0.1 inch of absorber and then



-157-

Fig. 52 Neutron and Gamma-Ray Absorption Properties of Boron-Carbide Plugs

a hardening of the beam due to the removal of the slow component. The fast U^{238} neutron detector indicates an efficient removal of fast neutrons from the beam with an average cross section of about 11.5 barns.

The initial drop of the naphthalene absorption curve can be interpreted as due to the removal of the neutron component. A subtraction of the gamma-ray tail gives a slope corresponding to the U^{238} detector indicating a naphthalene detection of the fast neutron component rather than that of the slow.

The average energy of the fission gamma rays appears to be about 2.2 Mev from the naphthalene curve for the boron-carbide absorbers.

APPENDIX C

PROPERTIES OF THE SPECIAL CONCRETE USED IN THE SANDSTONE GAMMA-RAY SHELTERS

Early plans for gamma-ray measurements at Sandstone indicated that good geometry experiments should be carried out. Such measurements required adequate shielding for both gamma rays and neutrons if the secondary effects of the latter were to be minimized. Pile types of shielding appeared to be more suitable and easier to set up than lead and water shields.

A special concrete for use in the Brookhaven pile had been tested and reported at the Oak Ridge meetings (October 1947). This concrete consisted of 12.8 per cent cement, 25.7 percent limonite, 56 per cent iron punchings and 5.5 per cent water, all by weight. The concrete was reported to have a density of 270 lb/cu ft and a strength of 3,500 lb/sq in. The limonite as brown hematite $2 \text{Fe}_2 \text{O}_3 \cdot 3 \text{H}_2\text{O}$ contains a considerable amount of water which greatly contributes to its effectiveness as a neutron shield. The mean-free-path for fast pile neutrons was found at Oak Ridge to be 5.86 cm and for pile gamma rays 6.85 cms.

These figures appeared to be very favorable and it was decided to construct the Sandstone gamma-ray shelters of a similar material. The shelter thickness was calculated on the basis of the following expected intensities from a 20-kiloton bomb at the proposed shelter distances.

Shelter Distance	Fast Neutrons /cm ²	Slow Neutrons /cm ²	Total R(gammas)	Temperature assumed const. for 20 ms, U _c	Peak Over-pressure psi
600 yards	9.5 x 10 ¹⁰	4.3 x 10 ⁹	20,000	2550°	24
1300 yards	6.2 x 10 ⁸	4.5 x 10 ⁷	550	545°	5.2
1800 yards	2.7 x 10 ⁷	~ 10 ⁶	80	284°	3.2

Using the above mentioned mean-free-paths the following figures were obtained for the shielding of the special concrete.

Wall Thickness	Fast Pile Neutrons	Pile Gammas
4 ft	3.7 x 10 ⁻⁷	2.5 x 10 ⁻⁵
3 ft	5 x 10 ⁻⁵	1.1 x 10 ⁻³
2-1/2 ft	5.6 x 10 ⁻⁴	7.7 x 10 ⁻³
2 ft	6.3 x 10 ⁻³	5 x 10 ⁻²

From these values the shelter wall thickness was made as follows:

Wall Thickness	Total Fast Neutron /cm ²	Gamma Ray Total R
4 ft	3.5 x 10 ³	0.005
3 ft	3.1 x 10 ³	0.006
2-1/2 ft	1.5 x 10 ³	0.006

These values are seen to reduce both the gamma rays and neutrons to very low values. The final shelter dimensions chosen are given below.

Station Distance	Inside Dimension	Front and Top	Sides	Back	Floor
600 yds	4 x 3 x 6	4 ft	3 ft	2 ft	1/2 ft
1300 yds	8 x 7 x 8	3 ft	2 ft	1 ft	1/2 ft
1800 yds	4 x 3 x 6	2-1/2 ft	1 ft	1 ft	1/2 ft

The sides were made thinner due to the small angle at which the radiation strikes. The back required even less

material due to the large angle scattering necessary for the radiation to strike. Neutrons were expected to be the worst in this respect, and it was therefore planned to stack cans filled with water and borax against the back door.

It is believed that the neutron and gamma-ray backgrounds observed and reported in neutron measurements (see references 20 and 3) are due to scattered radiation from the direct beams admitted through the collimators rather than any leakage through the shelter walls. Such backgrounds could be eliminated or greatly reduced by a more complete catcher arrangement for the beams, reducing the number of beam ports per shelter and always using some absorber in the collimators.

The actual concrete mixtures obtained in the shelters are reported in Sandstone 39 (Annex 16, Part II, of Scientific Director's Report). Excellent density values were obtained with even higher water content than was obtained in the Brookhaven tests.

Figure 53 summarizes measurements made on blocks made with the Sandstone gamma shelter concrete mix. These blocks were $4\frac{1}{4}$ inches by $4\frac{1}{4}$ inches in cross section and of several lengths. They fitted exactly into a pile port, and measurements were made in the geometry shown in Figure 50. The values obtained are total cross section measurements

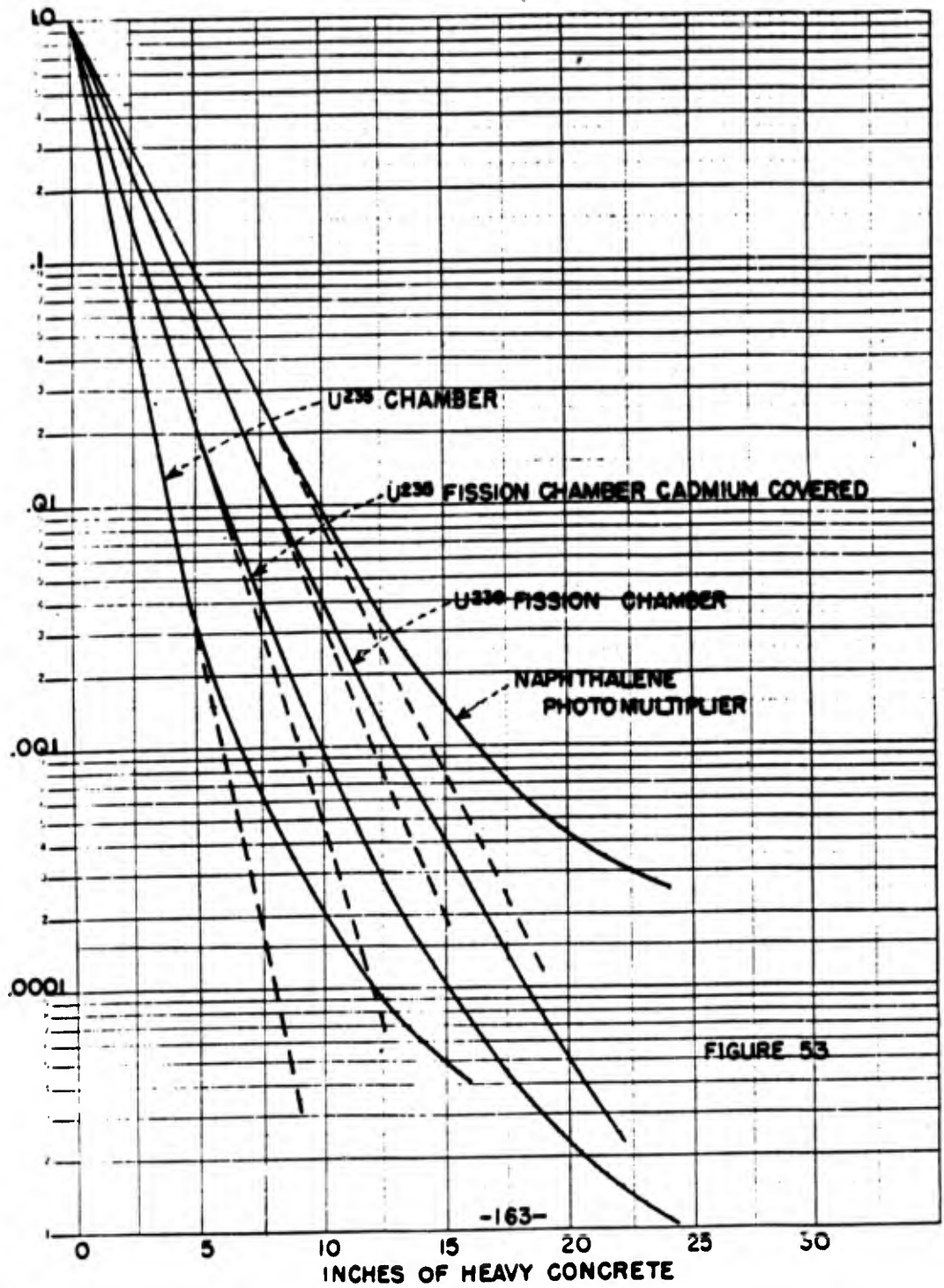


Fig. 53 Neutron and Gamma-Ray Absorption Properties of Special Concrete

and therefore give values which are presumably somewhat optimistic for a large shield. The material is seen to be extremely effective giving mean-free-paths for fission gammas of 5.2 cm and values of 4.5, 3.6 and 2.2 cm for fast, epithermal and slow neutrons for straight-line portions of the curves. These results are in rough agreement with Oak Ridge values. Hardening of the beam is quite apparent after a reduction in intensity of 10^3 .

Table I has been included since it may be helpful in designing future shelters. The table compares the values obtained here with fission-spectrum neutrons and gamma rays to those obtained by Gugelot and White⁽²¹⁾ using 16-Mev protons on beryllium. This reaction gives a neutron spectrum with a maximum at about 2 Mev and very hard gamma rays of average energy of about 7 Mev with some as high as 10 Mev. Our values as well as those quoted from Oak Ridge give better attenuation values. This is to be expected for the gamma rays since the fission gamma rays have energies of about 2 Mev instead of 7 Mev. The mix used at Sandstone had a lower cement and higher limonite content than that used at Princeton which might account for a slightly better

(21)

The Shielding Qualities of Different Concrete Mixtures, P.C.Gugelot and M.G.White, Palmer Physics Laboratory, Princeton, New Jersey, carried out with assistance by the Joint Program of the Office of Naval Research and the Atomic Energy Commission.

TABLE I

ATTENUATION THICKNESS FOR NEUTRONS (CM) GAMMA RAYS (CM)

Factors of 10	ATTENUATION		THICKNESS FOR NEUTRONS (CM)							SANDSTONE MIX			GAMMA RAYS (CM)						
	Number of Half Intensity Thickness	Water	Normal Concrete	Cement and Magnetite Ore	Cement and Limonite Ore	Cement and Limonite and Iron Scrap	U235 Chamber	U235 Chamber and Cadmium	U238 Chamber	Water	Normal Concrete	Cement and Magnetite Ore	Cement and Limonite Ore	Cement, Limonite and Iron Scrap	Sandstone Mix				
10 ⁻¹	3.33	18.3	35.6	28.3	16.0	17.5	5.1	7.6	10.2	49.4	44.4	30.0	30.0	26.3	12.1				
10 ⁻²	6.66	36.7	71.4	56.6	32.0	35.5	10.2	15.2	20.3	98.8	88.8	60.0	60.0	52.6	24.1				
10 ⁻³	9.99	55.0	107.0	85.0	48.0	53.5	16.8	25.4	33.0	148.2	133.2	90.0	90.0	78.9	30.8				
10 ⁻⁴	13.32	72.6	142.5	113.2	64.0	71.2	30.5	38.1	46.2	197.6	177.6	120.0	120.0	105.2	49.5				
10 ⁻⁵	16.65	91.5	178.1	141.5	80.0	89.0			61	247.0	222.0	150.0	150.0	131.5					
10 ⁻⁶	19.98	110.0	214.0	169.8	96.0	107.0				296.4	266.4	180.0	180.0	157.8					
10 ⁻⁷	23.31	128.2	250.0	198.1	112.0	125.0				345.8	300.8	210.0	210.0	184.1					

NOTE: All above values except column marked Sandstone Mix are results obtained at Princeton (Ref. 11) using neutrons and gamma rays from reaction of 16-Mev protons on Beryllium. Average γ ray energy 7 Mev with some intensity at 10 and 11 Mev. The neutrons had a spectrum with maximum at 2 Mev detectors for neutrons were Ag foils with and without cadmium measuring thermal and resonance neutrons (15 and 50 ev). The gamma rays were measured with a Geiger Counter. Sandstone measurements are for fission neutrons (1 Mev maximum intensity) and gamma rays (2 Mev) using fission chambers and naphthalene detectors.

neutron attenuation factor. The presence of such high-energy gamma rays for the Princeton measurements might produce secondary neutron effects in the absorber or detectors. Silver foils with and without cadmium were used to measure the thermal and resonance neutrons (50 and 15 ev) as compared with the fission chambers used here.

APPENDIX D

Figures

- 1 Picture of Camera and Dumont Type 256D Scope
- 2 Picture of Boron-Carbide Absorber Plugs and Spacers
- 3 Picture of Collimating Tubes and Frame
- 4 Picture of Collimating Frame in Position in Shelter
- 5 Picture of Collimators as Seen by Detectors
- 6 General View of 1300-yard Shelter
- 7 Shielding Over Door in Back of Shelter
- 8 Schematic Layout of Detectors in Shelter
- 9 Schematic Circuit Diagram of Equipment
- 10 View of Equipment in Position in Shelter
- 11 View of Equipment in Position in Shelter
- 12 Close-Up View of Detector Unit
- 13 Close-Up View of Detector Unit
- 14 View of Trigger Unit Mounted on Shelter
- 15 View of Trigger Unit Mounted on Shelter
- 16 Circuit Detail of Trigger Unit
- 17 Circuit Detail of Detector Unit
- 18 X-Ray Day Traces of Units 4, 5, and 6
- 19 X-Ray Day Traces of Units 4, 5, and 6
- 20 X-Ray Day Traces of Units 4, 5, and 6
- 21 Yoke Day Traces of Units 2, 3, 4, 5, and 6
- 22 Yoke Day Traces of Units 2, 3, 4, 5, and 6

Figures (continued)

- 23 Yoke Day Traces of Units 2, 3, 4, 5, and 6
- 24 Yoke Day Traces of Units 2, 3, 4, 5, and 6
- 25 Yoke Day Traces of Units 2, 3, 4, 5, and 6
- 26 Zebra Day Traces of Units 2, 3, 4, 5, and 6
- 27 Zebra Day Traces of Units 2, 3, 4, 5, and 6
- 28 Zebra Day Traces of Units 2, 3, 4, 5, and 6
- 29 Zebra Day Traces of Units 2, 3, 4, 5, and 6
- 30 Zebra Day Traces of Units 2, 3, 4, 5, and 6
- 31 Relative Sensitivity of Scope Assemblies
- 32 Geometry Used for Gamma Calibration
- 33 Spark Pulse Shape with Photocell
- 34 Spark Pulse Shape with Sensitive Unit No. 3
- 35 Spark Pulse Shape with Insensitive Unit No. 2
- 36 A, B, C Strobotak Calibrating Pulse Shape
- 37 Delay-Line Reflection Unit No. 2
- 38 Delay-Line Reflection Unit No. 3
- 39 Calibration Curves for Non-Linearity
- 40 Calibration Curves for Non-Linearity
- 41 Calibration Curves for Non-Linearity
- 42 Calibration Curves for Non-Linearity
- 43 Calibration Curves for Non-Linearity
- 44 Source Calibration Curves
- 45 Corrected Intensity Curves of Detectors

Figures (continued)

- 46 Final Composite Curves Semi-Log Plot
- 47 Final Composite Curves Log-Log Plot
- 48 Neutron Spectrum
- 49 Final Curve γ Intensity Curve 50 - 1000 Microseconds
- 50 Geometry Used in Experiments Described in Appendices A, B, and C
- 51 Relative Neutron Sensitivity of Naphthalene Units
- 52 Neutron and Gamma-Ray Absorption Properties of Boron-Carbide Plugs
- 53 Neutron and Gamma-Ray Absorption Properties of Special Concrete

TABLES

- I Summary of Relative Gamma Sensitivity of Units
- II Summary of Unit Arrangement for Tests
- III Summary of Absorbers Available for Each Test
- IV Summary of Results Obtained Without No. 2
- V Summary of Results Obtained Without No. 3
- VI Summary of Results Obtained Without No. 4
- VII Summary of Results Obtained Without No. 5
- VIII Summary of Results Obtained Without No. 6
- IX Transmission Through the Boron-Carbide Absorbers as a Function of Thickness and Energy (Calculated)
- X Summarized Neutron and Gamma-Ray Absorption Properties of Various Types of Concrete

SCIENTIFIC DIRECTOR'S REPORT
OF ATOMIC WEAPON TESTS
AT ENIWETOK, 1948

Annex 8

GAMMA-RAY MEASUREMENTS

Part III

GAMMA-RAY INTENSITY IN THE 100-MICROSECOND REGION
FOR NUCLEAR EXPLOSION OF MAY 15, 1948

GAMMA-RAY INTENSITY
IN THE 100-MICROSECOND REGION
FOR NUCLEAR EXPLOSION
OF MAY 15, 1948

By

Norris Nereson

September 1, 1948

TABLE OF CONTENTS

I. PREFACE 3
II. ABSTRACT 3
III. EXPERIMENTAL PROCEDURE 5
IV. RESULTS AND DISCUSSION 9

GAMMA-RAY INTENSITY IN THE 100-MICROSECOND REGION
FOR NUCLEAR EXPLOSION OF MAY 15, 1948

I. PREFACE

The experiment described in this report is being recorded more for guidance of personnel doing future experiments of this nature rather than for the experimental findings involved. Experimental results presented here are necessarily crude since the experiment received no stateside planning and the equipment in use consisted of gear available at the test site or stock items which could be flown out upon short notice. Due to the above reasons the results were not as beneficial and conclusive as might have been obtained with proper and sufficient detecting and recording equipment.

II. ABSTRACT

A large coaxial cylinder, gas filled, ionization chamber was used to investigate the shape of the gamma-ray intensity versus time relationship in the 100-microsecond region for the atomic bomb test explosion of May 15, 1948. The chamber in use was identical to that used in the alpha measurements and was located on top of the gamma B station at a distance of 1300 yards from the bomb. Slit collimation geometry was roughly provided by placing the chamber at the rear of the shelter and by placing a 6-inch-thick layer of lead on the top and the sides of the chamber. The chamber output signal was taken from a 100-ohm load resistor connected in series with the ionization chamber and then conveyed directly onto the vertical deflection plate of a cathode-ray tube; the horizontal plates of the same tube were connected to a linear sweep unit triggered by a gamma-ray sensitive, naphthalene-photomultiplier unit.

There is no evidence on the early part of the curve indicating any arrival of fast neutrons from the bomb or any other neutron effects. The general shape of the curve is in fair agreement with that obtained by L. D. P. King using a naphthalene-photomultiplier, gamma-ray detector.

A complicating feature of this experiment is the positive ion space charge which accumulates in the chamber when such large currents occur over sufficiently long time intervals. A rough calculation shows that the space charge is large enough at 2 microseconds to appreciably distort the true gamma intensity signal from the chamber. It is possible by a tedious and lengthy calculation to correct for the space charge and obtain the true gamma intensity curve,

but at this writing the end result does not appear to justify the work involved.

III. EXPERIMENTAL PROCEDURE

A more complete experiment of gamma-ray intensity versus time in micro-second regions is reported by L. D. P. King, who has used naphthalene-photo-multiplier detector units. The experiment described in this report is essentially a duplication of the above effort except that a different detector, an ionization chamber, has been used. The results obtained from a different detector unit would prove useful for a comparison of the relative shape of the intensity curve and a comparison of the absolute number of gamma rays recorded by the two detector units. Since the available oscilloscope-film combination could not record the fast rise of the initial gamma-ray intensity, the effort was directed towards obtaining the latter part of the gamma-ray curve and looking for any indications showing the arrival of neutrons from the bomb.

The chamber in use was identical to the chambers used by E. Krause of the Naval Research Laboratory for the measurement of alpha and transit time of the bomb. These chambers consisted of two concentric cylinders having a spacing of 1 cm, effective length of 60 inches, an outer diameter of 7 inches and outer wall thickness of 1/8 inch. The chamber was filled with a purified argon and carbon dioxide (about 2%) mixture to a gauge pressure of 25 psi.

As shown in Figure 1, the chamber was placed on the roof of gamma B shelter located 1300 yards from the bomb tower. The 3-foot thick, concrete-iron ceiling shielded the chamber from gamma-ray scattering from the ground and earth induced activity. In order to minimize air scattering a lead layer 6 inches thick and 2 feet wide was placed over the top of the entire chamber. The ends of the chamber were similarly shielded by a 4-inch thickness of lead. This essentially provided a slit opening facing the bomb for gamma rays entering the chamber volume.

The chamber was calibrated with various artificial sources at Los Alamos¹. A current measuring instrument was used to measure the steady ionization current when the source was placed at a great enough distance so that inverse square law conditions were in effect (distances larger than 5 feet). The calibration results shown below give the chamber current per source gamma per second when the chamber is placed at a distance of 2 meters from the source.

1.65 Mev RaLa gammas	1.82×10^{-20} amps/(source gamma/sec)
1.0 Mev Ra gammas	1.15×10^{-20} amps/(source gamma/sec)
0.85 Mev Po gammas	1.1×10^{-20} amps/(source gamma/sec)

The chamber was also calibrated for neutron sensitivity by using a Po-Be source and various absorbers¹. The following sensitivities were obtained at a chamber distance of 2 meters.

PoBe neutrons (mean energy of about 3 Mev)	0.7×10^{-20} amps/(source neutron/sec)
1 Mev neutrons (calculated)	0.2×10^{-20} amps/(source neutron/sec)

It is seen that for 1-Mev neutrons and gammas, the neutron sensitivity is down by a factor of about 6 as compared to the gamma sensitivity.

¹ See LAMS - 748 by R. F. Taschek

Electrical connections to the chamber and associated recording equipment for Zebra day are shown in Figure 2. The inner chamber cylinder was utilized for electron collection by giving it a positive potential of 2400 volts with respect to the outer cylinder. The output signal was taken across a load resistor of 100 ohms placed in series with the high voltage supply. The chamber capacity was $800 \mu\mu\text{fd}$ and the attached cable capacity was about $300 \mu\mu\text{fd}$. This made the chamber time constant about 0.1 microsecond and permitted rapid gamma-ray fluctuations to be observed. Since the high voltage battery supply was of rather high impedance, a $6 \mu\text{fd}$ capacitor was connected across it to supply the chamber surge current.

The chamber output voltage developed across the 100-ohm load resistor was condenser-coupled to the vertical deflection plate of a 5LP5 cathode-ray tube permitting chamber currents from 0.1 to 2 amperes (or voltage signals from 10 to 200 volts) to be recorded. Also, another oscilloscope coupled to an amplifier was in use for recording chamber currents in the range from 0.01 to 0.1

ampere (not shown in Figure 2).

The experiment for Zebra day was set up chiefly for the purpose of recording the delayed ~~gamma~~ intensity after the nuclear reaction. Since the available equipment would not record the fast writing speed associated with a trace of the initial ~~gamma~~ peak, effort was directed towards obtaining a time trace of the delayed activity. Also, it did not seem meaningful to attempt to record currents larger than of the order of amperes (for time intervals like 100 microseconds) due to the disturbing influence of large positive ion space charge effects occurring in the chamber at these large current values. After the Yoke day results, it was clear that in order to eliminate positive ion space charge effects, it would have been desirable to use a chamber with a gas pressure diminished by a factor 100 of that being used in the available chamber.

The sweep unit of the P4 synchroscope was modified so that it would operate as a servoscope sweep, i.e., sweep only when a trigger was applied. The trigger for the sweep was taken from the same naphthalene-photomultiplier unit which furnished a trigger for L. D. P. King's equipment.

The oscilloscope display on the 5LP5 tube was photographed with a camera having an f 2 lens and an image reduction of a factor 4. Unfortunately, the potential across the cathode-ray tube was only about 2 KV so fast writing speeds could not be photographed. The camera shutter was opened at minus 10 seconds and closed shortly after 0 time. Power for the oscilloscope was turned on at minus 15 minutes and turned off at plus $1/4$ second.

A time calibration of the sweep showing 10 microsecond markers is shown in Figure 3. A voltage calibration of the vertical or signal plate of the cathode-ray tube is contained in Figure 4. The central photograph represents

a 90-volt step function and the lower photograph shows 45- and 135-volt step functions applied to the vertical plate. (The superimposed signals on the steps were for the purpose of ascertaining the writing speed which could be photographed.)

IV. RESULTS AND DISCUSSION

The photograph obtained on Zebra day (Figure 5) shows that the rise of the gamma-ray intensity is not visible due to the fast writing speed and that the trace goes off the oscilloscope face for approximately the first 10 microseconds. Apparently, the signal returned at this point with a faster writing speed than the oscilloscope-film combination could record since it first becomes visible considerably inside the useful area of the oscilloscope screen. A graphical trace of this photograph is reproduced in Figure 6 with the ordinate given as chamber current in amperes as derived from the voltage output across the 100-ohm-load resistor.

The trace obtained does not represent a true picture of the gamma-ray intensity versus time. The error arises from the abnormally large number of slow-moving positive ions produced in the chamber which seriously distort the electric field within the ion collecting volume. When positive ions have accumulated in

sufficient number within the chamber so as to form a charge approaching that on the chamber, then the electric field at the anode approaches zero and the true electron current begins to be modified. Since the charge on the chamber is $Q = CV = 10^{-9} \times 2400 = 2.4$ microcoulombs, an average current of 2.4 amperes passing through the chamber for 1 microsecond releases this charge. Therefore, if the average current during the first microsecond is 3 amperes, the trace begins to be in error after approximately one microsecond.

The trace indicates that at least 15 microcoulombs were liberated during the first 10 microseconds. This charge would cause the electric field to reverse at the anode and affect the trace by reducing the electron current. The trace is also influenced by the relatively slow motion of the large number of positive ions. Therefore, in the first few microseconds the chamber current decreases faster than the gamma intensity because of the reverse field set up by the positive ions. Later the motion of positive ions may behave so as to increase the chamber current above the true intensity.

It is possible to calculate the true gamma intensity curve by using the trace obtained and assuming an initial chamber current. Preliminary calculations on this matter by B. Suydam indicate that such a calculation would require a month of work from the IBM machines. At the present time, this amount of work does not seem to justify the end result. These preliminary calculations show that the chamber current is distorted by 3% at 1.3 microseconds and by 10% at 2 microseconds.

The general shape of the trace agrees fairly well with that obtained by L. D. P. King using a naphthalene-photomultiplier detector. The chamber signal does not decrease as rapidly in the latter part and cover as large an intensity

range as the naphthalene detector. This is to be expected on the basis of the errors discussed above.

From the chamber calibration with a known gamma-ray source, it is possible to calculate the rate of emission of gamma rays from the bomb at a certain time. The calibration with the gammas from the RaLa source has been taken as that most closely approximating the gamma-ray energies present in the nuclear explosion. Using this calibration, the average number of gammas released per second from the bomb during the time region of the first few microseconds when the chamber current (assumed to be only electron current) was approximately 3 amperes is obtained as follows:

*300 meters has been taken as the average mean free path for gamma rays emitted from the bomb.

The above figures are in fair agreement with other experiments giving the number of gammas released per second from the Zebra bomb into the air. The 935 photocell and naphthalene detector unit of H. E. Edgerton's (Edgerton, Germeshausen & Grier, Inc.) gave a value of about

L. D. P. King's results from the 931 photomultiplier naphthalene units are also in the above range; his exact figures are not available at this writing.

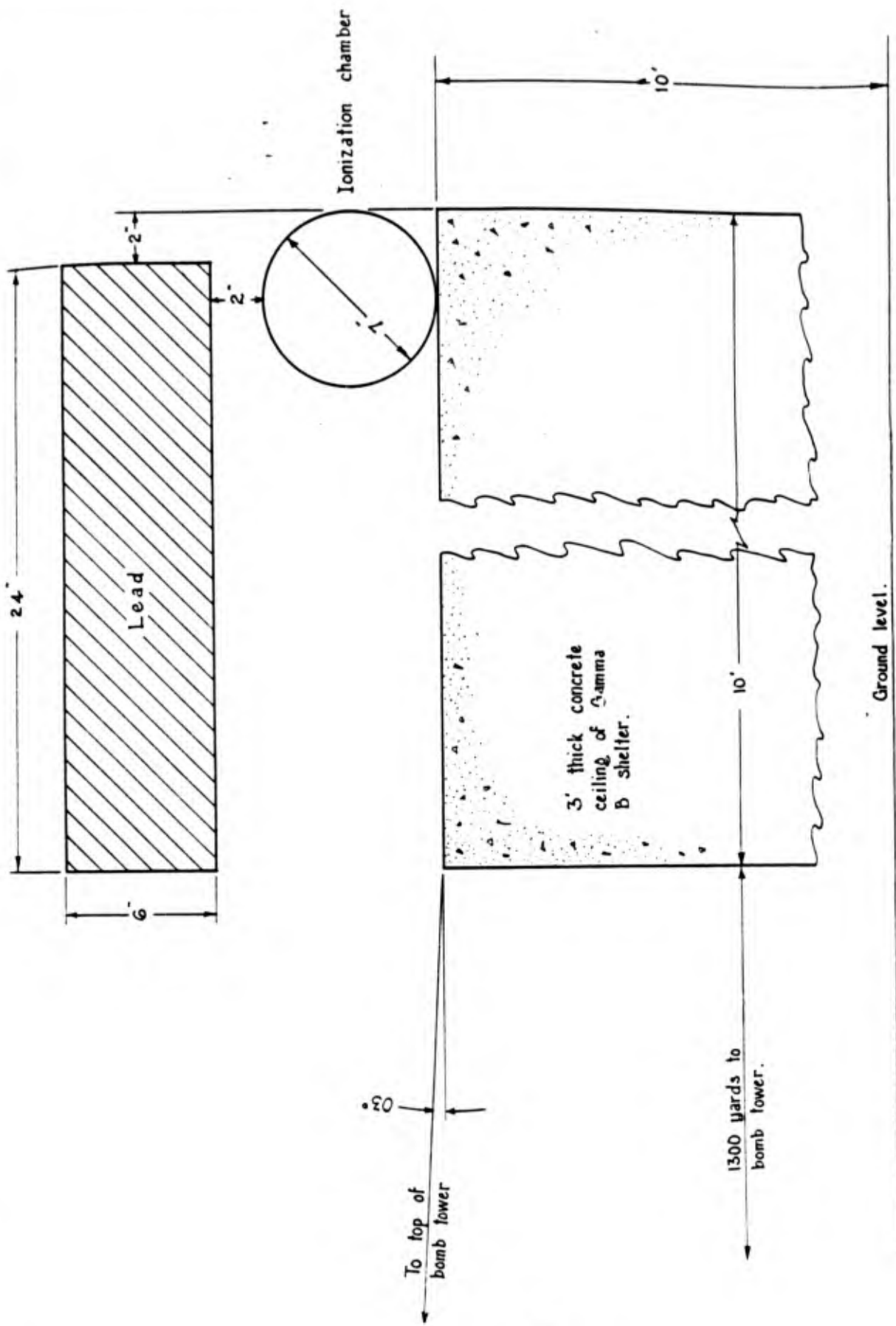
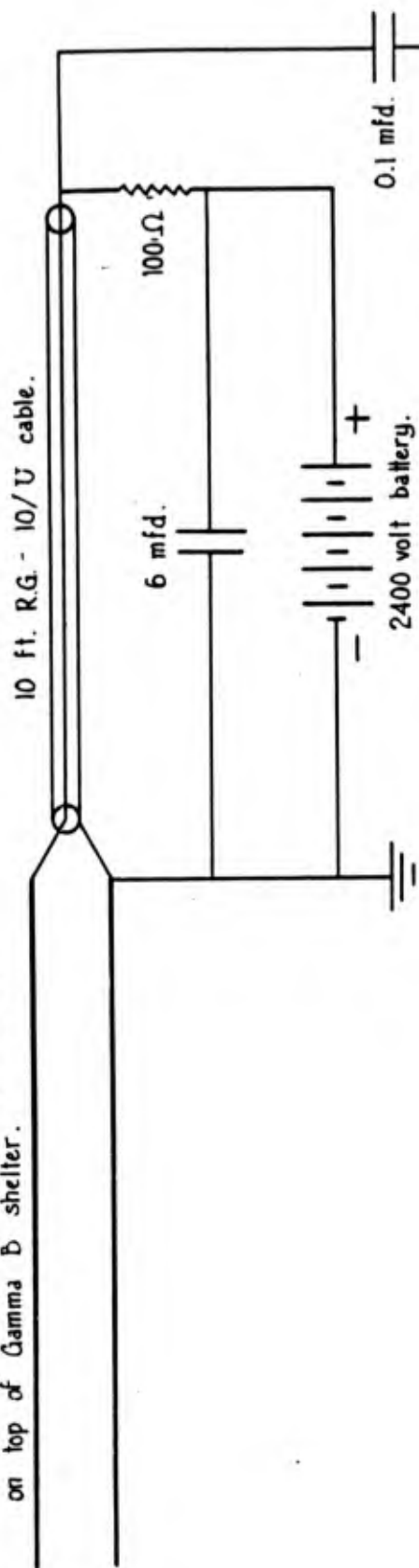
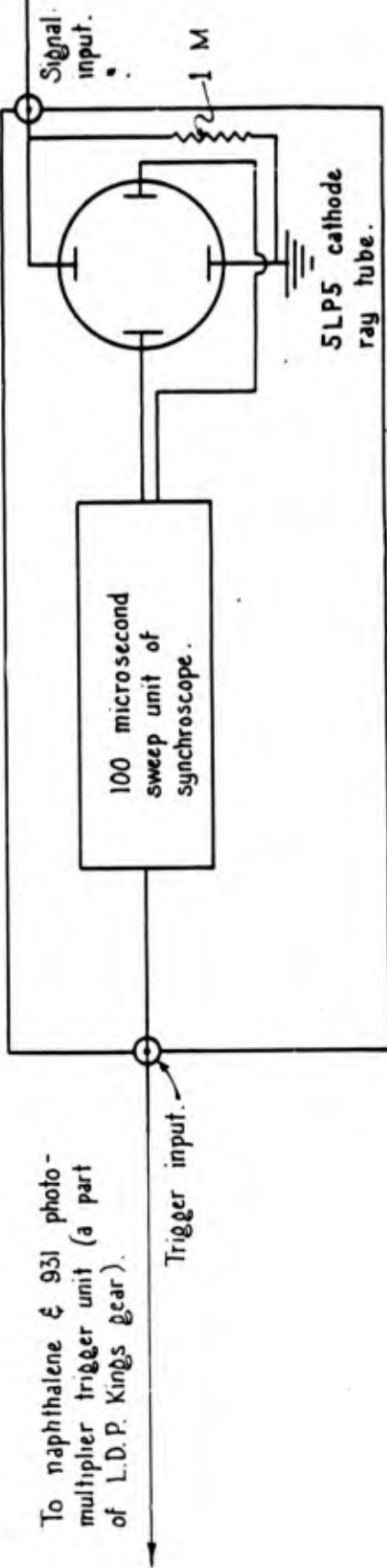


Figure 1. Location & Geometry of Ionization chamber detector.

Parallel plate Ionization Chamber located on top of Gamma B shelter.



To naphthalene ξ 931 photo-multiplier trigger unit (a part of L.D.P. Kings gear).



Modified model P-4 synchroscope

Figure 2. Simplified diagram of equipment used in the experiment.

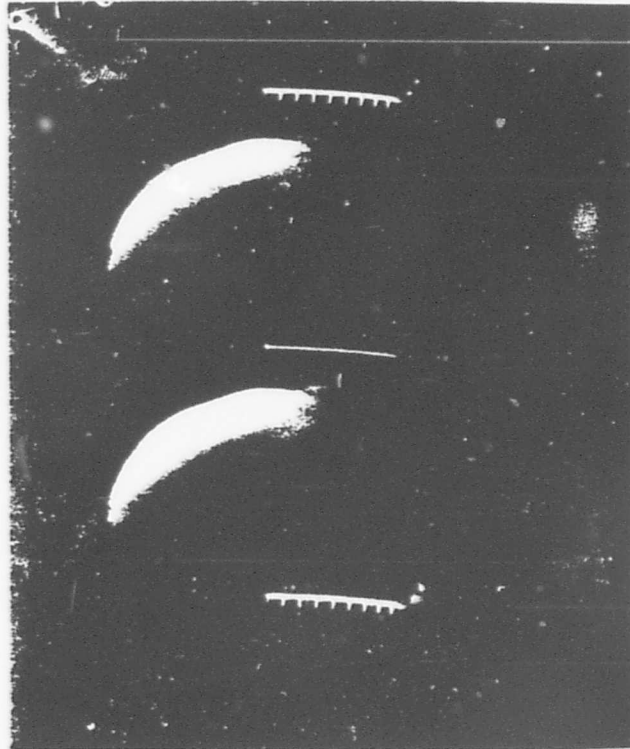


Fig. 3 Time Calibration of Sweep Using 10-Microsecond Markers



Fig. 4 Voltage Calibration of Vertical Signal Plate of Cathode-Ray Tube (See Text for Calibration Figures)

Fig. 5

Upper and Lower
Photographs

- Stationary Spot and Reference Base Line of
Cathode-Ray Tube

- 17 -

*page 18 is
deleted*

SCIENTIFIC DIRECTOR'S REPORT
OF ATOMIC WEAPON TESTS
AT ENINETOK, 1948

Annex 8

GAMMA-RAY MEASUREMENTS

Part IV

GAMMA RADIATION VERSUS DISTANCE

Task Group 7.6

Project Report

GAMMA RADIATION VERSUS DISTANCE

OPERATION SANDSTONE

by

Herbert Scoville, Jr.

CDR Edmund J. Hoffman, USN

LT Earl C. Vicars, USN

30 June 1948

Project 7.1-17/RS-1

TABLE OF CONTENTS

I	ABSTRACT	3
II	OBJECTIVE	3
III	HISTORICAL	4
IV	EXPERIMENTAL	5
	A. Theoretical	5
	B. Material and Equipment	6
	C. Distribution	7
	D. Calibration Procedures	9
V	RESULTS	11
VI	DISCUSSION	19
	A. Lethal Range	19
	B. Attenuation	19
	C. Strength of Gamma-Ray Source	24
	D. Residual Radioactivity from Ground Contamination	26
VII	CONCLUSIONS	27
	APPENDIX A	28

GAMMA RADIATION VERSUS DISTANCE

I. ABSTRACT

Gamma radiation exposures have been measured as a function of distance for the X-ray, Yoke, and Zebra tests. Film badges used for this measurement covered a range of exposure from 0.05 to 22,000 roentgens and their sensitivity was found to be practically independent of energy between 0.5 and 1.5 Mev. The lethal range of the gamma radiation as observed by these measurements was 1500, 1600, and 1350 yards for Tests X-ray, Yoke and Zebra respectively. Calculations made on the basis of measurements of the radiation intensity made by monitors upon re-entry to the test sites indicate that the residual contamination in the crater provides only a negligible contribution to the total gamma radiation exposure from the explosion. From the film data it has been possible to derive equations which satisfactorily express the variation of exposure with distance over the ranges measured, namely from 700 to 3000 yards. These equations indicate that the apparent mean-free-path of the gamma radiation in air is approximately 350 yards. It has also been possible on the basis of these equations to estimate the relative strength of the gamma-ray source for the three tests.

II. OBJECTIVE

The object of this project was to measure the gamma radiation exposure from each atomic weapon as a function of distance in order to evaluate the effectiveness of this radiation in producing casualties and to get the mean-free-path for absorption.

III. HISTORICAL

Calculations made prior to the Trinity tests did not indicate that the gamma radiation would be a major factor in the production of casualties from an atomic bomb detonation. However after the actual employment of the weapon at Hiroshima and Nagasaki it was found that the gamma radiation accounted for about 15 per cent of all deaths and a large number of casualties that survived. The median lethal range was estimated by the British as 1400 yards.

At Trinity, efforts were made to measure the gamma radiation exposure by means of films, but because of inability to recover the films promptly the experiment was not too successful. At the Bikini tests the gamma radiation was measured as a function of distance by Dr. Dessauer with considerable success. Some inaccuracy resulted from the uncertainty of orientation of the films with respect to the burst because of the semimobile nature of the target ships. Shielding and scattering by the ships' structures also interfered with the measurements.

When Operation Sandstone was proposed, a project was suggested by the Armed Forces Special Weapons Project for the measurement of this important phase of the weapons' action. This work was proposed in a memorandum from the Armed Forces Special Weapons Project dated 1 September 1947, to the Test Director and was subsequently approved and assigned to the Radiological Safety Group (Task Group 7.6) for detailed planning and accomplishment. This information was also requested by the Bureau of Ships, Department of the Navy, and the Chief of Engineers, Department of the Army. Various other offices of the Armed Services and the Los Alamos Scientific

Laboratory have also expressed interest in obtaining these data.

IV. EXPERIMENTAL

A. Theoretical

Gamma radiation may be emitted during and immediately following an atomic bomb detonation in four ways:

1. Gamma-ray emission in the fission process.
2. (n, γ) reactions with materials of the weapon and any other materials in its immediate vicinity.
3. Radiation from the fission products formed in the fission reaction.
4. Neutron and primary gamma-ray induced activity in materials in the neighborhood of the explosion.

No attempt was made in this experiment to estimate the relative quantities given off by the various processes since this was being done in experiments conducted by Dr. Shonka and Dr. King. However, the exposure recorded on the films from residual radioactive deposits up until the time the films can be safely collected might be of practical importance in wartime operations. Therefore, attempts were made to separate the prompt-gamma radiation from the residual. This was done by measuring with a portable meter, the intensity of the residual activity at the time the film was collected. From this and a knowledge of the decay rate, the exposure due to residual contamination can be calculated directly.

The attenuation of gamma radiation with distance will be due to two factors. The gamma radiation will decrease inversely as the square of the distance, and exponentially by absorption in the air. The relationship between the gamma exposure and distance may be expressed in the following form, assuming monochromatic radiation:

$$\text{Exposure, } E = \frac{E_0 \times 10^{-R/X}}{R^2} \quad (1)$$

This form of equation was observed at Bikini indicating that over the distances measured calculation of the air absorption coefficient may provide a check on the energy spectrum as measured by other investigators.

B. Material and Equipment

The total quantity of gamma radiation was measured by the use of film badges. This method was selected because of its simplicity, absence of need for auxiliary services at the test site, general reliability, and ease of obtaining duplicate data for checking. The badges consisted of seven films, each with a different emulsion which was designed to be useful over a different range of exposure. The film was obtained from the Eastman Kodak Company, and their designations with useful ranges follow:

Designation	Range in Roentgens
1. Type I	0.05 - 1.65
2. Type A	0.4 - 6.1
3. Cine Positive 5301	1.5 - 75
4. Cine Positive 5302	11 - 275
5. Translite single coat	50 - 2000
6-7. 548-0 single coat	1000 - 22,500

These films were packaged in three light proof packs, 1 and 2; 3, 4, and 5; and 6 and 7, with a 1/32-inch lead cross over the front of each unit. The three packs were then sealed in a larger single waterproof aluminum foil jacket which then constituted one total range

film badge as shown in Figure 1. In addition to the total range badges, 100 badges with an NTC emulsion on a film base were obtained. This emulsion has an extremely low sensitivity for gamma radiation and was used in an attempt to measure very high gamma exposures. The range of this film is 30,000 to 150,000 roentgens in dry air but unfortunately high humidity affected the sensitivity.

C. Distribution

The experimental installation designed to measure gamma radiation as a function of distance consisted of film badge stations at intervals of 100 yards, where possible. These commenced at a distance of 400 yards from the zero point and extended outward to about 3000 yards. In general the stations were placed upwind, but on some islands they were downwind in order to determine the seriousness of fall out from the cloud.

For test X-ray, angle iron stakes (2" X 2" X 3/16") were driven into the coral for stations out to 1000 yards from the zero tower and smaller stakes (1" X 1" X 3/16") were used for the remainder. At 1000 yards, four additional stakes were provided for additional film badges in order to obtain information regarding the uniformity and reproducibility of data obtained. In all cases, four badges were mounted on each stake and held to the stake by use of an adhesive cement. No additional protection for the badges other than the aluminum foil envelope was provided for in this test.

In Tests Yoke and Zebra, the same procedures as outlined above were carried out except that the badges were given additional protection from the effects of blast and heat which caused ignition of

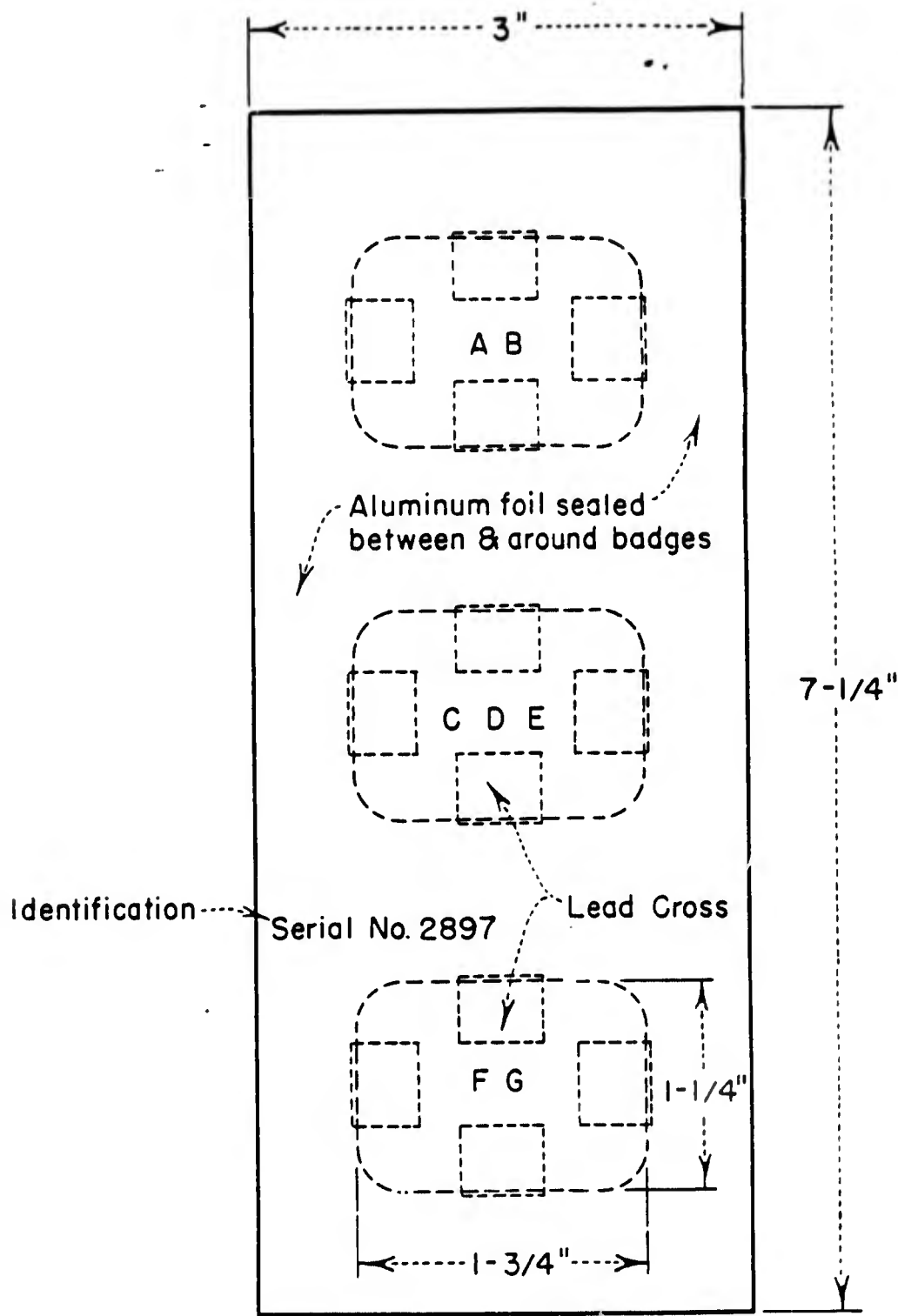


Fig. 1 Film Badge

the aluminum foil covering and spoiled many films in Test X-ray. This protection was accomplished by wrapping the film badges individually in a layer of glass cloth and placing an aluminum strip in front of the badges and bolting the strip to the angle iron stake. Small wooden blocks were placed between the aluminum strip and the angle iron stake in order to provide necessary clearance for the film badge and to protect the film badges from pressure due either to bolting or to blast. The assembly is shown by Figure 2.

All film badges were placed normal to the blast except for four badges at 1500 yards on Test Yoke. These badges were located parallel to the direction of blast in an attempt to observe the film reaction for this type of situation.

The film badges selected for this study were placed in the field on X-ray minus one day, Yoke minus two days and Zebra minus two days and recovered on test dates and test dates plus one. They were then shipped to the National Bureau of Standards for development and reading.

D. Calibration Procedures

Of a total lot of four thousand badges, 250 were sent to Dr. Lauriston S. Taylor at the National Bureau of Standards, Washington, D.C. There they were calibrated by exposure to X-rays with energies up to 1.5 Mev as given in Appendix A. Calibration at higher energies will be made at a later date. Until more information is available on the energy of the radiation from the explosion, the calibration at 1.5 Mev was used to determine the exposures of the films.

In addition, approximately fifty film badges were placed in several test positions where they were exposed to the unfavorable climatic

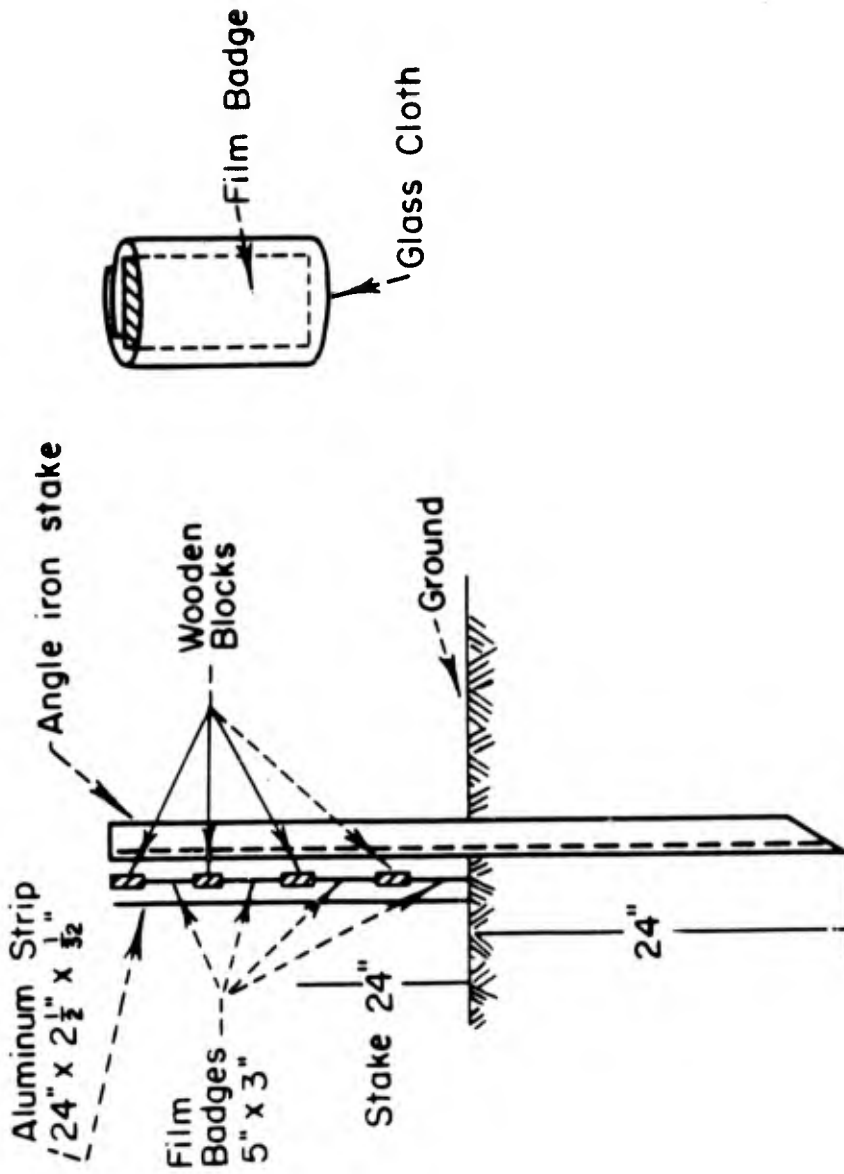


Fig. 2 Installation for Mounting Film Badges for Measuring Gamma Radiation as a Function of Distance. Film Badges are Wrapped in Glass Cloth and Attached to Angle Iron Stake with Adhesive Cement. An Aluminum Strip is Placed on the Stake to Protect the Film Badge from Heat and Sand-Elast. Wooden Blocks Serve as Spacers Between the Aluminum Strip and the Angle Iron Stake.

conditions for periods closely approximating the actual exposure time during the tests. These were returned to the Bureau of Standards for check calibration to assure that such treatment does not cause changes in the calibration. This check calibration made a compensation for the effect of age on the film. The type K was the only film which showed appreciable increase in the base reading. At each test on two stations, at least 16 additional badges were mounted in as nearly exactly the same position as practicable, in order to check the reproducibility or accuracy of individual readings. Details of the entire calibration procedure are included in Appendix A.

The exposure values contained in this report are subject to possible correction and refinement subsequent to the recalibration of the film emulsions employed during the test and re-reading certain of the exposed badges. This work will be undertaken by the Bureau of Standards in an effort to provide more reliable interpretation of exposures between 800 and 2000 roentgens. An additional project is also to be conducted at the Los Alamos Scientific Laboratory to determine the effect of neutrons on the film emulsions in the absence of gamma radiation. The effect of the above refinements to data presented herein cannot be defined at the present time for inclusion in this report.

V. RESULTS

The total gamma radiation exposure as a function of distance is shown graphically in Figures 3, 4, and 5 for Tests X-ray, Yoke and Zebra respectively. The data on which these curves are based are included in Tables I, II, and III. In general, the values listed for the exposure

*pages 12 through
14 are deleted*

are average values from at least four badges at each distance and in some cases a single badge had two or three films giving readings.

pages 16
and 17
are
deleted

In Test Zebra good results were obtained all the way from 450 yards to 2800 yards from the point of detonation and the values fall along a good smooth curve.

In Test Yoke the only distant stations which were valuable were on the islands downwind which became contaminated as a result of fall out from the radioactive cloud. As a consequence, they could not be used to measure the decrease in prompt-gamma radiation with distance. Because of the inability to obtain films which could accurately measure exposures greater than 22,000 roentgens, no accurate measurements of the exposure are available at distances less than 800 yards in Test Yoke. These two restrictions have therefore unfortunately limited the measurements in Test Yoke to a relatively short range between 800 and 2200 yards. Nevertheless, the data which were obtained within this range proved reasonably reproducible, and it was possible to obtain what is considered a relatively good curve for the variation of gamma radiation exposure with distance.

The results for Test X-ray are by no means as reliable as those for the succeeding tests since for all distances closer than 1600 yards the aluminum foil surrounding the films was ignited by the heat from the explosion and consequently the largest fraction of the films was destroyed. A few odd films were recovered which had by chance escaped the effects of the heat and these were used to provide some of the data at the closer ranges. In addition it proved possible, in several cases, to calculate the unshielded exposure by applying a suitable correction to the exposure obtained behind a thin shield. For example, badges were placed within the containers for biological material and a correction

factor of 20 per cent was estimated as necessary to convert these readings to unexposed readings. Similarly, unshielded readings were obtained by correcting values measured in the BuShips shields using the data from Test Yoke in order to obtain a proper correction factor. When final analysis of all badges is completed it may be possible to obtain more values for Test X-ray.

VI. DISCUSSION

A. Lethal Range

Examination of Figures 3, 4, and 5 indicated that the 400 roentgen lethal range for prompt-gamma radiation was approximately 1500 yards for Test X-ray, 1600 yards for Test Yoke and 1350 yards for Test Zebra. This is compared with a lethal range of 1400 yards as measured for Test Able at Bikini. It will be seen from these results that increasing the size of the explosion does not seriously increase the radius of the effectiveness, for the ratio of the lethal areas between the Zebra explosion and the Yoke explosion is only 0.7.

B. Attenuation

The attenuation of the gamma radiation can occur in two ways: First, the absorption by the air and second, by the inverse square law. These processes can be combined into a single equation of the following form

$$E = \frac{E_0 \times 10^{-R/K}}{R^2} \quad (1)$$

In order to calculate the constants for this equation, the product of the exposure times the distance squared has been plotted as a function

of distance for the three tests in Figures 6, 7, and 8. It will be seen that within the experimental error for Tests X-ray and Yoke, the points fall along a straight line over the range measured. For Test Zebra where the data are more reliable and the range of distance covered much greater a slight curvature is noted, and the slope of this curve at the extreme distances is somewhat greater than at the closer in locations. This would indicate a hardening of the dominant gamma radiation at extreme distances. If only gamma radiation is being measured by the films, then this hardening can be explained upon the assumption that some of the softer components of the emitted gamma radiation are absorbed in the shorter distances leaving only the harder rays at the extreme ranges. However, if part of the measured radiation is due to neutrons then this might explain the apparent hardening of the beam. Final resolution of the question must await the detailed analyses of the data obtained from several projects and from the projected calibration of the films with neutrons.

From the slopes of the straight lines in Figures 3 and 4 and from the slope at 1000 yards and 2000 yards of the curve in Figure 5 it has been possible to calculate values of the constant K in Equation (1). Substitution of values from the curve has permitted the calculation of the constant E_0 . Using these constants the following four equations have been drawn up to express the variation of the prompt-gamma radiation exposure as a function of distance for all three tests. In addition the equation obtained during Operation CROSSROADS for Test Able is included for comparison.

Test X-ray

(2)

Examination of these equations shows that the ten-folding distance K for Test Yoke and Test Able at Bikini is identical and that the value of E_0 for Test Yoke is approximately twice as great as that for Test Able. For Test Zebra at close range the ten-folding distance is less while at extreme ranges it is greater. Since the data were not available to determine any variation in K with distances for Yoke and Able it is probable that actually the value of K is the same for all three explosions. The value of K for Test X-ray is the same as that for Test Zebra at the extreme range, and this is probably explained by the fact that the best data obtained in Test X-ray were for the distance badges which were not ignited by the explosion.

C. Strength of Gamma-Ray Source

It is assumed that the gamma radiation produced in the explosion of an atomic bomb is not dependent on the characteristics of the

weapon; then the total number of gamma rays emitted should be proportional to the number of fissions occurring and consequently to the "tonnage". This should be expected if the decaying fission products are primarily responsible. If (η, δ) reactions with materials in the bomb are an important source of gamma rays, then the strength might depend more on such features of bomb construction as the quantity of material in the tamper. It is beyond the scope of this report to analyze this factor any further but it is interesting to make a rough comparison of the strengths of the gamma-ray source from the three explosions and compare these with Test Able at Bikini.

The value of E_0 in Equations 2, 3, 4, 5, and 6 should be a measure of the relative strengths of the gamma-ray source from each weapon. However, since these equations have different values for K and since the value of E_0 was obtained by taking a reading for E and substituting in the equation, the listed values of E_0 are dependent on the value of K selected. It would provide a better comparison if the same value of K was used in all cases. In order to check this the average value $K = 0.0001$ has been selected and from this the value of E_0 for the various tests calculated. These are summarized in Table IV. The values of the tonnage obtained from radio-chemical measurements are not available here so no comparison can be made at this time.

D. Residual Radioactivity from Ground Contamination

The contribution of the radioactivity resulting from the contamination in the crater has been calculated on the basis of measurements of intensity made by monitors entering the area after the detonation. If the intensity, I_2 , is known at a time, t_2 , when the monitor enters the area and if the time, t_1 , at which the contamination occurred is known, then the exposure due to this contamination can be calculated by the following methods:

$$E_c = \int_{t_1}^{t_2} I dt \quad (7)$$

Decay measurements on fission product mixtures indicate that

$$I = I_2 \left(\frac{t_2}{t} \right)^{1.2} \quad (8)$$

$$\text{Substituting, } E_c = I_2 t_2^{1.2} \int_{t_1}^{t_2} t^{-1.2} dt$$

$$\text{Solving } E_c = \frac{I_2 t_2}{0.2} \left[\left(\frac{t_2}{t_1} \right)^{0.2} - 1 \right] \quad (9)$$

where E_c = exposure in roentgens due to contamination

I_2 = intensity (r/hr) at the time badge was collected

t_2 = time (H plus hour) that badge was collected

t_1 = time (H plus hour) contamination occurred.

Substituting in equation (9) the value of $I_2 = 0.025$ roentgens per hour at $t_2 = H$ plus 27 hours and assuming values of t_1 for the time of

contamination of 1 second and 1 minute after the detonation, values of $E_c = 29$ and 11 roentgens are obtained. If the exponent in Equation (3) is 1.5, as measurements under Project 7.1-17/RS-3 indicate, then a value of $E_c = 53$ roentgens is obtained for $t_1 = 1$ minute. The value of I_2 used was that measured by a monitor at 750 yards following Test X-ray, and it is obvious from this calculation that the exposure resulting from contamination on the ground is inconsequential in comparison to the total exposure of greater than 10,000 roentgens obtained at this distance.

VII. CONCLUSIONS

The gamma radiation emitted directly at the time of explosion of the present models of atomic bombs is lethal about 1500 yards from the point of detonation. The variation in tonnage of the bomb between that used in Test Zebra and Test Yoke did not change the lethal range by more than 250 yards.

Calculations of the air absorption coefficient for the gamma radiation gave values for the ten-folding distance ranging from 790 and 900 yards, the value increasing slightly with distance from the center. The contribution of the radioactivity from the material deposited in the crater to the total exposure is negligible.

It is recommended that further development be carried out with a view to procuring films which cover the entire exposure range without any important gaps and also of films which are capable of measuring radiation up to several hundred thousand roentgens.

APPENDIX A

Preliminary Report

CALIBRATION OF FILM FOR GAMMA RADIATION EXPOSURES

by

Frank H. Day

X-ray Section

National Bureau of Standards

The following types of Eastman Kodak Film were exposed to measured exposures of X-rays of various energies as indicated in Figures 1-8.

	Film
Type A	a
Type K	b
Translite	c
Cine Positive 5302	d
Cine Positive 5301	e
548-0 Single Coat	f, g

The relationships between film density and gamma radiation exposure for radiation of 1.5 Mev are shown for these films and for the NTC emulsion in Figures 9-15. These were used for estimating the exposure in the films used at Eniwetok.

The exposure of film packets to X-rays was determined by varying the time of exposure to X-ray beams calibrated by Victoreen condenser r-meter in roentgens per minute under a given set of conditions of X-ray excitation potential and of filtration. Each film packet was exposed on a bakelite fork which was placed in the same position with respect to the tube target

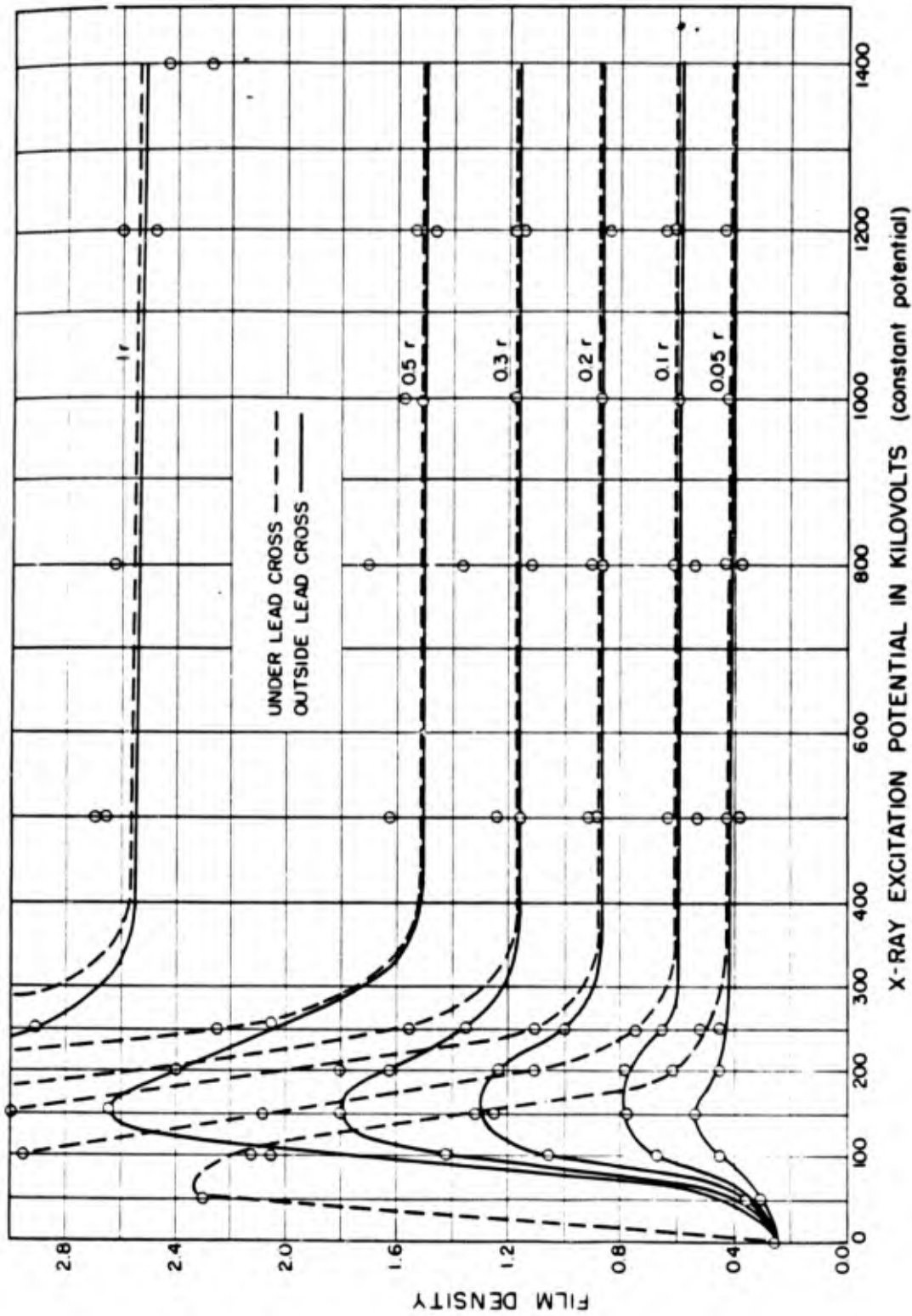


Fig. 1 Calibration of Eastman Type K Film. National Bureau of Standards Book 35,
 Preliminary Study Dated 24 March 1948

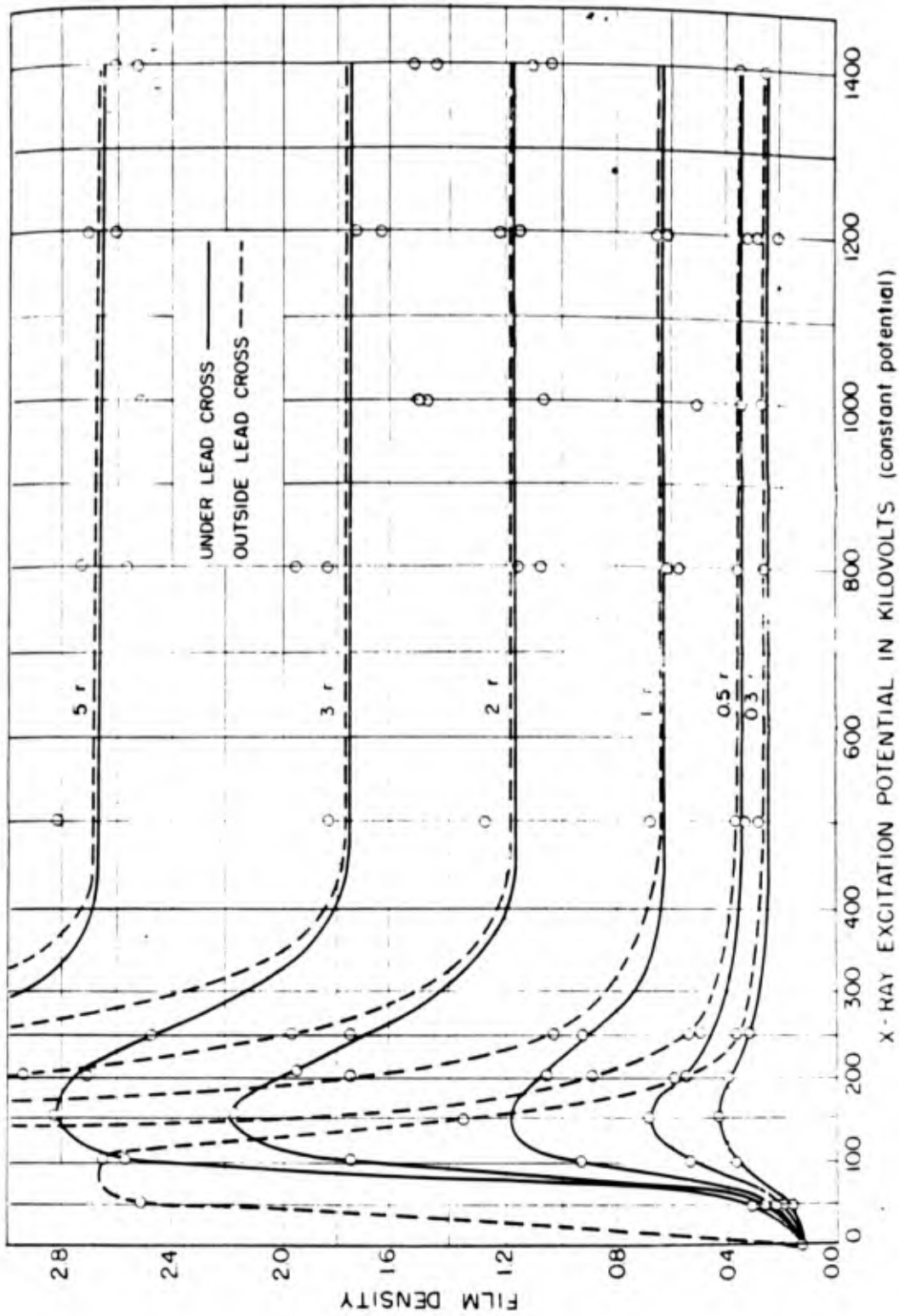


Fig. 2 Calibration of Eastman Type A Film. National Bureau of Standards Book 35, Preliminary Study Dated 24 March 194c.

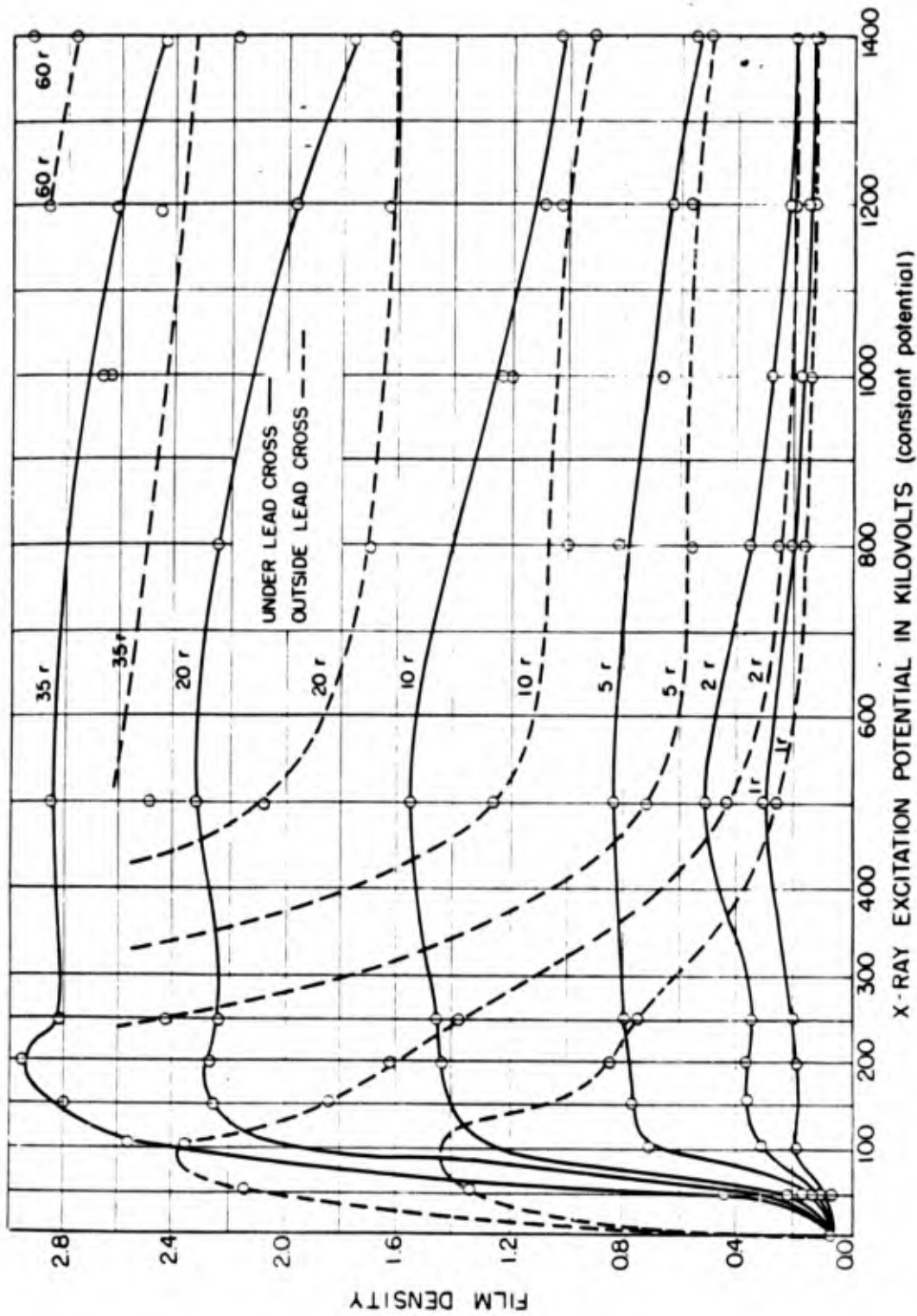


Fig. 3 Calibration of Eastman Film 5301. National Bureau of Standards Book 35, Preliminary Study Dated 24 March 1948.

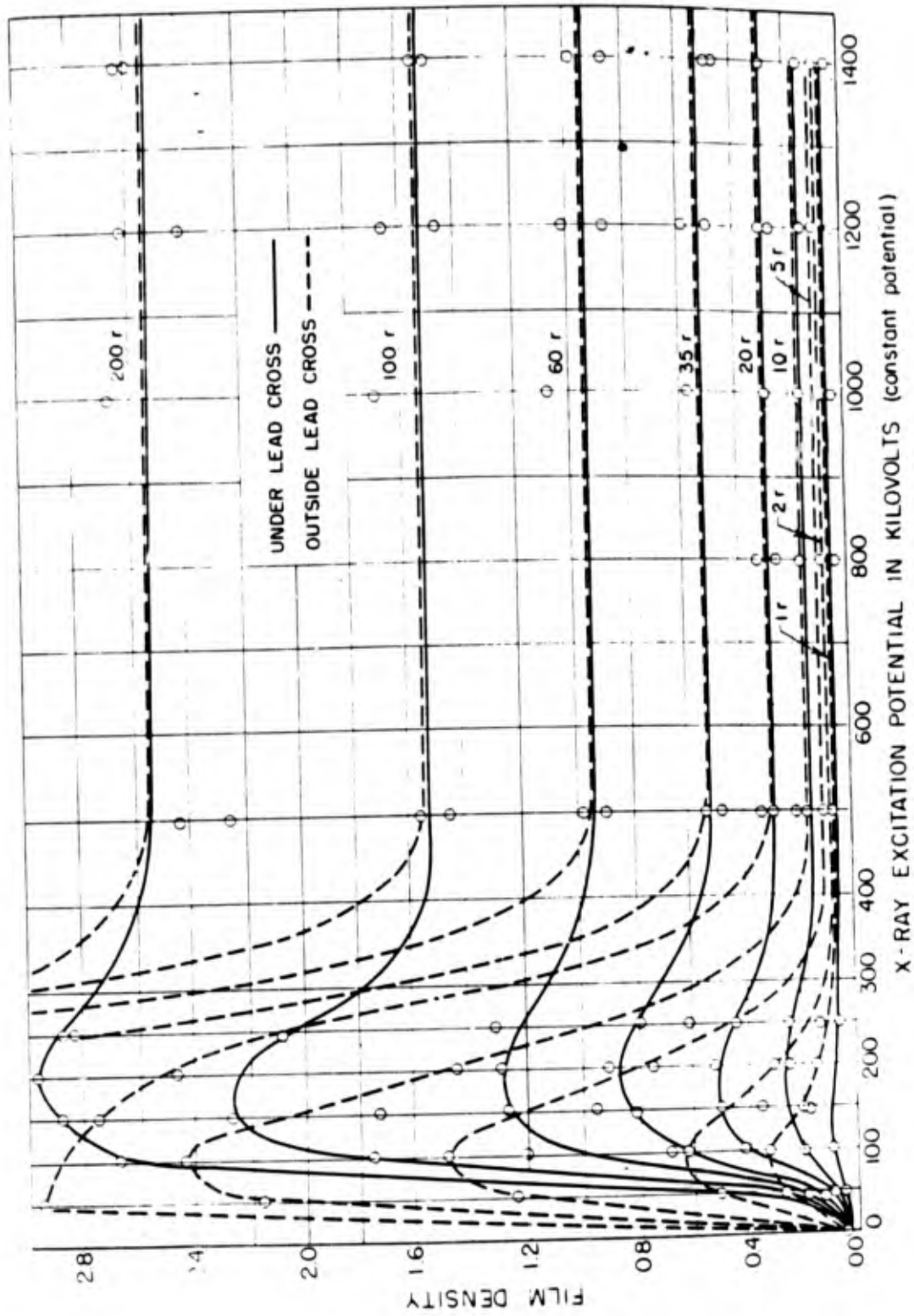


Fig. 4 Calibration of Eastman Film 5302. National Bureau of Standards Book 35, Preliminary Study Dated 24 March 1948.

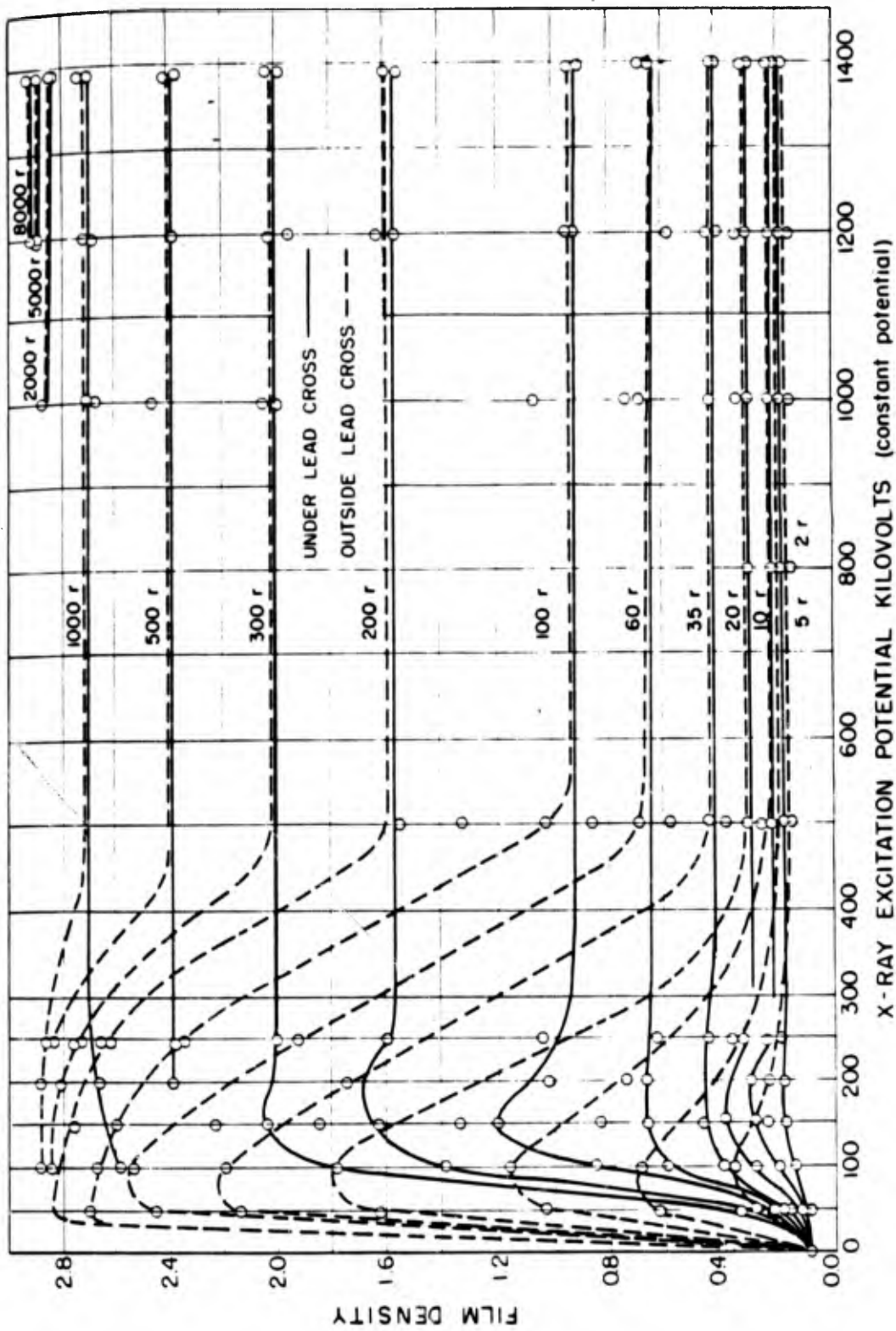


FIG. 5 Calibration of Eastman Translite Film. National Bureau of Standards Book 35,
 Preliminary Study Dated 24 March 1948.

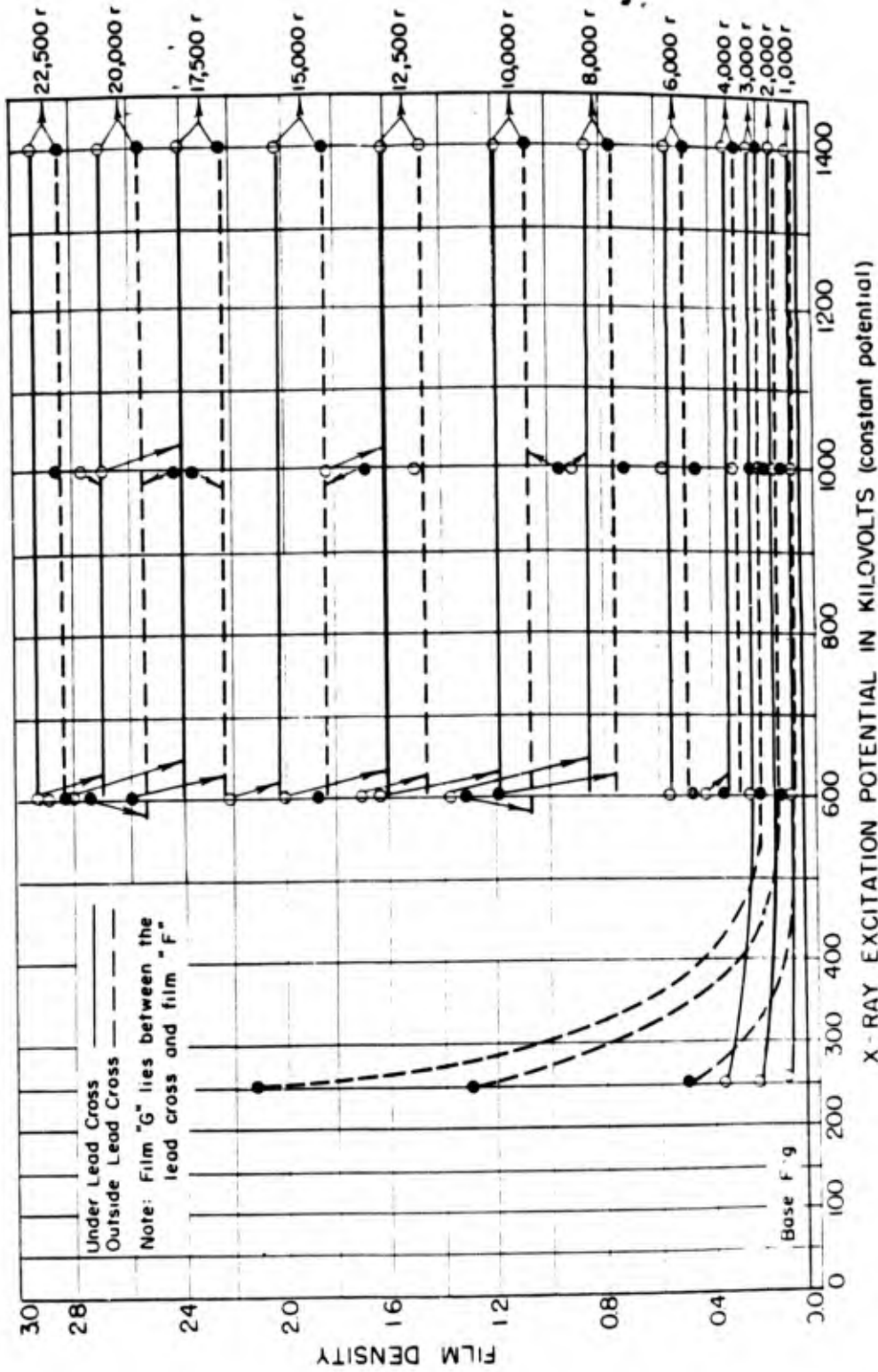


Fig. 6 Calibration of Eastman Type 548-0 Single Coat "f" Film Contained in Aluminum Foil Packet, National Bureau of Standards Test Number 35,154, Dated 24 June 1948.

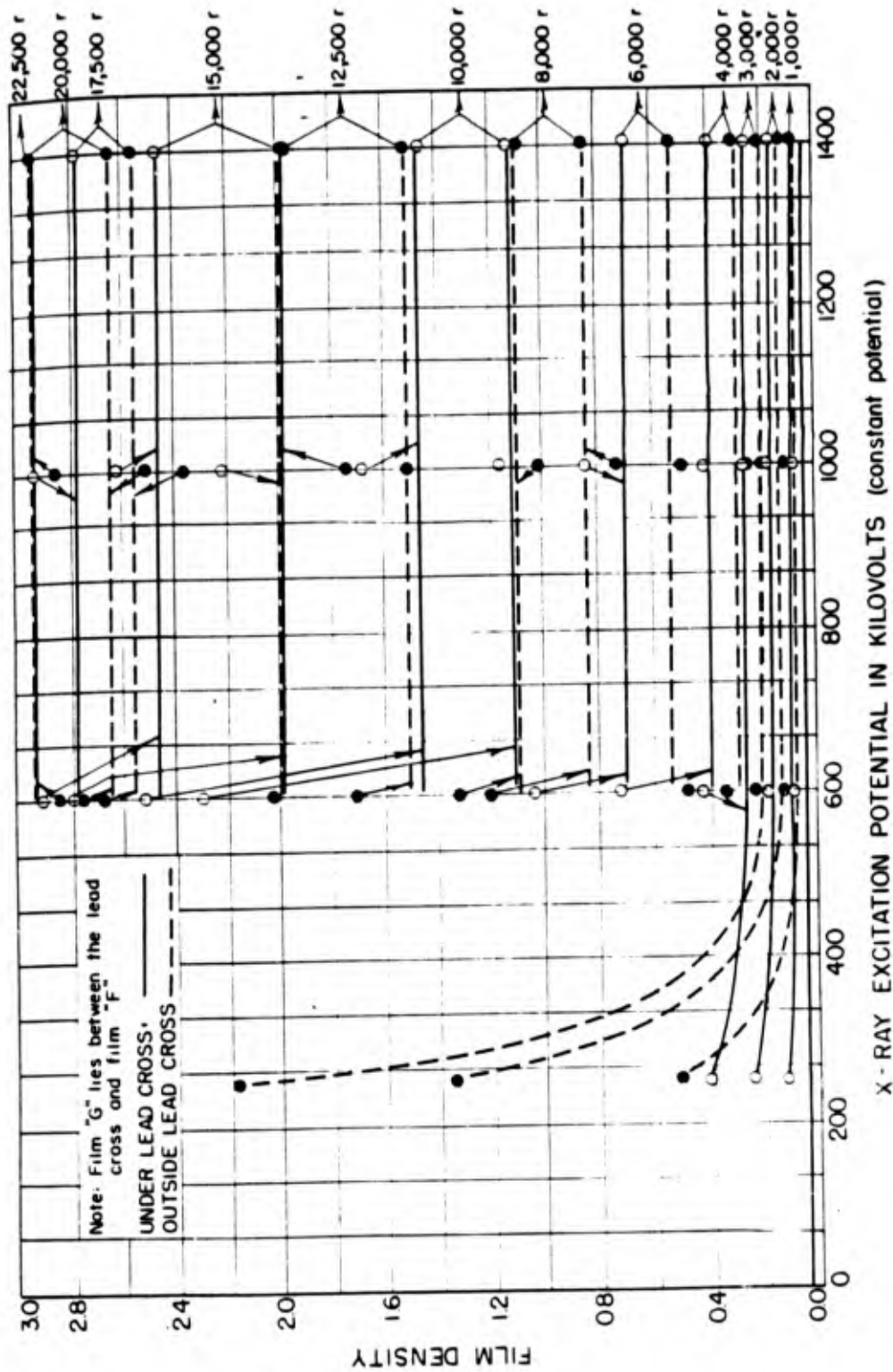


Fig. 7 Calibration of Eastman Type 548-0 Single Coat "g" Film Contained in Aluminum Foil Packet. National Bureau of Standards Test Number 35,154, Dated 24 June 1948.

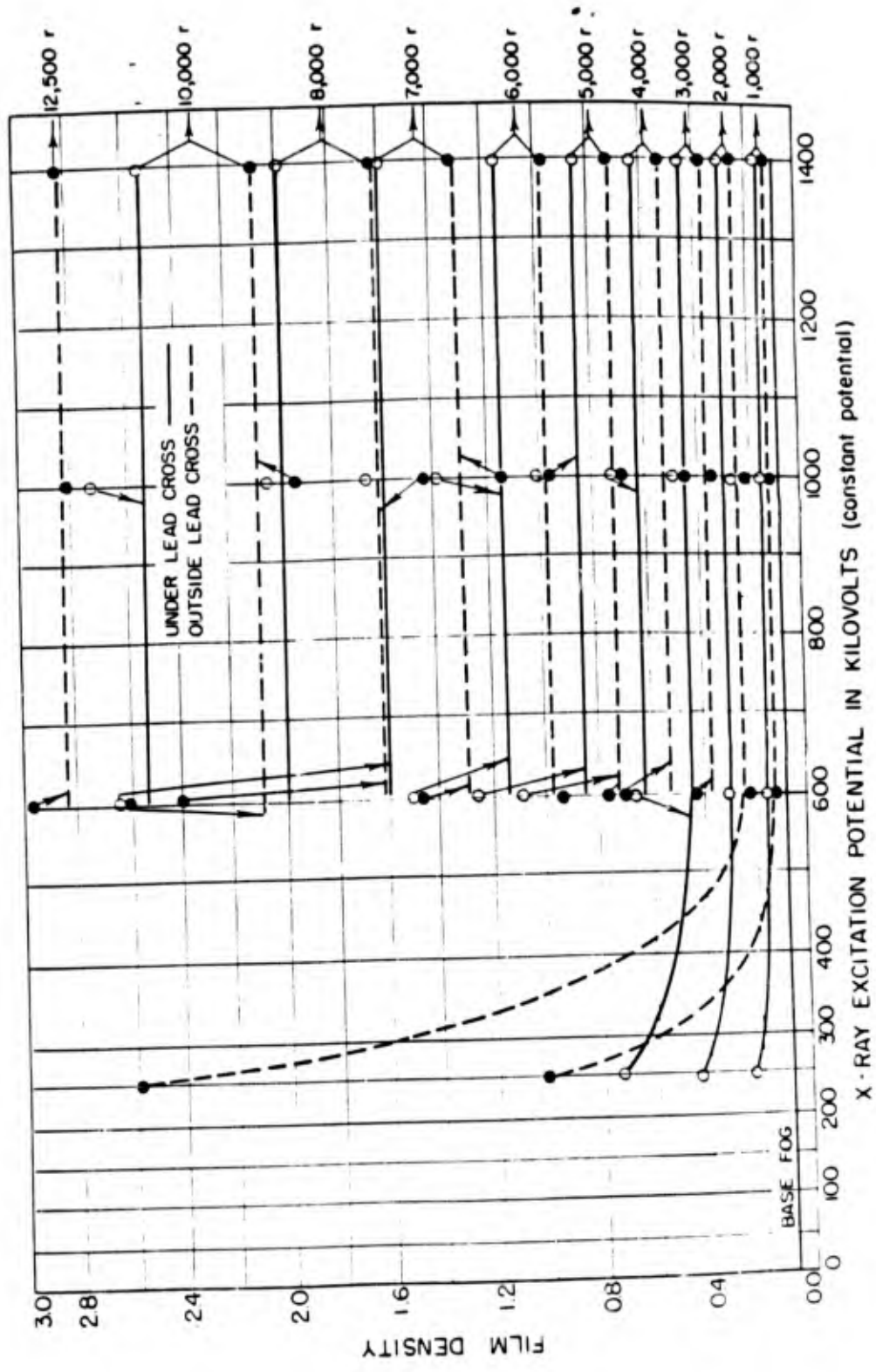


Fig. 8 Calibration of Eastman Type 548-0 Single Coat Film "f" and "g" Contained in Aluminum Foil Packet. National Bureau of Standards Test Number 35,154, Dated 24 June 1948.

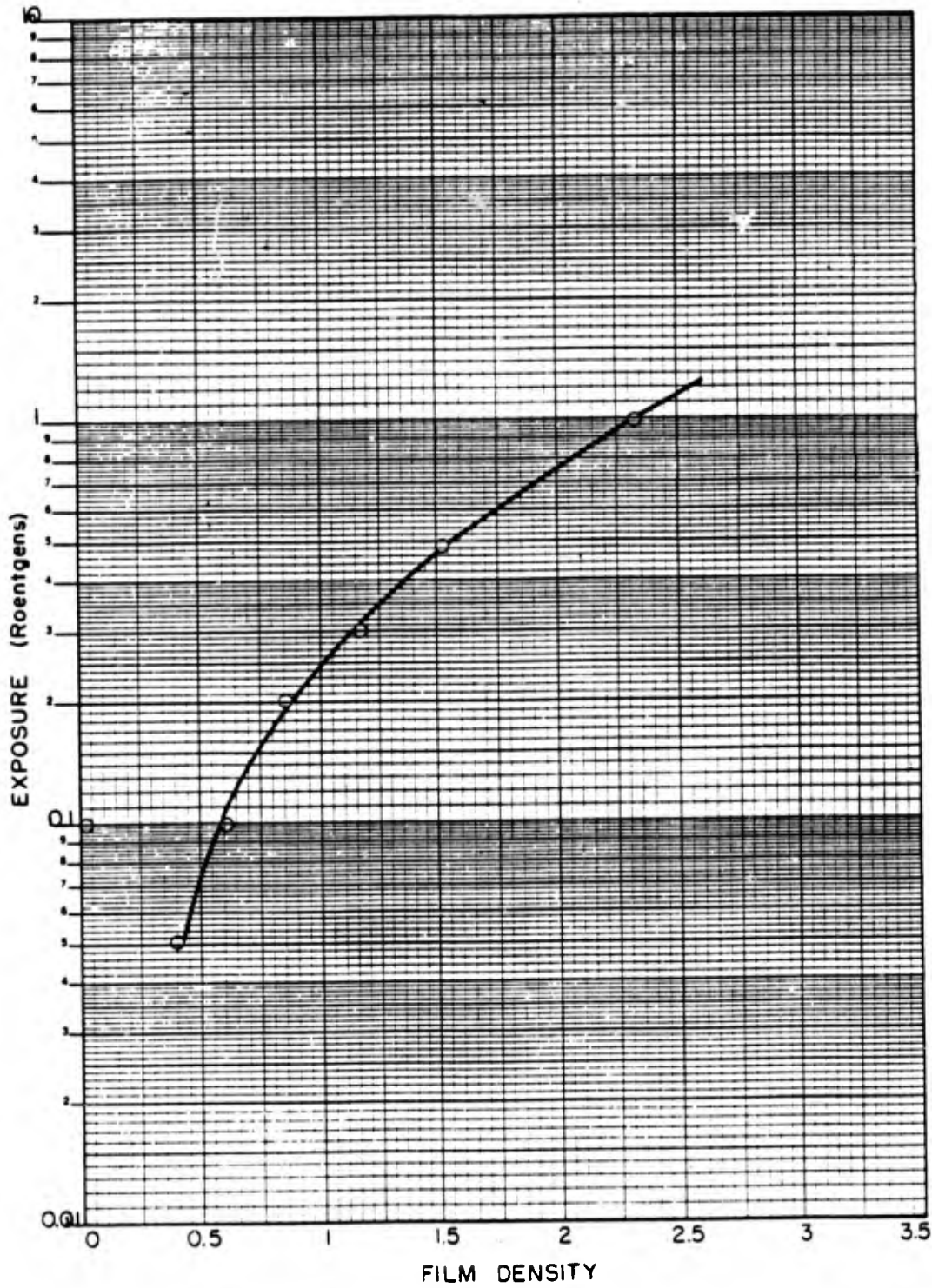


Fig. 9 Film Sensitivity - 1.5 Mev, Type K

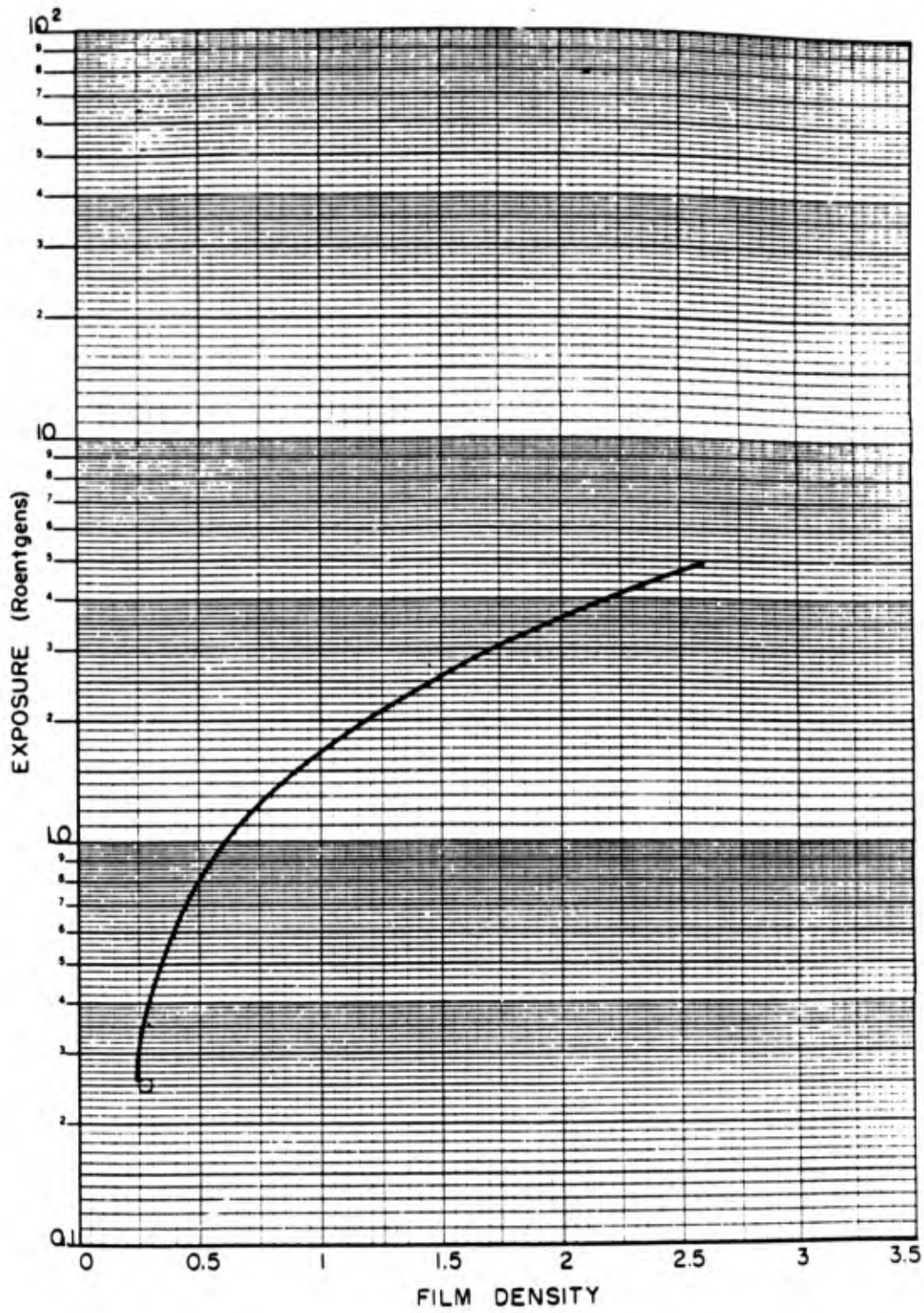


Fig. 10 Film Sensitivity - 1.5 Mev, Type A Film

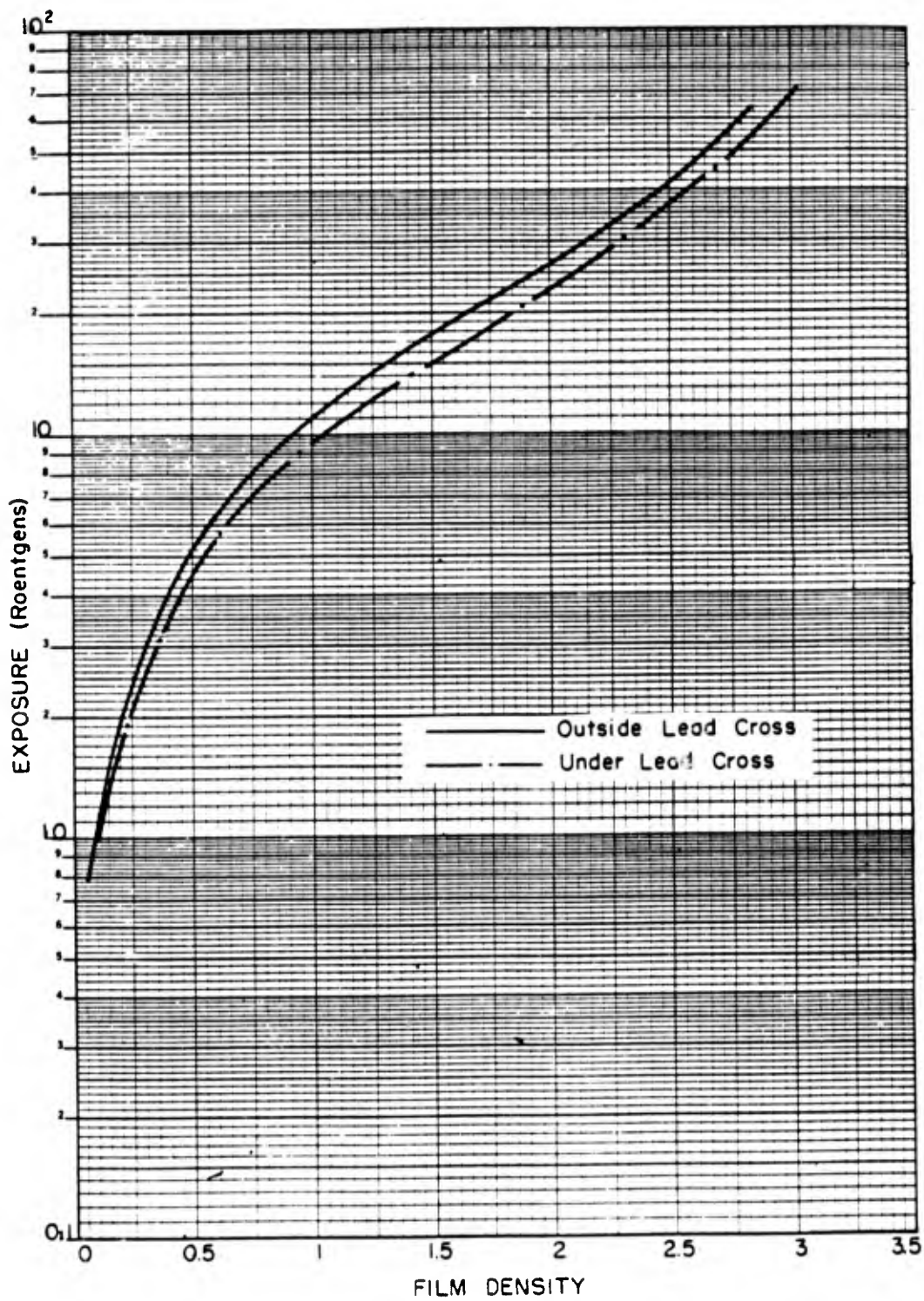


Fig. 11 Film Sensitivity - 1.5 Mev, Cine Positive 5301

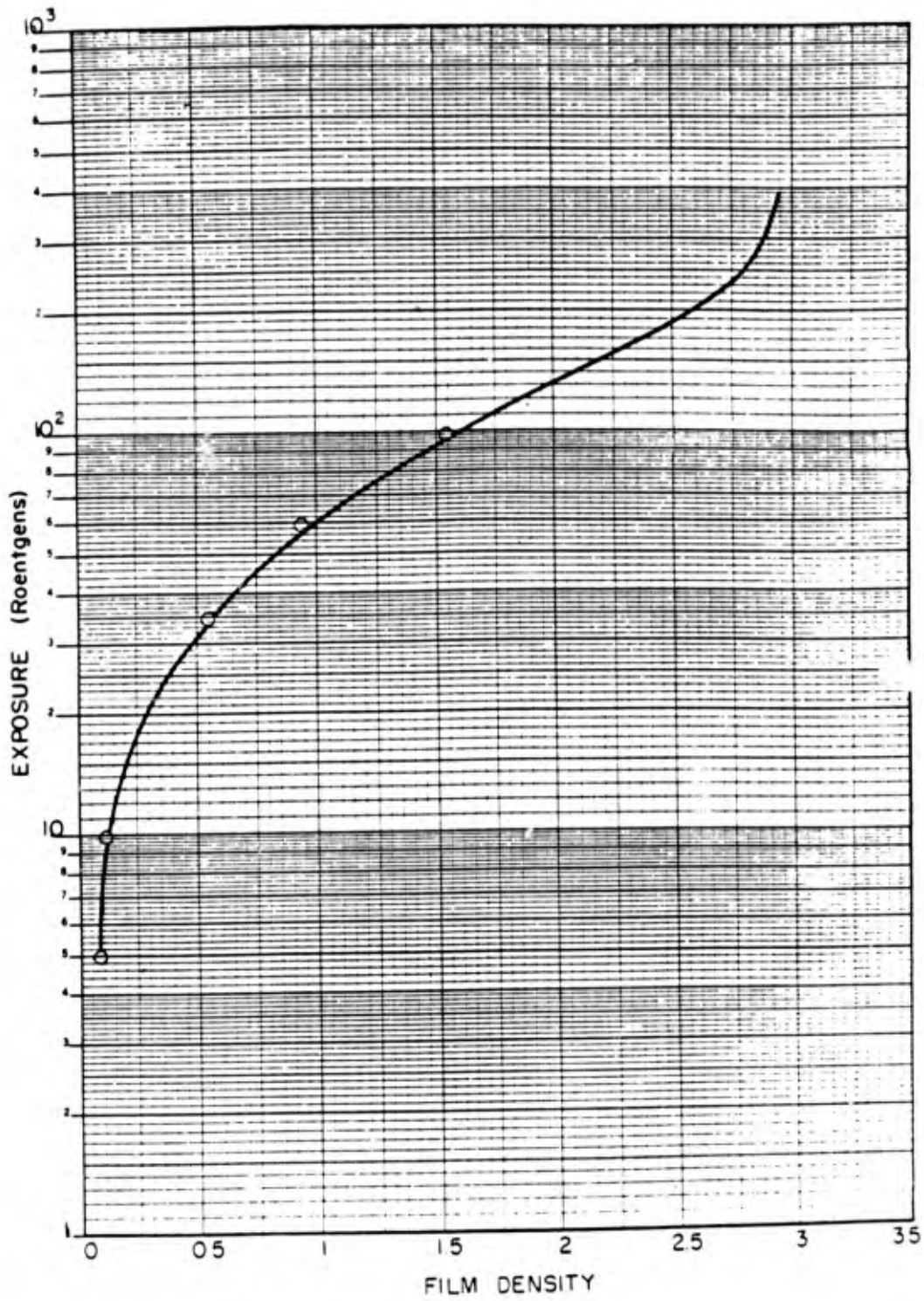


Fig. 12 Film Sensitivity - 1.5 Mev, Cine Positive 5302

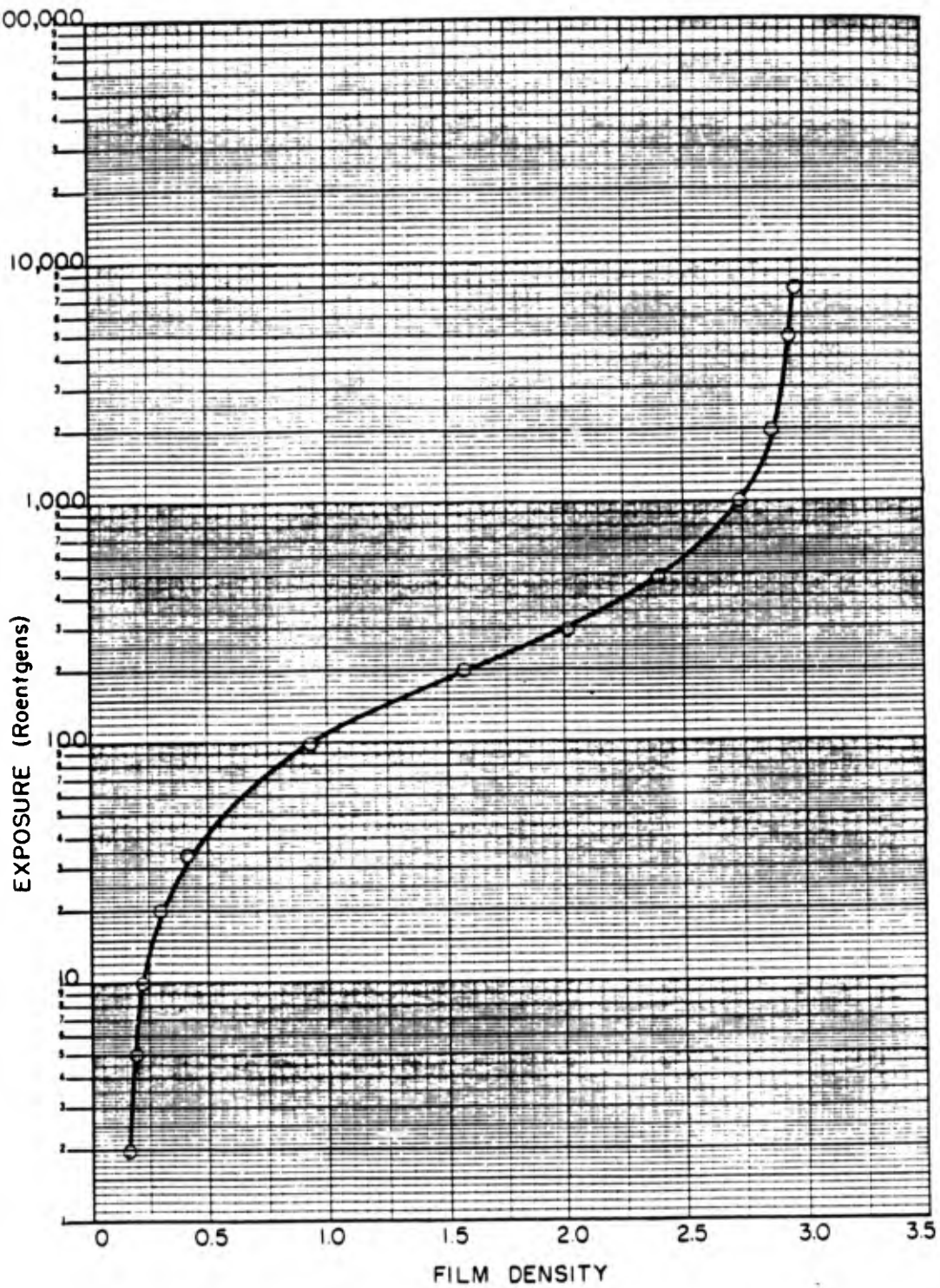


Fig. 13 Film Sensitivity - 1.5 Mev, Translite Film

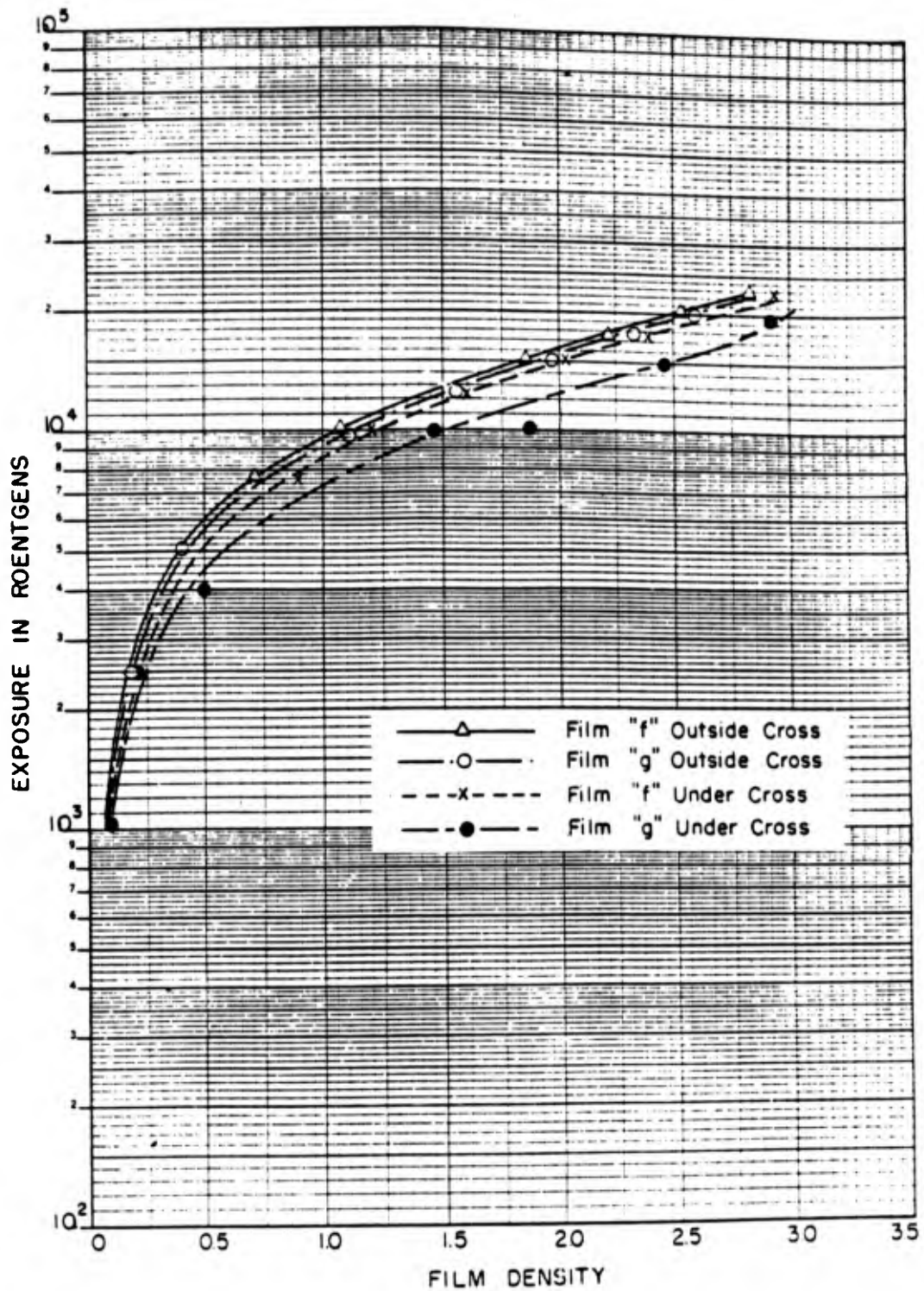


Fig. 14 Film Sensitivity - 1.5 Mev, Film: 548-0 Single Coat

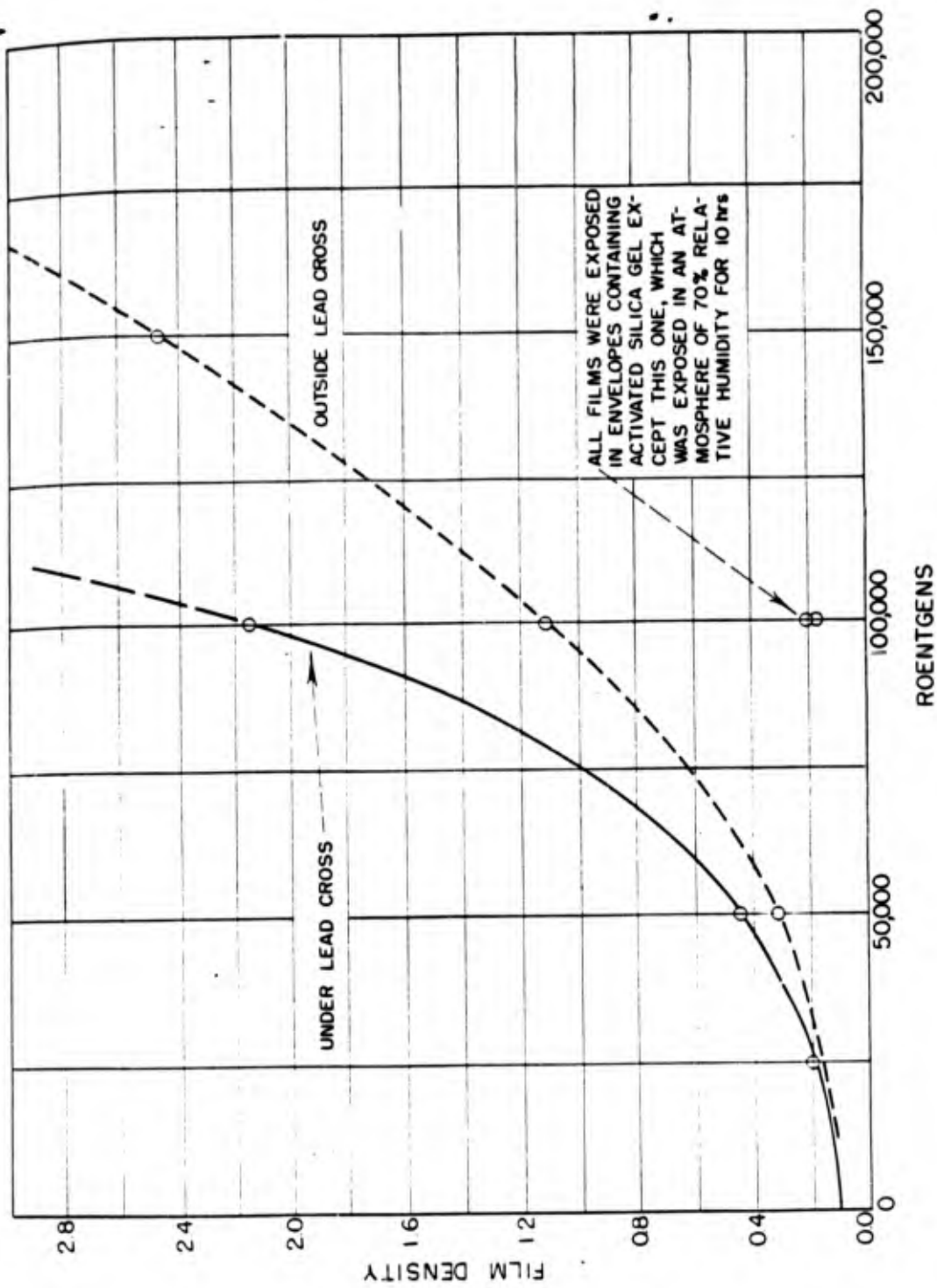


Fig. 15 Calibration of Eastman NTC Films on 1400-kv X-rays. National Bureau of Standards Test Number 35,161, Dated 16 June 1948.

as the thimble chamber was placed during the beam calibration. The side of the film on which the lead cross is complete was placed at all times facing the tube target.

It was necessary to vary the target-to-film distances from 19cm to 200cm, the periods of exposure from three seconds to one hour, and the added filtrations from 1.0mm of aluminum to $5/8$ inch of lead in order to span the range of exposures necessary. The inherent filtration of the tube used for generation of X-rays in the range of 50 to 250kv was equivalent to approximately 0.2mm of copper, and of the tube used in the 500 to 1400kv range, approximately 3mm of tungsten plus 6mm of copper plus 18mm of water.

Tests were made to determine the effect of added filtration on the film emulsion response. In the potential range of 100 to 250kv it was found that the addition of 0.5mm of copper plus 1.0mm of aluminum was sufficient to attain practical independence of the response at a given exposure. No filtration less than this was used at any excitation potential except at 50kv, where only 1.0mm of aluminum was added. In view of the relatively large inherent filtration in the million-volt tube, no noticeable dependence of film emulsion response upon added filtration was observed in the 500 to 1400kv range. However, in order to maintain a near-threshold quality for X-rays produced by a given excitation potential, maximum added filtrations were used at all times which were consistent with reasonable exposure periods.

Shutter control of exposures was available on the 250kv set but not on the million-volt equipment. Exposures were necessarily controlled in the latter case by means of turning the tube filament current on and off. Exposure periods with the million-volt equipment were maintained at one minute or more, in order to minimize the errors involved. A new anode housing with

motor-controlled shutter is now being assembled for the million-volt equipment and should be available for more exact exposure determination.

The exposure conditions at 1400kv for the 548-0 single-coat film were such that it is believed that the data are reliable within a few per cent. It is noted that at this X-ray quality there is an orderly progression of under-the-cross to outside-the-cross readings and that these are slightly different from the f and g films due to the photoelectron absorption in film g, which is the one nearest the lead cross, from which most of the photoelectron emission is given. It was hoped that by extending the X-ray excitation potential downward that a variation of these noted differences could be obtained, thus giving a clue to the incident radiation quality. Unfortunately, because of the loss of efficiency of X-ray production at lower X-ray excitation potentials (those used were 600 and 1000kv) it was necessary to place the films inside of the steel anode housing, thus entailing undesirable scattering. Furthermore, the necessity of placing the films within close proximity of the target reduced the accuracy of the exposure, causing divergence from the regular pattern which was observed at 1400kv. The exposures, which consisted of periods up to 90 minutes at 1400kv, were carried out at a target-to-film distance of 13 inches, which is outside the steel anode housing. However, those at 1000 and 600kv required exposures up to 7 hours at a distance of only 6 inches.

NTC films were calibrated at 1400kv using a target-to-film distance of 6 inches and requiring exposures up to 10 hours in length. The films were placed in envelopes containing silica gel because hydrogen peroxide formed, as the result of high relative humidity, in the film emulsion. This hydrogen peroxide reduces the amount of free silver present. At 100,000 roentgens

a difference of 10 to 1 in density is observed for films exposed with as compared without silica gel.

Tests have been conducted on the effects of pressure on the films contained in the aluminum foil packets. Pressures up to 2500 pounds per square inch have been applied to the packets with no observable change in density upon development.

Calibration films f and g were densitometered over an interval of twenty days and found to exhibit no change in density with time. A recheck will be made of these films in the future to determine any possible effect of aging.

The film processing was carried out at 20° Centigrade with a temperature variation of not more than $\pm 0.05^\circ$ Centigrade. The time of development was five minutes in Eastman "Kodak" liquid X-ray developer. Film density measurements were made on an Ansco-Sweet densitometer powered by a Sorensen electronic voltage regulator. A Weston densitometer of the double range type has been ordered for continuance of this work.

This work was carried out as a part of a project for the Armed Forces Special Weapons Project of the National Military Establishment. The above work is strictly of a preliminary nature.

Approved:

Lauriston S. Taylor
Chief, X-Ray Section
National Bureau of Standards

SCIENTIFIC DIRECTOR'S REPORT
OF ATOMIC WEAPON TESTS
AT ENINETOX, 1948

Annex 8

GAMMA-RAY MEASUREMENTS

Part V

GAMMA RADIATION SHIELDING

Task Group 7.6

Project Report

GAMMA RADIATION SHIELDING

--

OPERATION SANDSTONE

by

CDR E. J. Hoffman, USN

LT E. C. Vicars, USN

Herbert Scoville, Jr.

31 July 1948

Project 7.1-17/RS(BS)-2

TABLE OF CONTENTS

I ABSTRACT 3

II OBJECTIVE 3

III EXPERIMENTAL 4

IV RESULTS. 14

 A. Steel and Concrete Plates 14

 B. Corps of Engineers' Structures 14

 C. Bureau of Yards and Docks' Structures 16

 D. Multi-Sided Structures 21

 E. Angular Plates 22

V DISCUSSION. 22

VI CONCLUSIONS AND RECOMMENDATIONS. 26

APPENDIX 1 - STEEL AND CONCRETE SHIELDS 28

GAMMA RADIATION SHIELDING

I. ABSTRACT

The absorption of gamma radiation from an atomic bomb explosion by steel and concrete has been measured with films using simple plates and elementary structures for shields. Only a preliminary analysis of these data has been made to date but some tentative conclusions are drawn on the effectiveness of the various materials as shields. The Corps of Engineers' structures designed with two-foot-thick concrete walls would not have reduced the exposure to a sublethal amount within a distance closer than 750 yards from the zero point for an explosion similar to that at Test X-ray; for the structures with one-foot-thick walls this distance would be no closer than 1000 yards. None of the structures erected by the Department of the Navy, Bureau of Yards and Docks, would have provided protection to personnel inside, although many were apparently unaffected by the blast. The gamma radiation at appreciable distances from the point of detonation has an important soft component and consists partly of scattered rays requiring shielding in all directions to provide protection.

II. OBJECTIVE

The object of this project was to obtain by using simple shields and structures experimental data on the transmission of gamma rays through common construction materials and to attempt to derive from this data empirical rules applicable to more complicated structure. Such rules would facilitate design of ships and buildings for personnel protection.

The theoretical solution of most practical problems involves many assumptions the validity of which may be subject to question.

Since radiation shielding is of tremendous importance in the design of naval vessels and in any structure used for personnel protection against radiation, the Department of the Navy, Bureau of Ships and the Armed Forces Special Weapons Project requested that shielding experiments be performed in Operation Sandstone. The Bureau of Yards and Docks, and the Army Chief of Engineers, also expressed interest in the project.

III. EXPERIMENTAL

The absorption of gamma radiation by thick shields has been the subject of much theoretical work but because of the complicated nature of absorption processes, calculations are difficult and of dubious accuracy. The present experiments were designed to provide experimental data useable in evaluating the importance of various absorption processes. Simple plates were used to provide measurements under minimal scattering conditions. Angular shields and more complicated structures were to provide information which would assist in applying the results to practical situations. When all the data are complete, an attempt will be made to make an interpretation in terms of theory.

All gamma-ray measurements were made with film badges capable of being read when exposed to radiation intensities varying from 0.05 to 22,000 roentgens. Seven different emulsions to cover the total range were used. A complete description of the films and their calibration is given in Operation Sandstone No. 29 - Part IV "Gamma Radiation versus Distance". Exposure values contained in this report are a composite of the effects of gamma radiation and neutrons on the film emulsion. A study of the effects of neutrons on film emulsions in the absence of gamma radiation has been proposed as a part of Operation Sandstone No. 29.

The films were mounted in a variety of shielded positions. The shields consisted of the following:

1. Test X-ray

(a) Steel plates, 1 square foot in area were erected at 750, 1000, and 1400 yards, in thicknesses of 1, 2, 4, 6, and 12 inches. These thicknesses were built up of one-inch plates and eight film badges were mounted behind each plate. Details are given in Appendix 1.

(b) Steel plates, 4 square feet in area were mounted in two-inch thicknesses at 750, 1000, and 1400 yards, built up as before; 13 film badges were placed behind each plate. For details, see Appendix 1.

(c) Concrete shields, 1 square foot of total thicknesses, 3, 6, and 12 inches, built up of three-inch slabs and documented with films in a manner similar to the steel specimens, were erected at each station. For details see Appendix 1.

(d) Two each, Chief of Engineers' type A and type B concrete dugouts were documented by 126 film badges placed on a lattice within the structures and on the walls. Type A structure had two-foot walls and type B had one-foot walls. These structures were located at 1000, 1500, and 2500 feet from the zero point of explosion. Seventeen film badges were placed behind the Chief of Engineers' bunker located 2500 feet from zero point. (For construction and film badge placement see Operation Sandstone No. 24.)

(e) The Bureau of Yards and Docks' test structures for Test X-ray, which were located at 350, 500, 700, 1000 and 1250 yards were documented by placing film badges on a lattice within the various structures, each of which had significantly different shielding qualities. The remaining

structures had two badges placed near the center in each case. Detailed plans of the structures and of the placement of each badge are given in Operation Sandstone No. 24.

(f) A few additional film badges were distributed in incidental structures and buildings on the island, and their shielding adequately documented. (Unshielded exposures were reported in Operation Sandstone No. 29.)

2. Test Yoke

(a) Films were placed in a few typical Bureau of Yards and Docks' test structures.

(b) One shield, 4 square feet in area was mounted normal to the blast at 700, 1000, and 1250 yards. Documentation was accomplished in the same manner as had been done for Test X-ray.

(c) At 750 and 1250 yards, enclosures of two, three, four and five sides were erected. The sides were of one-inch plate, 1 square foot and were documented by placing 8 film badges behind each plate.

3. Test Zebra

(a) At 750 yards, steel plates, 1 square foot in area were provided in thicknesses of 1, 3, 6, and 12 inches, and at 1000 yards, in thicknesses of 1, 3, and 6 inches and documented as shown in Appendix 1.

(b) At 750 yards concrete shields in thicknesses of 3, 9, and 18 inches were documented as shown in Appendix 1.

(c) At 750 yards a badge was completely surrounded with at least 4 inches of lead in order to determine the importance of neutron flux on the badge.

IV. RESULTS

A. Steel and Concrete Plates

The arrangement of 8 and 13 badges behind the 1-square foot and 4-square feet steel plates respectively was designed to determine the reproducibility of results behind a given plate and to find out if any edge effects were present because of the small size of the shield used. Typical results behind some of these plates are summarized in Table I. The position numbers correspond to those used in Figure 3, Appendix 1. Examination of these results shows that the reproducibility behind a given plate is good and that there are no apparent edge effects. Therefore, for the analysis of the results obtained using the concrete and steel "sandwiches", the average value behind a given plate has been used.

The average exposures obtained between the steel plates have been plotted as a function of steel thickness for the various distances in Figures 1, 2, 3, and 4. In this preliminary analysis all sets of plates at a given distance are plotted together, no attempt being made to differentiate between the absorption in a sandwich of total thicknesses of 3, 6, and 12 inches. In Figures 5, 6, and 7 the shielding provided by the concrete blocks has been plotted in the same manner.

B. Corps of Engineers' Structures

Practically 100 percent of all the film badges exposed in the two type B and type A Corps of Engineers' structures at 1500 feet were recovered but nearly all of the badges within the 1000-foot type A structure were destroyed. The few miscellaneous badges which were recovered and which could be developed to give any reasonable results, gave readings between 8000 and 15,000 roentgens. In the other structures no obvious difference

in the exposures at the various locations was apparent so for the purpose of this preliminary analysis, average values on the various walls and in the middle have been recorded in Table II. For comparison purposes the exposure outside the structure is also listed.

TABLE II
GAMMA RADIATION EXPOSURE
OCE STRUCTURES

C. Bureau of Yards and Docks' Structures

For the purpose of preliminary analysis only the average values within the various Yards and Docks' structures have been used. These are summarized in Tables III and IV. In the case of structures which were partially buried or which had a single barricade providing additional shielding, the average reading at ground level was taken rather than the

average of all the badges within the structure. In addition to listing the exposures obtained within these various structures the percent reduction from the unshielded exposure at the same distance has also been tabulated.

pages 18 through
20 are
deleted

D. Multi-Sided Structures

The purpose of these erections was to obtain experimental data concerning the scattering of gamma radiation within enclosures. This information was considered to be of importance for use in analysing CROSSROADS data and in the evaluation of shielding characteristics of conventional ship designs. All film badges were recovered from the 1250-yard station and the five sided figure only was recovered at the 700-yard station. The exposures determined within these structures are tabulated in Table V. These exposures were frequently in the dubious range of from 800 to 2000 roentgens.

The results to date do not appear to show any obvious differences in exposure between the various structures.

E. Angular Plates

The results of this test are shown in Table VI. Due to the exposures being within the inaccurate range of the film badges it is considered that this test is inconclusive. However, it is recommended that similar experiments be carried out with more stations and with close control of the variables inherent in such tests.

V. DISCUSSION

Detailed analysis of the data obtained as a result of this project can not be made at this time because of the necessity of re-evaluating all

film badges and the need to calibrate the films with radiation of the same energy as was produced by the detonation. The calibration carried out to date has indicated a nearly consistent response between 0.2 and 1.0 Mev for most films, but it is quite possible that this independence of response with energy will not continue at the higher energies. When the energy of the gamma radiation is known from the experiments carried out by Shenka and King and the calibration at higher energies completed, then the exposures will be recalculated.

A further problem which has arisen in the analysis of these films was an inability to obtain satisfactory and reproducible readings in the exposure range of 800 to 2000 roentgens. This range lies just between the exposure which could be measured accurately with the translite film and the 548-0 single coat. Some improvement in this range is anticipated by reading the duplicate 548-0 films together, thereby increasing the total density in the lower ranges of this film. A densitometer which has greater accuracy in these ranges will also be used for this work. It is hoped therefore that as a result of the re-reading of these 548-0 films it will be possible to increase the reliability of the results obtained. Unfortunately, a large number of the badges used in this experiment fell within the range of 1000 to 2000 roentgens since this was an exposure which might be reduced to sublethal by the normal shielding provided by naval vessels.

It should be noted at this time with respect to the data obtained with the steel and concrete shields that higher readings were obtained on the back plate than on many of the inside plates. This might result from neutron-gamma reactions in the shield, the absorption of fast and scattered neutrons by the film badge itself, and finally from scattered gamma radiation

from the air and surrounding ground. The extent of this exposure on the last shield is approximately 15 percent of the unshielded exposure at the same location. Since the badges on the next to last plate show no increase in gamma radiation it appears likely that the high readings on the outside are due to low-energy scattered rays. This energy would, however, appear to be greater than 0.2 Mev since for lower energies, the relationship of intensity under the lead cross on the film to that outside the lead cross would be abnormal. No such abnormal behaviour was noted.

The exposure decreased within thick shields to a background exposure which did not appear to be lowered by further increase in shielding. This might be due to neutron-gamma reactions in the shielding material, neutron effects on the film or scattered radiation entering along the edges of the plates. Comparison of this background level with the exposure observed on badges surrounded on all sides by lead to eliminate scattered radiation and permit transmission only of neutrons indicates that this background is probably caused by the neutrons. This would appear reasonable since the distance between plates was no greater than 1/8 inch, leaving an exceedingly small solid angle unshielded to permit entrance of the scattered rays. A question of whether the neutron effect is due to n- γ reactions or to a direct effect on the film cannot be definitely determined until neutron calibrations are made, but calculations indicate the former to be most likely. The total background observed is somewhat less than 5 percent of the unshielded exposure, indicating that under most conditions the neutrons are not contributing appreciably to the exposure recorded by the film badges.

If this background reading is subtracted from the observed exposure in the shields, then a derived curve is obtained which should be representative

of the efficiency of the shield in removing gamma radiation. This has been done in Figures 1, 2, 3, and 4. Examination of these derived curves indicates that the half thickness of steel decreases from about 1.1 inches behind 3 inches of steel to about 0.8 inch behind 10 inches of steel. The first inch of steel plate appeared to have a very much higher efficiency of removal than the succeeding plates. This probably results from the absorption of some of the softer components of the beam in the outer shield. The magnitude of the soft component which is completely removed by the first inch of steel is about one third of the total.

The data with the concrete blocks are not as complete or reproducible as they are with the steel, but these indicate that 1 foot of concrete will reduce the exposure by a factor of 10. The same sharp decrease of exposure in the first 3 inches of concrete is observed as with the steel, and there is also evidence of the reduction of exposure to a background value similar to that obtained with steel.

Examination of the results obtained within the Corps of Engineers' structures show that while these provided considerable protection against the gamma radiation, they failed to reduce it below the median lethal exposure. This type B structure which had 1-foot concrete walls cut the exposure to about 7.5 percent of the unshielded value and the type A with 2-foot walls to about 2 percent. These results indicate that the type A structure would have prevented a lethal exposure from a Test X-ray type explosion at a distance of about 750 yards and the type B at 1000 yards. In all probability this range is greater than the range at which the structures would withstand the blast effects from the detonation.

No attempt has yet been made to correlate the shielding provided

by the Yards and Docks' structures with the type of construction. It should be noted, however, that in all the structures tested by the Bureau of Yards and Docks the average gamma radiation exposure is greater than 400 roentgens, indicating that while these structures were satisfactory to withstand the blast pressure, they would not have provided protection against the nuclear radiation effects.

VI. CONCLUSIONS AND RECOMMENDATIONS

It is too early to draw any firm conclusions as a result of this experiment, but the following tentative statements can be made at this time.

The gamma radiation obtained at moderate distances from the point of detonation has an appreciable soft component which can be removed by relatively thin shields. Once this soft component has been removed approximately one inch of steel is required to reduce the exposure by a factor of two. About one sixth of the total exposure results from the back scattered radiation, so that some shielding is required in all directions in order to provide complete protection from the gamma radiation.

Apparently neutrons do contribute a small amount to the total exposure as measured by the film badges, but this contribution is negligible in comparison to the gamma radiation except under conditions of heavy shielding.

The Corps of Engineers' structures with two-foot-thick concrete walls would have prevented a lethal exposure to gamma radiation at a distance of 750 yards while that with one-foot walls would have been effective at 1000 yards.

None of the structures erected by the Bureau of Yards and Docks provided sufficient shielding to reduce the gamma radiation to a sublethal

exposure.

No striking distribution effect was noted within any of the structures tested nor behind any of the shields.

These data will be given further detailed analysis. Arrangements have been made to determine the film response to neutron exposure. No recommendations appear warranted pending the completed analysis.

APPENDIX 1
STEEL AND CONCRETE SHIELDS

The experimental installations for the measurement of gamma-radiation shielding consisted of assemblies of one-inch steel and three-inch concrete plates. These assemblies were completely documented with film badges. The individual film badge is illustrated by Figure 1. These plates were grouped together to provide over-all thicknesses of steel of one, two, four, six and twelve inches as shown in Figure 2. They were set up at distances from the zero point as given in Table I. In every set eight film badges were placed behind each plate. The arrangement is illustrated by Figure 3. Steel washers were inserted between the individual steel plates to provide bearing areas and to remove the possibility of pressure between plates having an adverse effect on the film badges. In order to provide the structural characteristics necessary for these installations to withstand the effects of the blast and shock waves following the detonation, the sets of steel plates were mounted on angle iron stakes, 2 x 2 x 3/16 inch, which were driven into the coral to a depth of about two feet. The plates were held together as a unit and attached to the steel angle iron stake by means of 3/8 inch threaded rods bolted at each end. In the case of the installation made up of the twelve one-inch plates, it was necessary to provide the angle iron supports at the four corners of the set whereas in all other sets, the plates were attached to only two stakes which were located on the side of the plates facing toward the zero tower.

Steel plates having an area of four square feet and one inch in thickness were also made up in groups to provide an over-all thickness of two inches

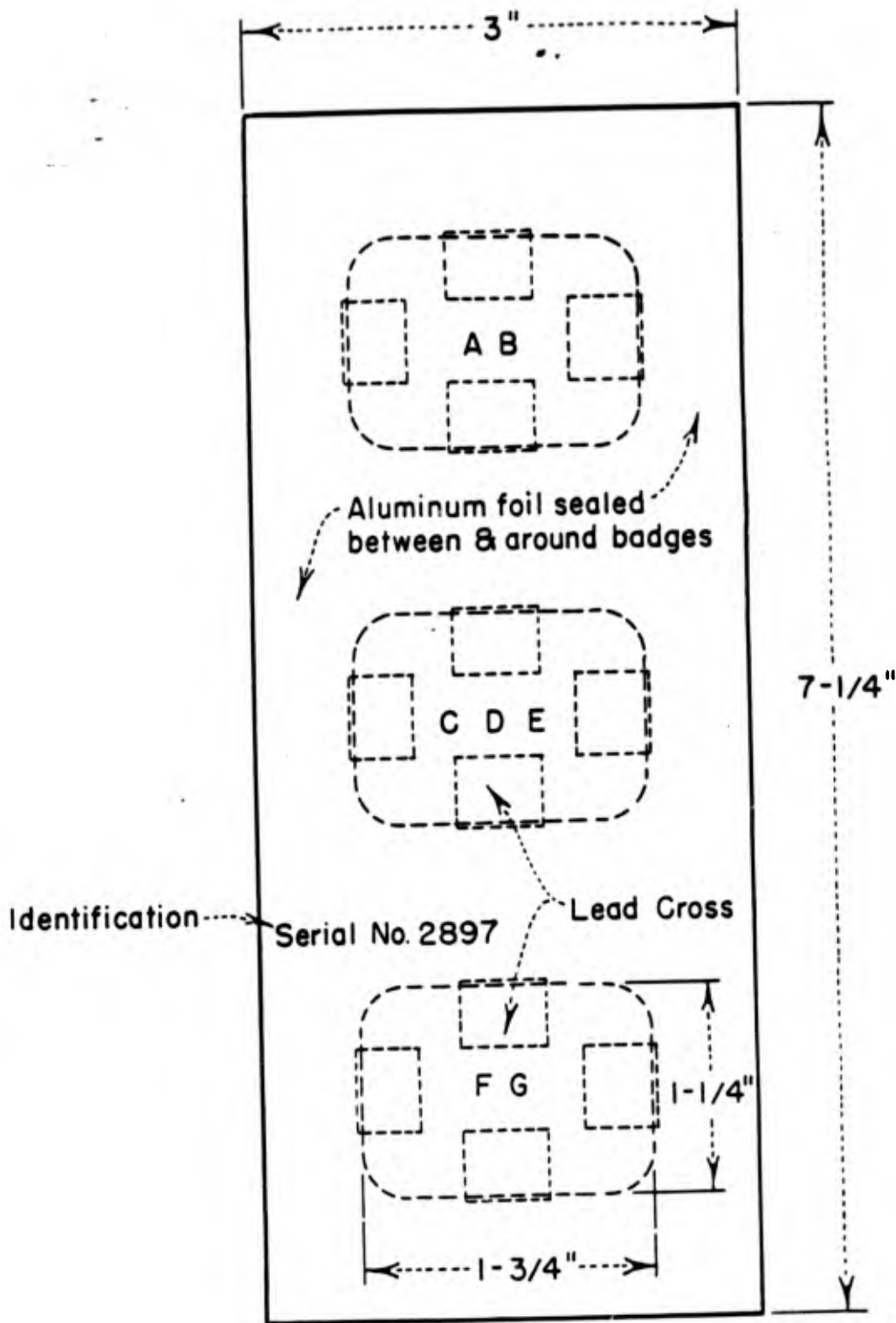
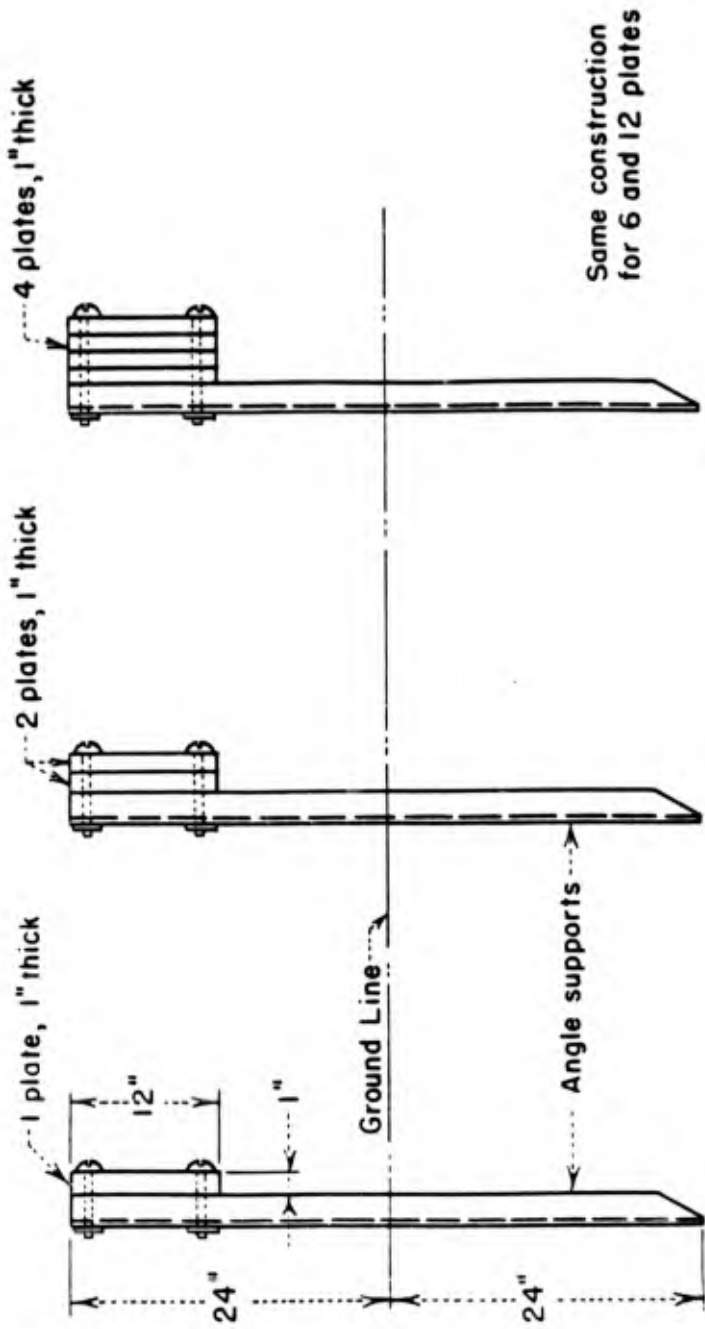


Fig. 1 Film Badge



Same construction
for 6 and 12 plates

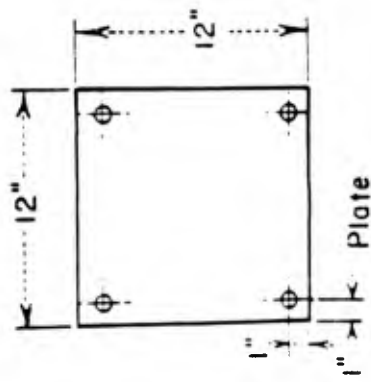


Fig. 2 Gamma Shielding Assemblies. The Assemblies as Shown were Held Together by 3/8-inch Bolts Through the Four Corners of the Steel Plates and Angles.

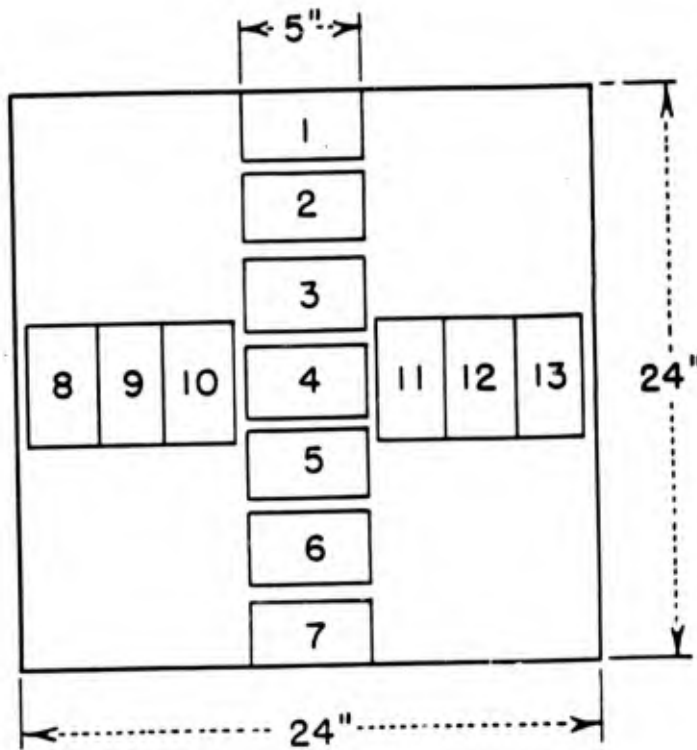
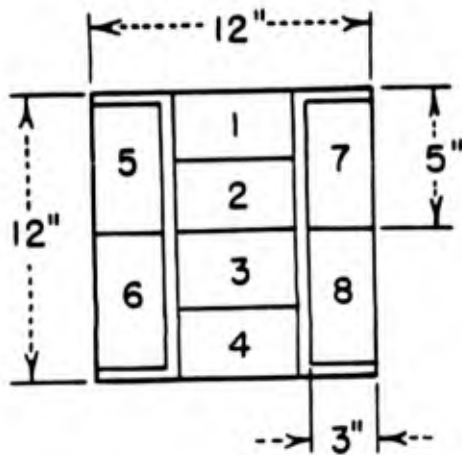


Fig. 3 Arrangement of Film Badges Behind 12" x 12" x 1" Steel Plates
 12" x 12" x 3" Concrete Block, and 24" x 24" x 1" Steel Plate
 for Measurement of Gamma Radiation Shielding.

TABLE I

LOCATIONS FOR STEEL AND CONCRETE INSTALLATIONS

<u>Test X-ray</u>			
Distance in Yards	Area of Plate In Square Feet	Steel Thickness In Inches	Concrete Thickness In Inches
750	1	1, 2, 4, 6, 12	3, 6, 12
750	4	2	
1000	1	1, 2, 4, 6, 12	3, 6, 12
1000	4	2	
1400	1	1, 2, 4, 6, 12	3, 6, 12
1400	4	2	
<u>Test Yoke</u>			
700	1	2	3, 6, 12
	4	2	3, 6, 12
1000	1	2	3, 6, 12
	4	2	
1250	1	2	3, 6, 12
	4	2	
<u>Test Zebra</u>			
750	1	1, 3, 6, 12	3, 9, 18
1000	1	1, 3, 6	

as shown in Figure 4. The plates were similarly mounted and bolted together as were the smaller plates, but additional strength to withstand the blast was provided by attaching two angle iron stakes at the upper corners of the vertical stakes and driving them diagonally into the coral to a depth of about 18 inches. These plates of larger area were documented by thirteen film badges placed in the form of a cross on the reverse side of each plate in lieu of the eight badges used with the smaller plates, as shown in Figure 3.

For the purpose of comparison, the concrete blocks were installed at the same distances from the zero tower as were the steel plates. The concrete installations were composed of individual blocks one square foot in area and three inches thick, containing no reinforcing material. The concrete blocks were grouped together to provide units having over-all thickness of three, six, twelve and eighteen inches of concrete and were used with compatible thicknesses of steel plates.

In order to securely mount the concrete blocks, wooden racks, consisting of lengths of four-by-four inch and two-by-four inch timbers, were constructed. These were so designed to provide for a base and a backing support for the blocks as shown in Figure 5. The rack was secured to the ground by means of 5/8-inch steel pins which were driven through drift holes in the timbers of the rack. The concrete blocks were placed in an upright position and held together and to the rack by means of wire rope.

On Test Zebra, small envelopes containing individual samples of arsenic, phosphorous, and sulphur together with one film badge were interposed between the steel and concrete shields in lieu of the type of documentation used for Tests X-ray and Yoke which has been previously described. This departure from the previous documentation methods was employed for the purpose of

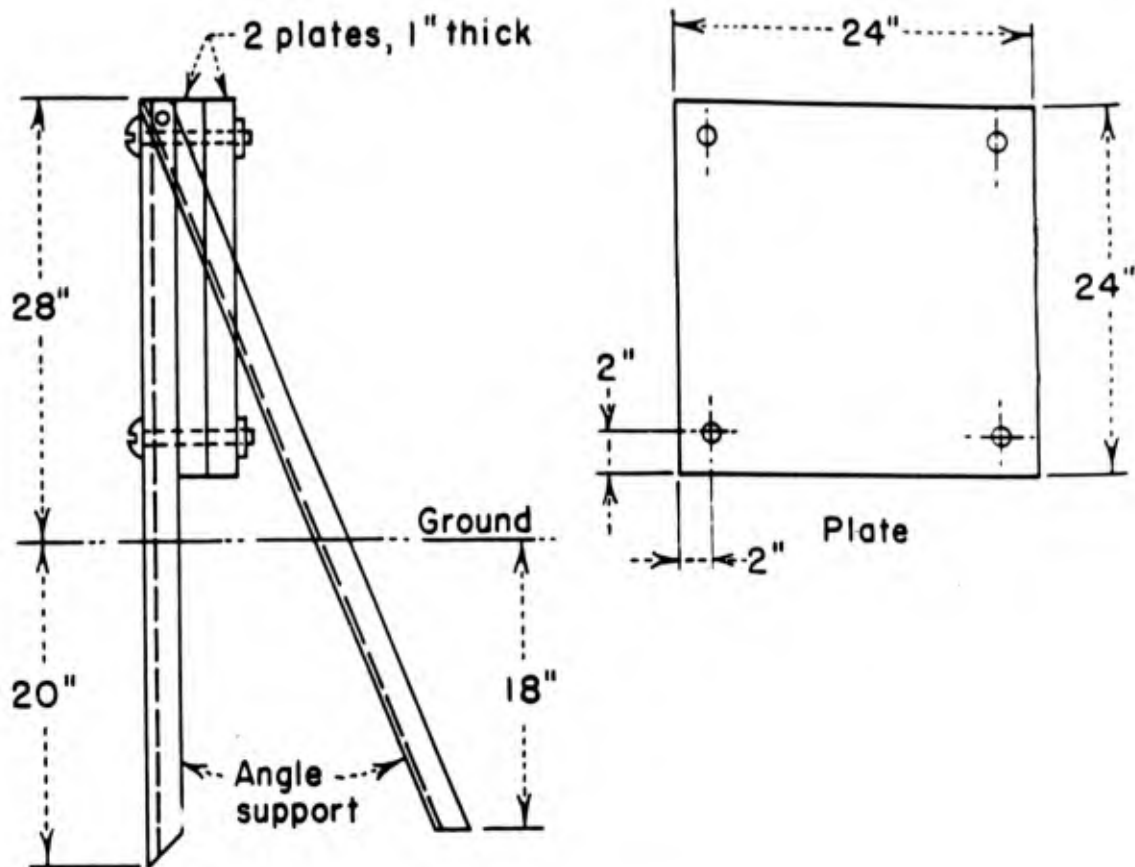


Fig. 4 Gamma Shielding Assembly. The Increased Plate Size Over That Shown in Fig. 2 Necessitated the Addition of a Rear Angle Iron Brace.

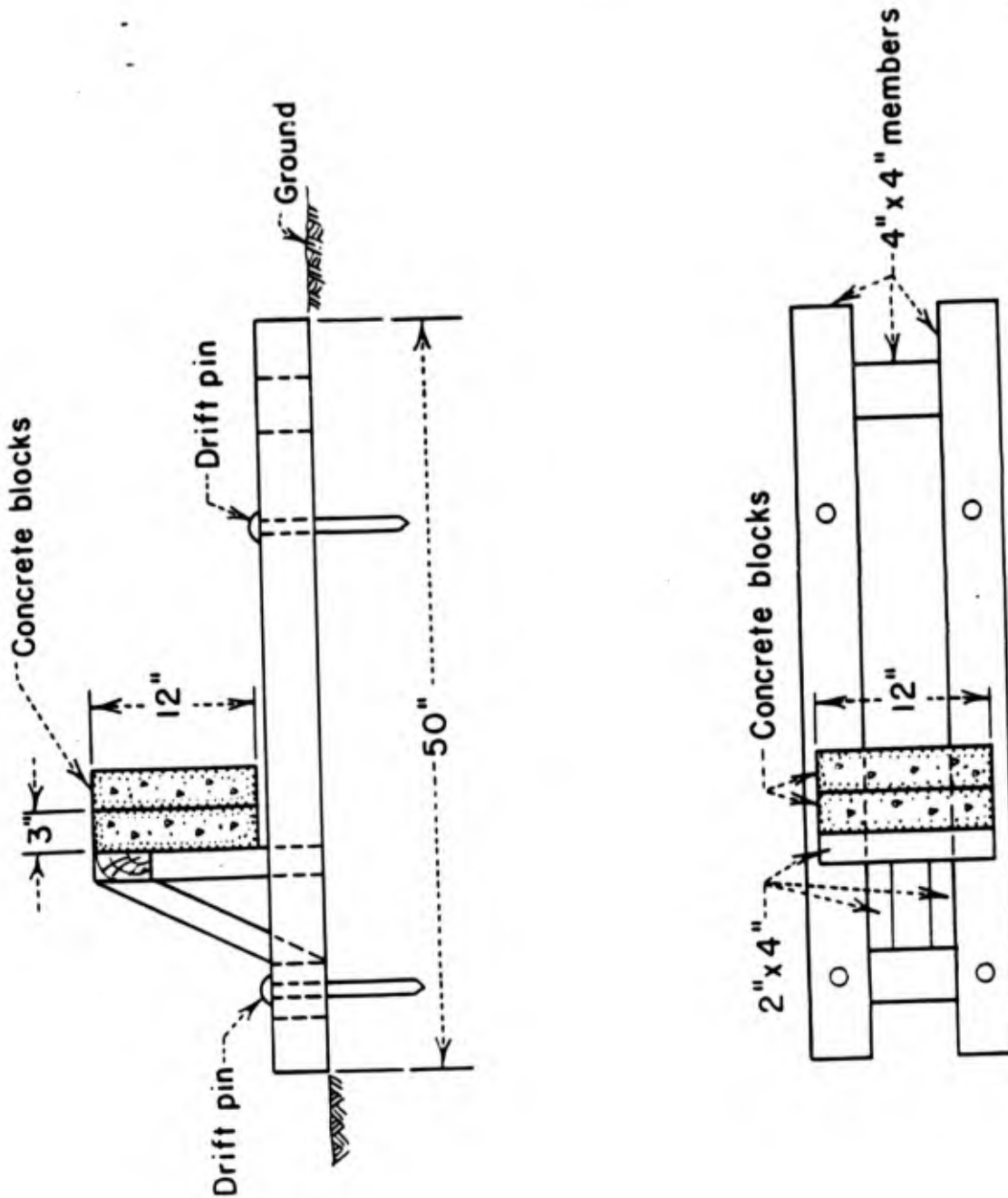


Fig. 5 Two Concrete Blocks and Rack for Measurement of Gamma Radiation Shielding Characteristics. Similar Installations were Provided for 1 and 4 Concrete Blocks.

determining the neutron flux within the shield while simultaneously recording the exposure registered by film. Calibration of these films for neutron sensitivity will enable correlation to be made with observed results. The arrangement of the neutron-sensitive material and the film badge is shown in Figure 6.

An aluminum strip about nine inches long was placed between the envelopes containing the As, P and S and the film badges in order that the β -particles from the activated materials would be absorbed by the aluminum and not affect the film badges. The aluminum strip, sample envelopes and film badge were held in place by use of an adhesive cement. In addition, for each set of shield four series of envelopes and film badges were placed on the front side of the plates or concrete shields nearest the zero tower. An aluminum panel twelve inches square and 1/8 inch thick was placed in front of the test envelopes and film badges to protect them from burning.

Installation of the film badges was commenced on test day minus two days for all tests. The installation of the plates for each group had been effected much earlier than these dates but actual placing of the film badges was delayed so that the weathering effect on the badges prior to the test could be held to a minimum. To this end, it was also considered advisable to cover the plates with white paint in order to keep their temperature to a minimum. The badges were made up aboard ship into their individual groups of eight or thirteen, depending upon the area of the plate behind which they were to be placed. They were provided with lengths of white cotton line to facilitate lowering into their assigned position between the plates which were already installed and bolted together. Adhesive cement was used to hold the badges which were placed on the outside of the sets. These methods proved to be satisfactory.

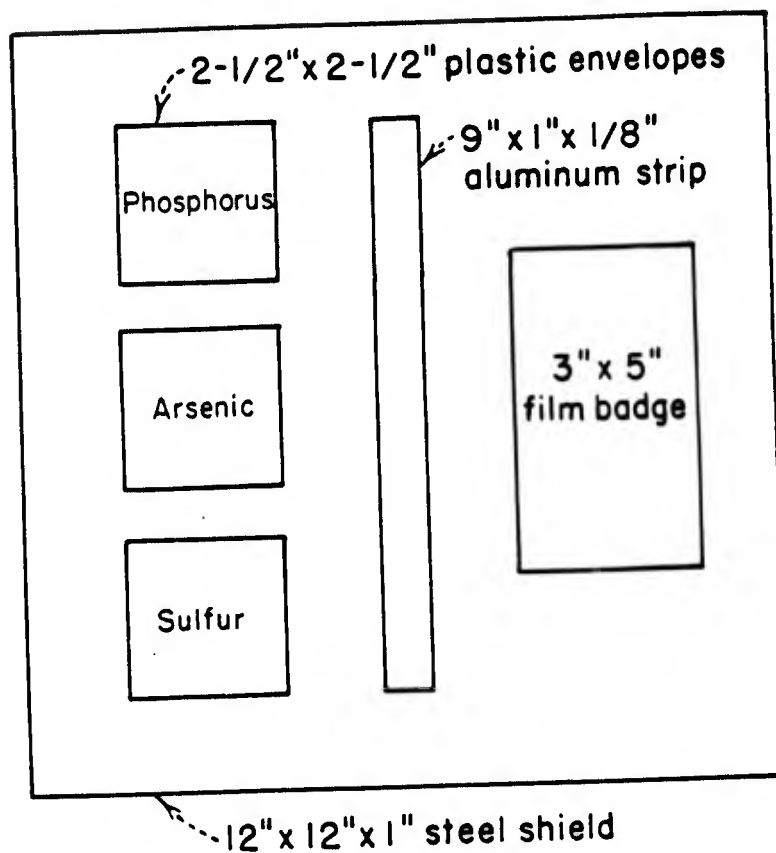


Fig. 6 Arrangement for Test Zebra of Film Badge for Measuring Shielded Gamma Radiation and the Position of Chemical Elements for Measuring Shielded Neutron Intensities. An Aluminum Strip is Interposed Between the Film Badge and the Plastic Envelopes Containing the Elements in Order to Shield the Film Badge from Beta and Gamma Rays Emitted by the Elements after Neutron Capture.

The installations were covered with heavy waterproof paper as a protection against rain until X-ray minus one day.

Following the detonation and upon re-entry of the survey parties, film badge recovery from the plates was begun. The percentage recovery was considered to be very good with one hundred percent at 1400 and 1000 yards and about ninety percent from 750 yards. The recovery was accomplished by loosening the plate holding bolts and withdrawing the sets of badges by grasping the tapes that held the groups as a unit. Radiation intensities and times were recorded at recovery. Since no significant contamination was observed none of the exposure can be attributed to this source.